

CRANFIELD UNIVERSITY

SAYYAM KHURANA

LOAD INTRODUCTION IN BOLTED UD-SMC HYBRID  
COMPOSITE STRUCTURES

SATM  
MSc AEROSPACE MATERIALS

MSc  
Academic Year: 2019 - 2021

Supervisor: Andrew Mills  
Associate Supervisor: David Ayre  
August 2021



CRANFIELD UNIVERSITY

SATM  
MSc AEROSPACE MATERIALS

MSc

Academic Year 2019 - 2021

SAYYAM KHURANA

LOAD INTRODUCTION IN BOLTED UD-SMC HYBRID  
COMPOSITE STRUCTURES

Supervisor: Andrew Mills  
Associate Supervisor: David Ayre  
August 2021

This thesis is submitted in partial fulfilment of the requirements for  
the degree of MSc Aerospace Materials  
***(NB. This section can be removed if the award of the degree is  
based solely on examination of the thesis)***

© Cranfield University 2021. All rights reserved. No part of this  
publication may be reproduced without the written permission of the  
copyright owner.



## **ABSTRACT**

There is a growing need for lightweight composite parts that can be mass produced for the automotive industry. Conventional continuous fibre composites are too expensive, and Sheet Moulding Compound (SMC) parts have very high variability. Hybrid composites made of Uni-directional (UD) Tapes and SMC lie in the goldilocks zone to fulfil this market.

A suspension arm of a multi-link suspension system is chosen as a target part for the project. A complex I-beam with a cross-section similar to a suspension arm is moulded using hybrid composites. An original UD placement layout is designed to increase the net tensile strength of the part.

Six inserts are designed, manufactured, and embedded into hybrid I-beams to reduce the stress concentration and increase the bearing strength of the parts. Pin-bearing tests are performed on the parts to evaluate the impact of insert shape, projected area, and texture. The resultant hybrid parts have a higher strength than Aluminium but have lower stiffness.

Keywords:

Compression Moulding, SMC, UD, Insert, Automotive, Suspension Arm



## **ACKNOWLEDGEMENTS**

I would like to thank my Supervisor Andrew Mills for his continuous support ever since I first approached him for my IRP in 2020. This project wouldn't have been possible without the support and feedback from Krutarth Jani. I would like to thank Jim Hurley, for without him the lab work would have stalled.

I would like to thank my course coordinator Dr Sue Impey for guiding me throughout my MSc. I am thankful for the input and feedback I have received from Dr. David Ayre and Lawrence Cook. I would like to thank Mick Purton from Crown Precision Engineering to take on the challenge of machining my designs and Steve Pope and Ben that made it possible to test them.

I would like to thank my colleague Oliver for being my comrade through the project and for especially lending an ear when nothing was working. Last but not the least, I would like to thank the SAS Leads Soumayah and Sarah who helped me a lot in navigating the deadlines in these final days.





# TABLE OF CONTENTS

ABSTRACT .....	i
ACKNOWLEDGEMENTS.....	iii
LIST OF FIGURES.....	viii
LIST OF TABLES .....	xii
LIST OF EQUATIONS.....	xiv
LIST OF ABBREVIATIONS .....	xv
1 Introduction.....	1
2 Project Definition .....	3
3 Literature Study .....	7
3.1 Automobile Parts vs Aerospace Parts.....	7
3.2 Composites.....	7
3.2.1 Continuous fibre composites.....	8
3.2.2 Discontinuous fibre composites.....	8
3.2.3 Hybrid composites.....	13
3.3 Prepreg Compression Moulding .....	17
3.4 SMC Compression Moulding .....	18
3.4.1 SMC Manufacturing and Properties .....	18
3.4.2 Fibres .....	20
3.4.3 Resin.....	20
3.4.4 Charge Placement and Flow.....	21
3.4.5 Charge stacking sequence.....	23
3.4.6 High Flow Moulding.....	23
3.4.7 Disadvantages of high flow .....	26
3.4.8 Compression Pressure.....	27
3.4.9 Scalability .....	27
3.4.10 Shrinkage .....	28
3.4.11 Internal Mould Release .....	28
3.4.12 Temperature.....	29
3.4.13 Dwell Time .....	29
3.4.14 Mould Closing Speed .....	29
3.4.15 Compression under vacuum .....	29
3.5 Hybrid Compression Moulding.....	30
3.5.1 UD Flow .....	30
3.5.2 Adhesion of UD and SMC .....	31
3.5.3 Difference in Compression Pressure.....	31
3.5.4 Stacking of UD and SMC .....	31
3.5.5 Charge Placement.....	32
3.5.6 Predictability and Testing .....	33
3.6 Mechanical Properties of Hybrid Composites .....	34
3.6.1 Modulus.....	34

3.6.2 Strength.....	35
3.7 Composite Joining Methods.....	35
3.8 Inserts.....	39
3.8.1 Location.....	40
3.8.2 Modes of Failure .....	42
3.8.3 Shapes & Texture Inserts.....	45
3.8.4 Adhesion .....	52
3.8.5 Material .....	52
3.8.6 Corrosion.....	52
3.8.7 Pre-Load .....	53
3.8.8 Viscoelastic effects /Creep .....	53
3.8.9 Aging .....	54
3.9 Knowledge Gap .....	54
3.10 Goals of a Hybrid Composite .....	55
3.11 Goals of an Insert.....	55
4 METHOD.....	57
4.1 Design.....	57
4.1.1 Material Properties .....	58
4.1.2 Design Loads .....	58
4.1.3 Hybrid Structural Design .....	59
4.1.4 Insert Design .....	61
4.1.5 Design of Experiments .....	67
4.1.6 Predicted Strength and Modulus .....	68
4.1.7 Summary of Hypothesis's being tested .....	69
4.2 Manufacturing .....	70
4.2.1 Charge Design .....	71
4.2.2 SMC Moulding.....	72
4.2.3 Hybrid I – Beam Moulding .....	73
4.3 Testing .....	75
4.3.1 Sample Preparation.....	75
4.3.2 Machine Set up .....	75
5 RESULTS.....	77
5.1 Qualitative Results .....	77
5.1.1 Moulding Results.....	77
5.1.2 Test Results .....	81
5.2 Quantitative Results.....	82
5.2.1 Geometric Properties .....	82
5.2.2 Mechanical Properties.....	82
6 Discussion .....	85
6.1 Mechanical Performance .....	85
6.1.1 Strength.....	85
6.1.2 Stiffness .....	87

6.2 Manufacturing Process .....	88
6.3 Comparison with aluminium.....	89
6.4 Proposed Design .....	89
7 Conclusion.....	91
8 Recommendations and Future Work.....	92
REFERENCES.....	93
APPENDICES .....	101
Appendix A Force Displacement Graphs.....	101
Appendix B Datasheets .....	105
Appendix C Adhesion of Metals and Composites .....	110
Appendix D Risk Assessment & Mitigation Plan .....	113
Appendix E .....	114

## LIST OF FIGURES

Figure 1: Render of a multi-link rear suspension arm.....	3
Figure 2: Location of Suspension arm.....	4
Figure 3: Bushings in a Suspension Arm .....	4
Figure 4: Render of an I-Beam .....	5
Figure 5: Composite strength as a function of fibre length (Visweswaraiah et al., 2018) .....	8
Figure 6: Orientation of discontinuous fibres in the x-y plane (Visweswaraiah et al., 2018).....	9
Figure 7: Classification of discontinuous fibres (Visweswaraiah et al., 2018).....	9
Figure 8: Cost of materials (Granta design, 2020).....	10
Figure 9: Boeing 787 window frame (Bale and others, 2015).....	13
Figure 10: Ways to increase the stiffness of a composite (Visweswaraiah et al., 2018) .....	14
Figure 11: Processing vs performance of different composite architectures (Selezneva and Lessard, 2016).....	15
Figure 12: Net Shape Hybrid Compression Moulding .....	15
Figure 13: Mitsubishi Rayon Hybrid Structural Floor (Corbridge, 2018) .....	16
Figure 14: Prepreg Compression Moulding (Akiyama, 2011).....	17
Figure 15: SMC Manufacturing Process (Mazumdar, 2001) .....	18
Figure 16: Diameter, Width and Edge Distance of a specimen .....	19
Figure 17: 1d Flow, 2d Flow and 3d Flow Scenarios.....	22
Figure 18: Flow Mechanisms: (A) Fountain flow usually observed in thermoplastic moulding;(Papathanasiou and Guell, 1997) (B) Preferential flow usually observed in thermoset compression moulding (Lee and Tucker, 1987) ....	22
Figure 19: Pyramid Stacking Sequence to avoid voids and out of plane fibre distortion (REVELLINO, SAGGESE and GAIERO, 2000) .....	23
Figure 20: Defects in SMC ribs.....	25
Figure 21: Material Break Charge Design (Corbridge, 2018) .....	25
Figure 22: SMC flow creating a weld line (Sentis et al., 2017) .....	26
Figure 23: Knit line formed past an insert (Sasdelli, Karbhari and Gillespie, 1993) .....	27

Figure 24: Increased likelihood of proximity of fibre bundle ends and transverse fibres in larger parts .....	28
Figure 25: UD waviness inside hybrid .....	30
Figure 26: Two stage hybrid compression moulding .....	30
Figure 27: Flexural modulus of different UD-SMC orientations (Hopmann et al., 2017) .....	32
Figure 28: Difference in mechanical properties of SMC and hybrid composite sections in charge region and flow region.....	33
Figure 29: Difference in longitudinal and Transverse strength as a function of UD (Evans et al., 2017) .....	35
Figure 30 : Damage due to drilling (Faraz, Biermann and Weinert, 2009) .....	39
Figure 31: Bonded insert for bolt in composite laminate (Camanho and Matthews, 2000) .....	39
Figure 32: Top Insert (BigHead, 2017) .....	40
Figure 33: Middle/Embedded Insert (Gebhardt and Fleischer, 2014) .....	40
Figure 34: Through Insert (Troschitz, Kupfer and Gude, 2019) .....	41
Figure 35: Modes of Failure in Composite plates (Ataş and Soutis, 2013).....	42
Figure 36: Typical Bearing failure load curve (Turvey and Wang, 2007).....	44
Figure 37: Different insert options (Reller, 2008).....	45
Figure 38: Load capacity of inserts (Reller, 2008) .....	46
Figure 39 : Pin Joining of metal inserts in composites (Graham et al., 2014)...	47
Figure 40: Optimised tapered ends for inserts (Camanho et al., 2005) .....	48
Figure 41: Deformation of an insert with and without a bead pattern (Gebhardt and Fleischer, 2014) .....	48
Figure 42: Z-pins reinforcement in bonded joints (Löbel et al., 2013).....	49
Figure 43: Through Insert design with an undercut (Troschitz, Kupfer and Gude, 2019) .....	49
Figure 44: Hybrid Titanium sheet reinforcement (Camanho et al., 2009) .....	50
Figure 45: Fibre Steering around a hole (Li, Kelly and Crosky, 2002) .....	50
Figure 46: Bighead Insert with holes (BigHead, 2017) .....	51
Figure 47: Quasi-Linear Insert (Muth et al., 2018).....	51
Figure 48: I-Beam to Test Specimen.....	57

Figure 49: Tapered I-Beam Cross-section Drawing .....	57
Figure 50: Hybrid Specimen Layout .....	59
Figure 51: Net Tension Failure of Hybrid Specimen .....	60
Figure 52: Cylinder .....	64
Figure 53: Knurled Cylinder .....	64
Figure 54: Flying Saucer .....	65
Figure 55: Yoyo .....	65
Figure 56: 2d Yoyo .....	66
Figure 57: Butterfly .....	66
Figure 58: Predicted Failure Loads of all Configurations .....	68
Figure 59: Predicted Modulus based on Rule of Hybrid Mixtures .....	69
Figure 60: Compression Moulding Press .....	70
Figure 61: Male and Female Moulding Tool .....	71
Figure 62: Charge Design with a Punched Hole .....	72
Figure 63: SMC I-Beam Moulding Process .....	72
Figure 64: SMC Moulded Specimen .....	73
Figure 65: Hybrid I-Beam Moulding Process .....	73
Figure 66: Elastomeric Tool Iterations .....	74
Figure 67: Hybrid I-Beam Moulding .....	74
Figure 68: Specimens with their respective inserts .....	75
Figure 69: Pin-Bearing Test Set Up .....	76
Figure 70: Gel Tearing on Surface .....	77
Figure 71: Voids in Specimens .....	78
Figure 72: UD-SMC Delamination .....	78
Figure 73: Dry Region from Resin Squeeze Out .....	79
Figure 74: Resin-rich Region at the UD-SMC Interface .....	79
Figure 75: Fibre Waviness near Insert .....	80
Figure 76: Fibre Flow around Flying Saucer Insert .....	80
Figure 77: Fibre Flow around Yoyo Insert .....	80

Figure 78: Asymmetric Failure of Specimens .....	81
Figure 79: Failure Loads Proportional to the Cross-Section Area of the Specimens.....	83
Figure 80: Hybrid Specimen with Knurled Insert .....	84
Figure 81: Hybrid Specimen with Butterfly Insert.....	84
Figure 82: Comparison of Predicted and Tested Failure Loads .....	85
Figure 83: Gripping Effect of the Knurled Insert .....	86
Figure 84: Comparison of Predicted and Tested Modulus .....	87
Figure 85: Angled UD Strips to Increase Stiffness .....	90
Figure 86: Tie Fighter Insert Design .....	90
Figure 87: SMC Specimen .....	101
Figure 88: SMC Specimen with Cylindrical Insert.....	102
Figure 89: Hybrid Specimen.....	102
Figure 90: Hybrid Specimen with Cylindrical insert .....	103
Figure 91: Hybrid Specimen with Yoyo Insert.....	103
Figure 92: Hybrid Specimen with 2d Yoyo Insert.....	104
Figure 93: Hybrid Specimen with Flying Saucer.....	104
Figure 94: Surface Energy of different materials (Candotape, 2016) .....	110
Figure 95: Aluminium surface microstructure after Phosphoric Acid Anodization (Vander Voort et al., 2004) .....	111
Figure 96: Tensile strength of stainless-steel carbon fibre lap joints with different surface treatments on metal (Gebhardt and Fleischer, 2014).....	111
Figure 97: Tensile and Bending strengths of embedded inserts with different surface treatments (Gebhardt and Fleischer, 2014) .....	112
Figure 98: Impact of Insert Tolerance on Loading.....	114
Figure 99: Medium Flow Trapezoidal Charge Design .....	115
Figure 100: Hybrid Flat Sample Moulding .....	115

## LIST OF TABLES

Table 2: Differences in Aerospace and Automotive Design .....	7
Table 3: Comparison of Various Manufacturing Processes (Corbridge, 2018; Granta design, 2020) .....	11
Table 4: Specific Strength and Stiffness of Different Materials (Granta design, 2020) .....	12
Table 5: Summary of advantages of UD, SMC, and Hybrid Composites .....	16
Table 6: Stress Concentration Factors Around Holes in Different Materials D/W 0.375 (Bond et al., 2019) .....	19
Table 7: Stress concentrations factors in infinite width materials (Woodhead Publishing, 2012) .....	20
Table 8: Properties of Different Resins (Bücheler, Griesbaum and Henning, 2018) .....	21
Table 9: Advantages and Disadvantages of different composite joining methods .....	37
Table 10: Locations of Inserts inside Composites .....	40
Table 11: Recommended Part Width/Diameter and Edge Distance/Diameter Ratios for Bearing Failure in Single Pin Joints .....	44
Table 12: Reinforcement Options for Composite Joining .....	47
Table 13: Material Properties of the Composites .....	58
Table 14: Predicted Pin-Bearing Failure Loads of SMC Specimen .....	59
Table 15: Predicted Failure Pin-Bearing Failure Loads of UD-SMC Hybrid Specimens .....	60
Table 16: Mechanical, thermal, electrochemical, and cost properties of material options (Granta design, 2020) .....	61
Table 17: Material Selection Trade-off Table .....	62
Table 18: Insert Properties .....	64
Table 19: Design of Experiments .....	67
Table 20: Specimen Geometric Properties .....	82
Table 21: Comparison of Hybrid Composite and Aluminium under Pin Loading .....	89
Table 21: Risk Assessment and Mitigation Plan .....	113





## LIST OF EQUATIONS

Equation 3-1: Rule of Hybrid Mixtures .....	34
Equation 3-2 Modulus of Random Fibre Composites .....	34
Equation 3-3: Net-Tensile Strength of a Specimen .....	42
Equation 3-4: Shear Stress on a Specimen .....	43
Equation 3-5: Bearing Stress on a Material .....	43

## **LIST OF ABBREVIATIONS**

UD	Uni Directional
SMC	Sheet Moulding Compound
RoHM	Rule of Hybrid Mixtures



# 1 Introduction

Climate change is the biggest threat to modern humans. It is crucial that we reduce our greenhouse emissions through every avenue. Transport emissions account for 30% of EU's total CO<sub>2</sub> emissions, majority of which is caused by road transport.<sup>1</sup> One of ways to reduce emissions is to reduce the weight of the vehicles in turn leading to higher energy efficiency.

Most structural parts of the automobiles are made from metals. It is possible to reduce the weight of these parts by replacing them with continuous fibre composites. While this strategy has worked for the aerospace industry, continuous fibre composites are expensive and have high manufacturing cycle times. Short fibre composites on the other hand are price competitive, low production times, but have lower strength, stiffness, and reliability. Hybrid composites with short and continuous fibres combined synergistically utilises the advantages of both composites. While, the strength and stiffness of hybrid composites has been investigated in lab conditions, load transfer in real world applications occurs using bolted joints. Therefore, this report investigates the load transfer using bolted joints in hybrid composites.

The project is defined in Chapter 2. Chapter 3 presents the literature study and points out the knowledge gap. The design, manufacturing and testing method is presented in Chapter 4. Chapter 4.3 displays the results of the testing followed by their discussion in Chapter 6. The conclusion of the project is presented in Chapter 7 followed by recommendations for future work in Chapter 8.

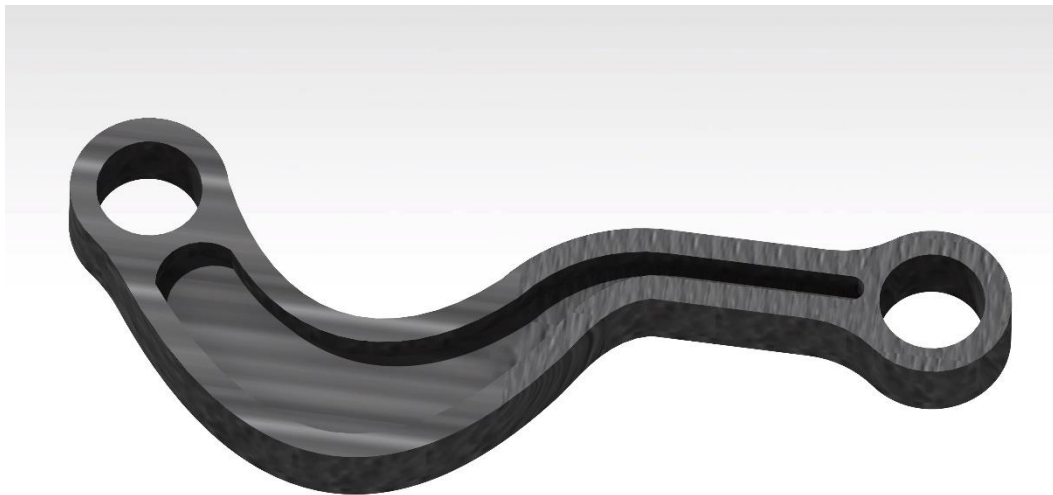
---

<sup>1</sup><https://www.europarl.europa.eu/news/en/headlines/society/20190313STO31218/co2-emissions-from-cars-facts-and-figures-infographics>



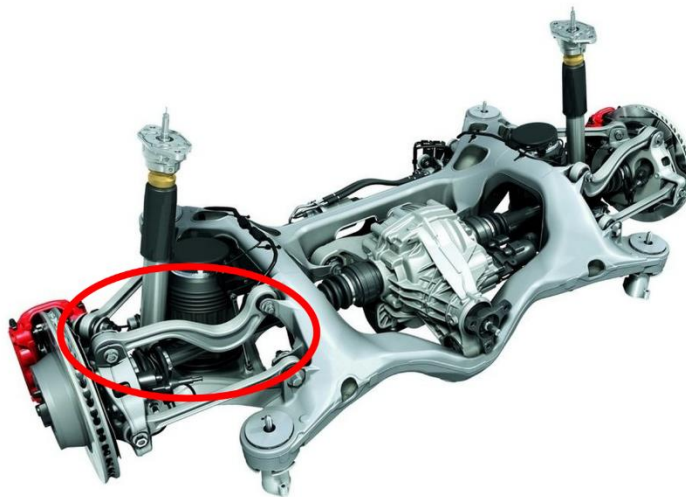
## 2 Project Definition

The aim of the project is to establish design rules for hybrid bolted composite joints. Amongst the various structural components in an automobile, the rear suspension arm of Porsche Panamera is chosen for redesign with hybrid composites. Currently, the arm is produced using forged Aluminium. A render of the suspension arm is shown in Figure 1.



**Figure 1: Render of a multi-link rear suspension arm**

The car uses a multi-link suspension system, which provides design flexibility, improved comfort, and simple loading on the arms. The location of the suspension arm is displayed in Figure 2. The design requirements for a consumer car state a minimum travel distance of 200,000 km. Apart from simulating “stop brakes” and “bends”, the suspension arm also must withstand misuse scenarios such as car travelling at 50 km/hr over an obstacle 100 mm high and 100 mm long.



**Figure 2: Location of Suspension arm**

In a multi-link suspension system, the suspension arm is limited to tensile and compressive loading.<sup>2</sup> The loading is applied via a bushing shown in Figure 3. As a sudden catastrophic failure is unacceptable, a gradual bearing failure of the suspension arm is desired.



**Figure 3: Bushings in a Suspension Arm**

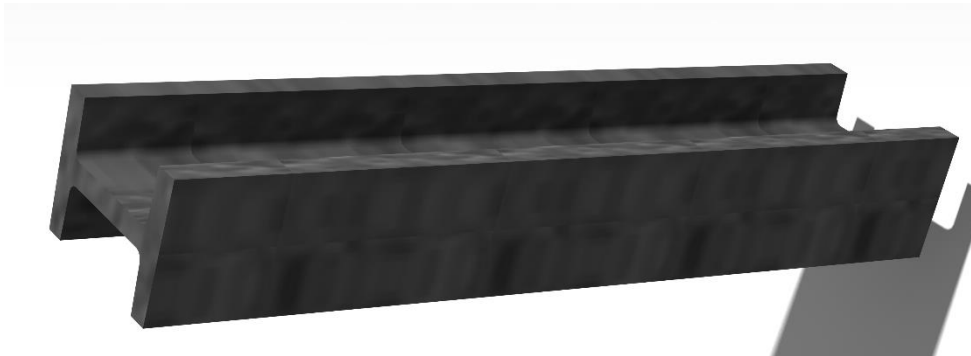
Every manufacturer has their own in-house loading criteria and safety factors for the suspension system. Therefore, to design a useable component, the hybrid suspension arm must meet the same technical criteria as the aluminium one.

---

<sup>2</sup> <http://www.multibody.net/teaching/msms/students-projects-2020/multi-link-suspension/>



To minimize design variables, an I-beam was chosen as a simplified model of a suspension arm because of its similar cross-section.



**Figure 4: Render of an I-Beam**

The objectives of the project are to:

- Develop a compression moulding technique for complex I-section test elements using hybrid composites.
- Develop a change in the failure mode of a SMC specimen from net tension to bearing using UD fibre tapes and shaped inserts.
- Determine the influence of insert shape on the failure of hybrid part bolted joints.
- Design a hybrid Suspension Arm with 30 % weight reduction with less than 3x the cost of forged aluminium.

The risk assessment and mitigation plan can be found in Appendix D.



### 3 Literature Study

This chapter provides a comprehensive review of the hybrid composites, metal inserts in composites, and effective ways to transfer loads through them. The aim of the chapter is to present and analyse the problem, probe the work that has previously been undertaken and identify the knowledge gap and potential challenges.

#### 3.1 Automobile Parts vs Aerospace Parts

Composites have a significant flight heritage in the aerospace sector. However, there are some key differences in aerospace and automobile requirements that must be considered when designing composite parts as outlined in Table 1.

**Table 1: Differences in Aerospace and Automotive Design**

	<b>Aerospace</b>	<b>Automotive</b>
<b>Design Safety Factors</b>	~1.5	~3
<b>Handling</b>	Certified Technician	Garage Mechanic
<b>Maintenance checks</b>	Regular scheduled checks	Irregular checks
<b>Operating Conditions</b>	Narrow operational envelopes with specific operational limits	Broad operational envelopes
<b>Right to Repair</b>	Can require custom tooling for repair	Should be repairable/replaceable using standard tooling

#### 3.2 Composites

Composites in this report are used to define fibre reinforced polymers. There are two broad categories of composites namely continuous and discontinuous fibre composites.

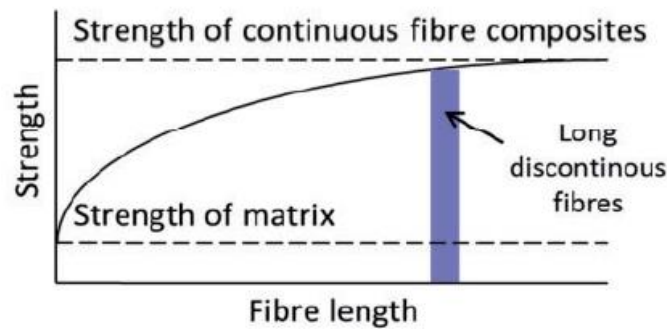
### 3.2.1 Continuous fibre composites

Continuous fibre composites utilize long fibres that encompass the entire structure. They can be uni-directional (UD) tapes, woven fabrics, knitted fabrics, braided shells, etc. While each type of continuous fibre has its own advantages, UD's are the simplest form of composites with the highest specific strength and stiffness.

UD's are anisotropic composites which comprise of continuous glass or carbon fibres aligned in one direction and are held together using a polymer. They are relatively expensive. Resin can be injected in them during moulding or can be pre-impregnated in the case of pre-pregs.

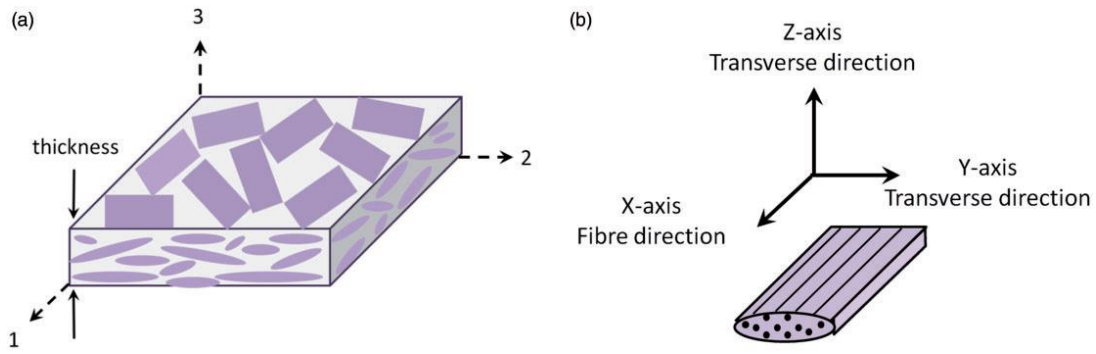
### 3.2.2 Discontinuous fibre composites

SMCs (Sheet moulding compounds) are made from discontinuous fibre composites. They are planar isotropic and can be easily moulded in complex shapes using high pressure. The relationship between strength of composites and fibre length is demonstrated in Figure 5.



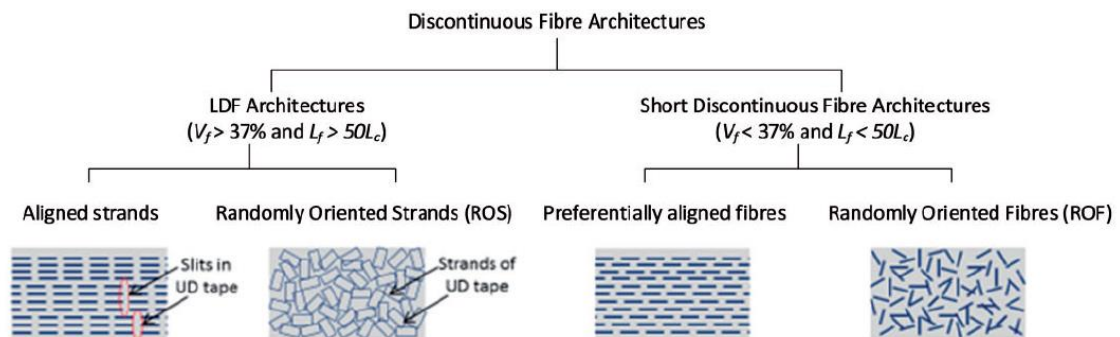
**Figure 5: Composite strength as a function of fibre length** (Visweswaraiah et al., 2018)

As the length of the fibres is shorter, SMCs are relatively less strong and stiff. The fibres in SMC are randomly oriented in the X-Y plane as displayed in Figure 6. SMC's gain their relative isotropicity from the random orientation of fibres. The level of isotropicity is dependent on the mould and the processing characteristics.



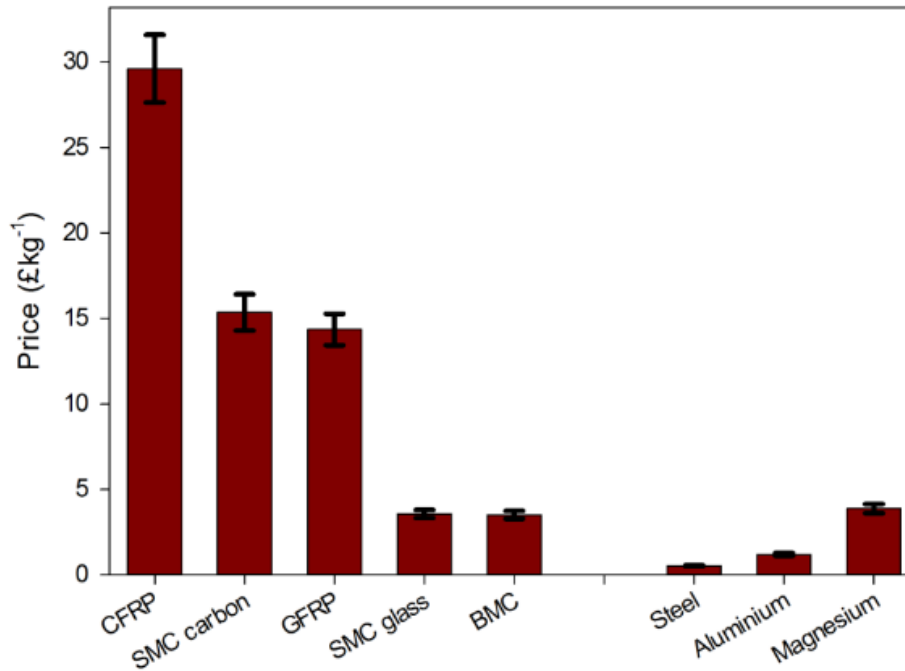
**Figure 6: Orientation of discontinuous fibres in the x-y plane** (Visweswaraiah et al., 2018)

Figure 7 demonstrates the different types of discontinuous fibre architectures. Long discontinuous fibres (LDF) are made from continuous fibre pre-pregs. This provides with long fibres, higher wetting (better adhesion) and higher cost. Short discontinuous fibre architectures are made using tows of dry fibre and resin sheet. They have relatively lower mechanical properties but are significantly cheaper.



**Figure 7: Classification of discontinuous fibres** (Visweswaraiah et al., 2018)

SMCs are significantly cheaper than UD which makes them viable for automotive applications. The cost of UD and SMC along with other materials is displayed in Figure 8.



**Figure 8: Cost of materials** (Granta design, 2020)

SMCs are compression moulded. Compression moulding is a relatively low-cost process suitable for medium to high production batches. The final cost of any part is dependent on both the material cost and the process cost. A comparison of processing parameters and process cost of different manufacturing methods for composites and metals is presented in Table 2.

**Table 2: Comparison of Various Manufacturing Processes** (Corbridge, 2018; Granta design, 2020)

<b>Manufacturing Process</b>	<b>Pressure (MPa)</b>	<b>Temperature (°C)</b>	<b>Cycle Time (min)</b>	<b>Relative Cost Index (£)<sup>3</sup></b>	<b>Economic Batch Size</b>
<b>Autoclave</b>	0.3-0.7	30-350	300-600	183	1-500
<b>Resin Transfer Moulding (RTM)</b>	0.1-6	30-350	3-30	20.8	500-5000
<b>Compression Moulding (SMC)</b>	1-20	30-350	1-15	21	5000-1000000
<b>Injection Moulding</b>	10-100	30-350	1-2	13.1	10000-1000000
<b>Steel Stamping</b>	140-200	30-800	0.16	10.2	25000-250000
<b>Sand Casting (Aluminium)</b>	-	700	0.2-3	11.9	1000-100000
<b>Aluminium Forging</b>	50-130	400	0.2-6	25.1	100-10000000

The use of SMCs in structural parts is limited because of low mechanical properties and lack of repeatability in parts. A comparison of specific strength and stiffness of different materials is presented in Table 3.

---

<sup>3</sup> “The relative cost index approximates the cost of making a 'unit' or a component by the process. Its value is calculated with the 'Process Cost Model’. The complexity of the part, batch size, material, manufacturing location, etc will all have an impact on the final cost, however relative cost index is a helpful tool for process comparison.

**Table 3: Specific Strength and Stiffness of Different Materials** (Granta design, 2020)

<b>Material</b>	<b>Specific Tensile Strength (kN.m/kg)</b>	<b>Specific Stiffness (MN.m/kg)</b>
<b>Aluminium 6082</b>	95	26.5
<b>Aluminium 6060</b>	60	26.5
<b>Low Carbon Steel 1020</b>	38	26.6
<b>High Carbon Steel 1095</b>	48	26.5
<b>Stainless Steel 316L</b>	38	24.8
<b>Gray Cast Iron (EN GJL 350)</b>	33	18.5
<b>CF UD (Epoxy)</b>	1650	105.8
<b>CF SMC (Vinyl Ester)</b>	77	18
<b>GF SMC (Vinyl Ester)</b>	104	7.4
<b>CF HexMC (Epoxy)</b>	193.54	24.5

Tensile loading is the critical loading for the SMCs followed by compression loading and flexural loading (Feraboli et al., 2009). Compressive strength of SMCs can be up to 1.7 times higher than tensile strengths (Caprino et al., 2002). SMCs have higher fracture toughness than continuous fibre laminates and are notch insensitive. SMC parts can be designed with local thickness variation. SMCs are also more sustainable than continuous fibre composites as they can be made from recycled composite fibres.

SMCs have already found use in aerospace and automobile applications such as Boeing 787 window frame as shown Figure 9.



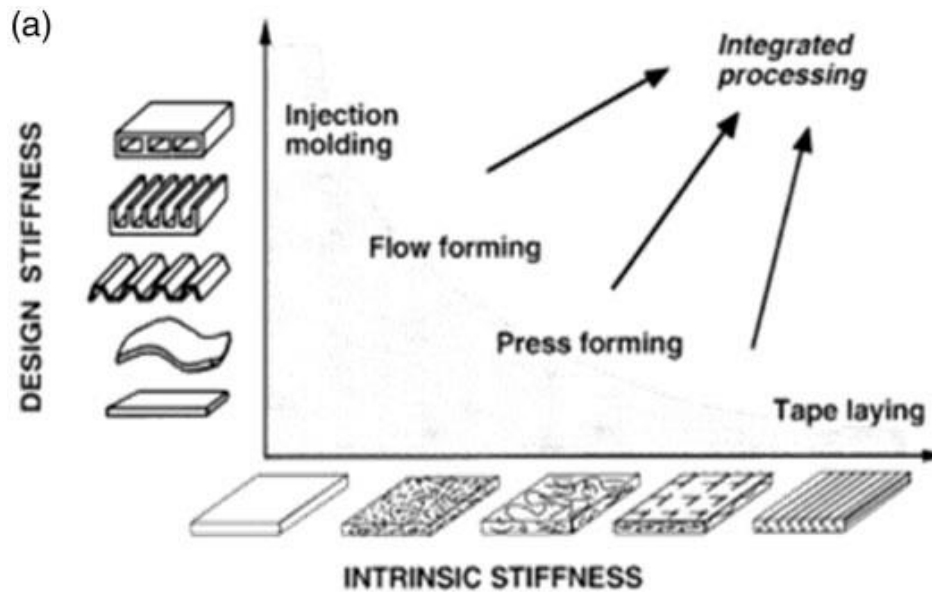


**Figure 9: Boeing 787 window frame** (Bale and others, 2015)

### **3.2.3 Hybrid composites**

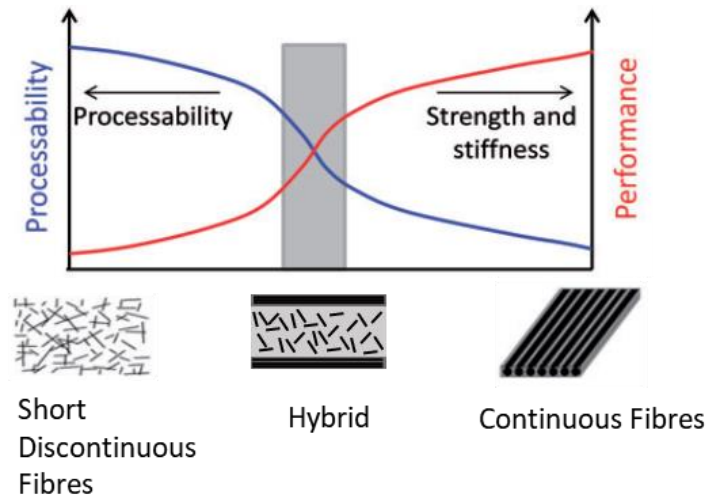
Hybrid composites is a term used for any combination of composite materials. The scope of this report is limited to a hybrid of UD-SMC thermoset composites.

Figure 10 shows that the two ways of increasing stiffness of a composite structure are by increasing the moment of inertia or intrinsic material stiffness. SMC parts can be compression moulded into complex shapes with high moment of inertia, whereas UD can add stiffness, strength, and predictability in critical load paths.



**Figure 10: Ways to increase the stiffness of a composite** (Visweswaraiah et al., 2018)

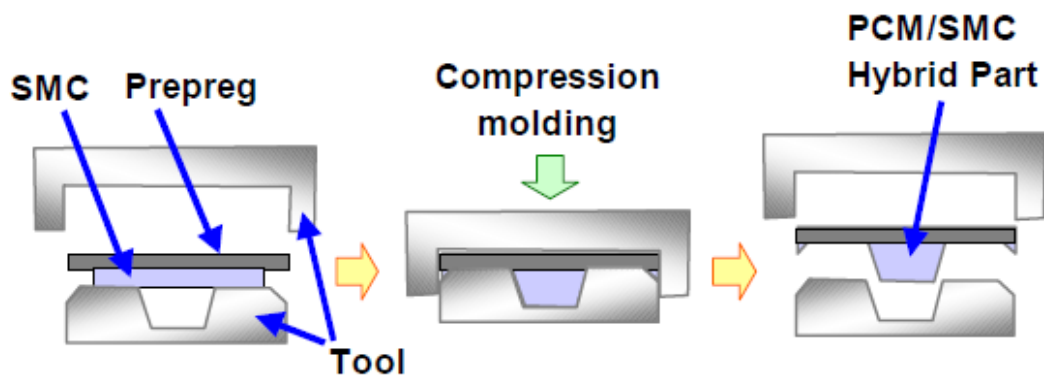
Therefore, hybrid composites are a way to synergistically utilise the strengths of SMC and UD. The strength and stiffness of the specimen can be tailored by changing the amount of location of the UD. Wulfserg et al doubled flexural, tensile moduli and tensile strength through hybridization (Wulfserg et al., 2014). Hybrid composites are notch insensitive for low volume fractions of UD (Visweswaraiah and others, 2017). Additionally, they provide higher repeatability when compared to SMCs (Akiyama, 2011). Figure 11 displays the processing and performance of different composite architectures and hybrid composites lie in the middle.



**Figure 11: Processing vs performance of different composite architectures**

(Selezneva and Lessard, 2016)

Hybrid composites offer a unique opportunity to reduce the cost of high performance structural composites (Hitchen and Kemp, 1996). They can be manufactured using same compression moulding technique as SMC with high production rates. An example of a single shot hybrid compression moulding can be seen in Figure 12.



**Figure 12: Net Shape Hybrid Compression Moulding**

Hybrid composites have gained a lot of interest in the past few years for automotive applications as they can reduce weight of metallic parts without significantly increasing the cost. One of the earliest adoptions of hybrid composites in automobiles is the Mitsubishi Rayon hybrid structural floor

displayed in Figure 13. It uses the UD to add strength and stiffness in straight paths and uses SMC to form the complex shapes.



**Figure 13: Mitsubishi Rayon Hybrid Structural Floor** (Corbridge, 2018)

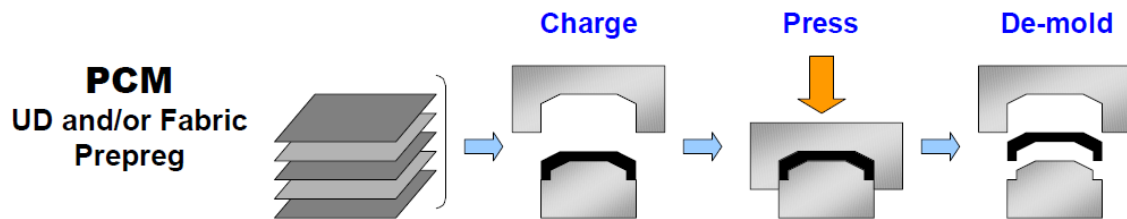
Table 4 summarises the ways in which hybrid composites adopt advantages of SMC and UD composites.

**Table 4: Summary of advantages of UD, SMC, and Hybrid Composites**

UD	SMC	Hybrid
High specific strength	Mouldability	Mouldability
High specific stiffness	Medium specific stiffness	Tailorable specific strength and stiffness
Repeatability	Low cost	Medium cost
Directional properties	High production rate	High production rate
	Notch insensitivity	Tailorable notch sensitivity
	Sustainable	Sustainable
	Planar isotropic	Repeatability
	Progressive failure	Progressive failure

### 3.3 Prepreg Compression Moulding

UD prepregs are cut and stacked in near net shape and moulded using heat and pressure as shown in Figure 14. Prepreg manufacturing is expensive, so they are generally made from carbon fibre and fast curing epoxy. The recommended compression pressure is 5-35 bars.



**Figure 14: Prepreg Compression Moulding** (Akiyama, 2011)

Prepreg compression moulding has a low cycle time, can be automated, and produces net shape parts. However, it doesn't extract voids like an autoclave. The prepregs need to be symmetric to prevent warping.

### 3.4 SMC Compression Moulding

#### 3.4.1 SMC Manufacturing and Properties

SMC is manufactured by chopping carbon fibre and randomly dropping them on a layer of resin as showed in Figure 15. The manufacturing process is supposed to result in homogenous properties, but because of machine design, there is often an orientation bias in the SMC sheet.

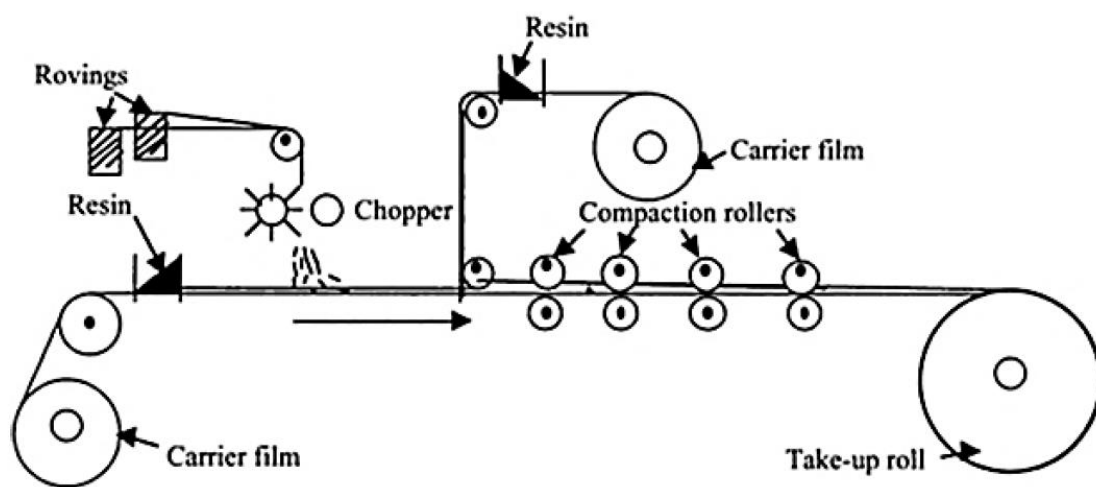


Figure 15: SMC Manufacturing Process (Mazumdar, 2001)

SMCs are notch insensitive, as the stress concentrations at the edge of fibre bundles are greater than holes. Table 5 shows the stress concentration factors in a specimen with a Diameter to Width Ratio of 0.375. It can be observed that SMCs distribute stress around a hole better than isotropic materials but has higher stress concentration at bundle ends.

**Table 5: Stress Concentration Factors Around Holes in Different Materials  $D/W$  0.375** (Bond et al., 2019)

Material	Location	Stress Concentration Factor
Metals/Isotropic	Hole	2.26
SMC	Hole	1.4
SMC	Bundle End	3.95

Figure 16 shows the width ( $W$ ), diameter of the hole ( $D$ ) and the edge distance ( $E$ ) of a specimen.



**Figure 16: Diameter, Width and Edge Distance of a specimen**

As the stress concentration factors depend on the dimensions of the specimen, Table 6 shows the stress concentration factors at hole of metals and composites in an infinite width scenario. It can be observed that UD [0] has high stress concentrations and UD [45] has the lowest stress concentration in continuous fibre laminates.

**Table 6: Stress concentrations factors in infinite width materials** (Woodhead Publishing, 2012)

<b>Material</b>	<b>Location</b>	<b>Stress Concentration Factor</b>
<b>Metals</b>	Hole	3
<b>UD [0]</b>	Hole	6.6
<b>UD (45)</b>	Hole	2
<b>Quasi Isotropic [0/± 45/90]</b>	Hole	3
<b>Cross- Ply [0/90]</b>	Hole	3.5
<b>[0/45/0]</b>	Hole	4.1
<b>45/0/45</b>	Hole	3

### 3.4.2 Fibres

As SMCs are relatively inexpensive, they are made with both glass fibre and carbon fibre. Glass fibre is inexpensive, strong, chemically resistant and has low galvanic potential. Carbon fibre is relatively stiff and strong but is also expensive and has high galvanic potential.

### 3.4.3 Resin

SMCs are manufactured with different fast curing resins for different applications. Some properties of the available resins are presented in Table 7.



**Table 7: Properties of Different Resins** (Bücheler, Griesbaum and Henning, 2018)

<b>Resin</b>	<b>Tensile Strength in MPa</b>	<b>Young's Modulus in GPa</b>	<b>Elongation at break in %</b>
<b>Epoxy</b>	115	2.8	6
<b>Vinyl Ester (VE)<sup>4</sup></b>	35	3.5	1.25

Epoxy is expensive and it binds well with carbon and glass fibre. It also has a high elongation at break.

VE is cheaper than epoxy. It has relatively lower strength and elongation at break. It bonds well with glass fibre but doesn't bond well with carbon fibre. Carbon fibre VE SMC has poor strength because of poor bonding but still has high stiffness. VE releases styrene during curing which is not very sustainable. Versions of VE that don't release styrene have been developed and are undergoing proliferation.

Resin in SMC needs thickening to avoid fibre matrix separation at high pressures during moulding. In epoxies, this is achieved using B-staging and in VE, thickening agents are added.

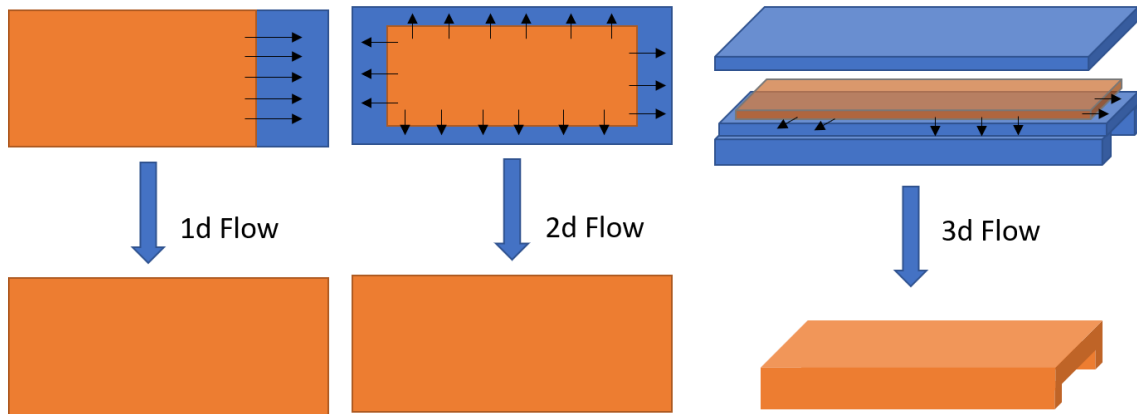
#### **3.4.4 Charge Placement and Flow**

Charge refers to the material placed in the mould before pressing. SMC is usually shipped in a roll of 1 mm sheet. Multiple sections of the sheet are cut and stacked together to make a charge for a product. Charge shape, area, location, and stacking can have an impact on the final product.

Charge area is the percent of the total cross-section area of the mould covered by the charge. A higher charge area results in low flow of material and vice versa. Different values of charge coverage ranging from 60%-95% are recommended by manufacturers. Charge flow can take place in either one, two or three dimensions as shown in Figure 17.

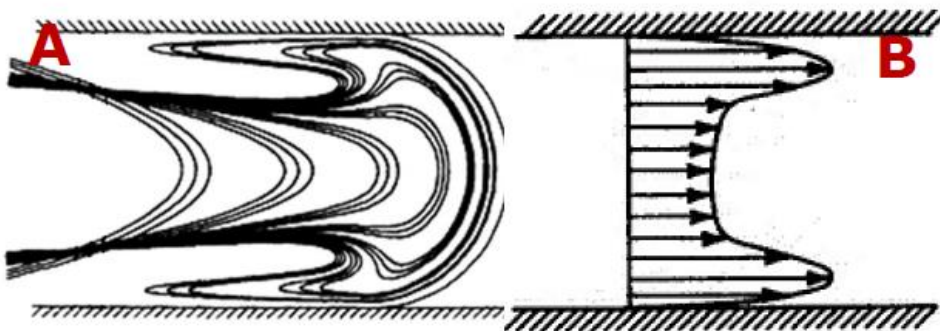
---

<sup>4</sup> From datasheet in Appendix B



**Figure 17: 1d Flow, 2d Flow and 3d Flow Scenarios**

SMC flow inside a mould is often not uniform. Figure 18 shows the two non-uniform flows observed during compression moulding. Fountain flow is usually observed in thermoplastics as the polymer cools and becomes more viscous around the edges, whereas preferential flow is observed in thermosets where the heat from the edge of the tool reduces viscosity and promotes flow. Because of preferential flow, the fibre volume fractions are often higher near the edges of a tool. This can lead to high stiffness on the edges and lead to a fracture prone core (Corbridge, 2018)(Orgéas and Dumont, 2011).



**Figure 18: Flow Mechanisms: (A) Fountain flow usually observed in thermoplastic moulding;**(Papathanasiou and Guell, 1997) **(B) Preferential flow usually observed in thermoset compression moulding** (Lee and Tucker, 1987)

Apart from charge coverage and charge placement, variables such as charge viscosity, fibre volume fraction, mould shape, mould surface roughness, mould

temperature, mould closing speed, and dwell time of charge on the mould affect the flow and quality of the SMC.

### 3.4.5 Charge stacking sequence

Charge stacking sequence refers to the attribute of SMC sheets stacked in the Z-direction. Best practice guidelines suggest that small pieces of charges should be avoided when possible. Additionally, a pyramid charge structure as shown in Figure 19 should be used to avoid trapping voids.

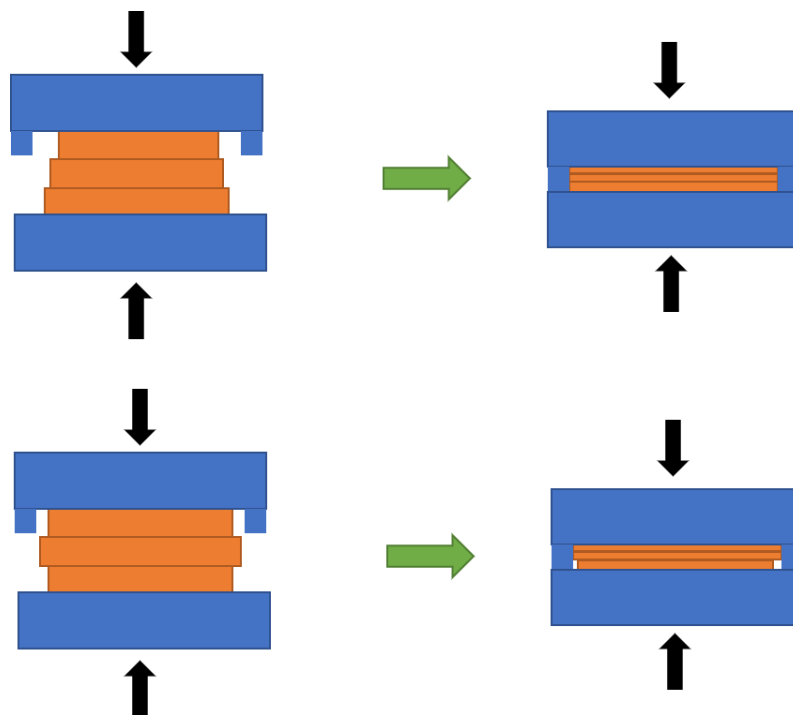


Figure 19: Pyramid Stacking Sequence to avoid voids and out of plane fibre distortion (REVELLINO, SAGGESE and GAIERO, 2000)

### 3.4.6 Advantages of High Flow Moulding

There are two design philosophies of SMC manufacturing: high/medium flow and low flow moulding.

#### 3.4.6.1 Orientation of Fibres – Mechanical Properties

High amount of flow leads to preferential orientation of fibres. This can be an advantageous if desired. Extremely high flow can also lead to tangling and

orientation of fibres in the z-direction, increasing loss and variability of mechanical properties.

#### **3.4.6.2 Voids**

SMC charge sheets have voids. High flow in combination with high pressures leads to low void content which increases predictability. This is because the flowing material allows the air pockets to escape.

#### **3.4.6.3 Manufacturing Complexity**

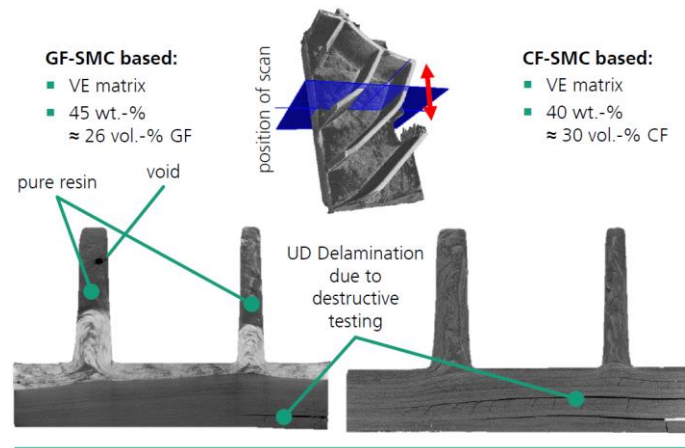
High Flow design requires charge to be placed on a smaller (and often imprecise) section of the mould. Therefore, it reduces the complexity during the moulding process.

#### **3.4.6.4 Flow in Ribs**

One of the techniques used to enhance the stiffness of polymer parts is to add ribs. Adding ribs is often not possible in a low flow design without manually placing the charge in the cavity.

However, the flow and orientation of fibres in the z directions leads to a variety of issues such as:

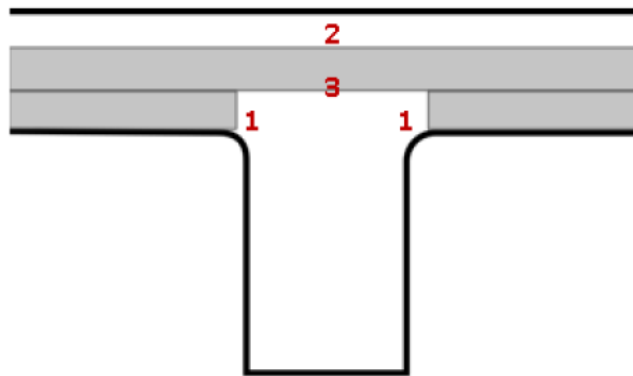
- Voids and resin rich regions which leads to higher shrinkage which leads to sink marks as seen in Figure 20
- Fibre matrix separation (Jeong, Kim and Im, 1996)
- Fibre bridging/entanglement



**Figure 20: Defects in SMC ribs**

A few strategies that have been successfully used to counter these issues:

- Increasing surface roughness at rib corners to encourage earlier rib filling (Kia, 1993)
- Increase rib thickness to prevent fibre bridging. However may lead to difference in local cure times, residual stress and consequently sink marks (Fan et al., 1989)
- Material break charge design as shown in Figure 21.



**Figure 21: Material Break Charge Design** (Corbridge, 2018)

### 3.4.6.5 Independence from manufacturing alignment bias

High flow can reduce the impact of the alignment bias in SMC charge sheets formed during SMC manufacturing.

### 3.4.7 Disadvantages of high flow

#### 3.4.7.1 Fibre Matrix Separation

High flow increases the likelihood of fibre matrix separation as the fibres and resin face higher shear loads during moulding.

#### 3.4.7.2 Weld Line

When two edges of flow meet, they can form weld lines as shown in Figure 22 which can significantly reduce mechanical properties. Weld lines should be avoided near joints.

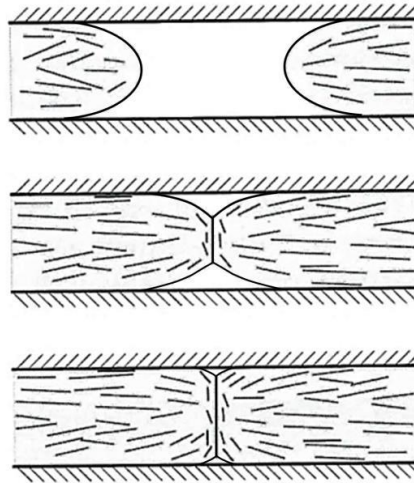


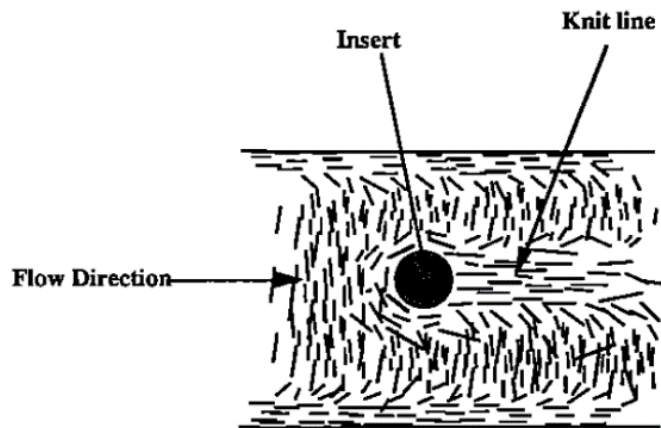
Figure 22: SMC flow creating a weld line (Sentis et al., 2017)

#### 3.4.7.3 Fibre waviness and alignment

Higher flow leads to fibre waviness which reduces the planar properties of the composite. Additionally, variable fibre alignment reduces the predictability of the part and reduces the isotropicity of the material.

#### 3.4.7.4 Flow around inserts

Flow around holes and inserts can form knit lines as shown in Figure 23. They can significantly reduce strength. One way to tackle knit lines is to place the charge on top of the insert avoiding flow over around the hole.



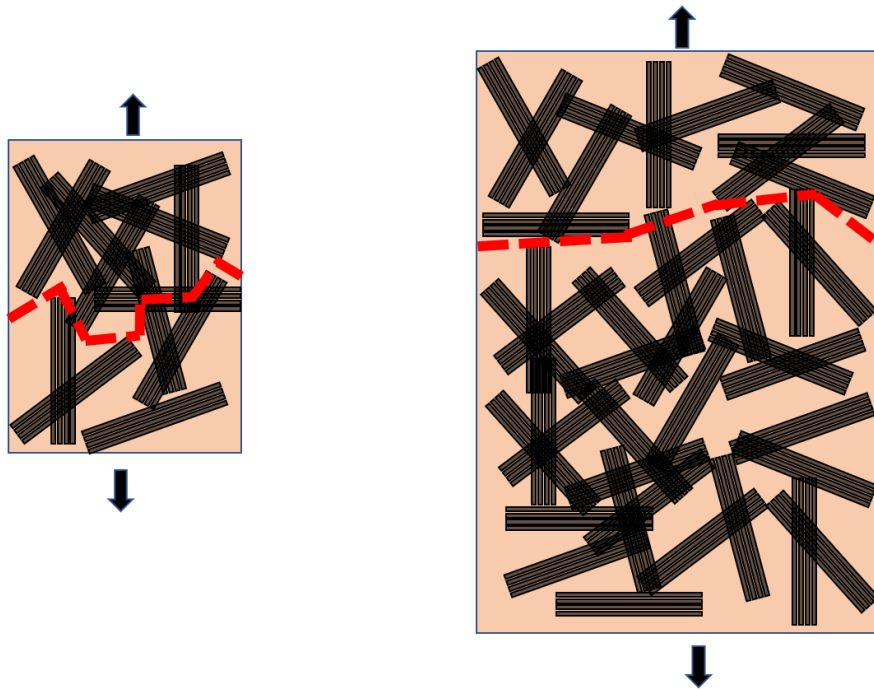
**Figure 23: Knit line formed past an insert** (Sasdelli, Karbhari and Gillespie, 1993)

### **3.4.8 Compression Pressure**

The compression pressure recommended by the manufacturer is 80-120 bars. In low flow moulding, a higher pressure leads to low voids. In high flow moulding, a higher pressure doesn't have any conclusive impact on the void content.

### **3.4.9 Scalability**

Modulus of a material is a volume averaged property and is not impacted by the size of the part. Strength on the other hand is limited by the critical load path. In a SMC part, fibre bundles oriented transversely to the load direction and ends of fibre bundles are regions of high stress concentrations as shown in Table 5. Large changes in local modulus make these locations ideal for crack initiation. Cracks propagate on the boundaries of bundle ends. Figure 24 shows that the likelihood of proximity stress concentrations increases with the size of the part. Therefore scalability of strength from small to large parts is unlikely. (Bond et al., 2019)



**Figure 24: Increased likelihood of proximity of fibre bundle ends and transverse fibres in larger parts**

### 3.4.10 Shrinkage

Thermoset polymers shrink when cured. The shrinkage is higher for polyester and vinyl ester resins. Fibres reduce the shrinkage, so resin rich regions often experience larger shrinkage leading to voids and sink marks. Shrinkage also increases transversely with fibre alignment. Shrinkage of resin also leads to residual stresses which can lead to warping. Additives that expand are often added to minimize shrinkage, however this can have a negative impact on the material strength.

### 3.4.11 Internal Mould Release

Internal mould release is added to the SMC resin to allow for easier removal from the mould tool. During curing, the mould release diffuses through the SMC charge and collates towards the metal mould. Mould release makes it harder for metal inserts to stick to the resin. The impact of the internal mould release on co-curing of multiple composites is not known yet.



### **3.4.12 Temperature**

Temperature during moulding has a significant impact on the final product as thermoset resins get less viscous with temperature until gelation. A higher temperature leads to a more uniform flow and preheating SMC epoxy charge to 60-65 degrees has shown promising results. On the other hands, a higher temperature increases the risk of fibre matrix separation and squish effect.

### **3.4.13 Dwell Time**

Dwell time refers to the duration that the SMC is left on the moulding tool to heat without force. It minimises preferential flow as large parts of the SMC preheat to the same temperature. On the other hand, it reduces viscosity which may lead to fibre-matrix separation. It increases the risk of premature gelation. As SMC is heated only on the bottom surface during dwell time, it may lead to unequal flow in the z direction. This issue is more critical for thick parts (Olsson, Lundström and Olofsson, 2009). Dwell time can be reduced by using fast mould closure speed or simplifying charge placement.

### **3.4.14 Mould Closing Speed**

A faster mould closing speed results in a more uniform fibre distribution in SMC parts (Olsson, Lundström and Olofsson, 2009). It also reduces the fibre matrix separation when moulding ribs. This is likely because faster moulding speed reduces the impact of non-uniform heating of the charge in the mould.

### **3.4.15 Compression under vacuum**

Applying vacuum during compression moulding leads to lower void content and pressure build-up in tool from confined air (Olsson, Lundström and Olofsson, 2009). It also leads to uniform flow at low closing speeds. On the other hand, it adds manufacturing cost. It is also not suitable at high temperatures when using polyester or vinyl ester because of styrene boiling.

### 3.5 Hybrid Compression Moulding

Hybrid compression moulding is very similar to SMC moulding with a few additional considerations.

#### 3.5.1 UD Flow

One of the key issues with moulding UD and SMC together is that UD can flow and result in fibre waviness, wrinkling, buckling and fibre distortion as seen in Figure 25 (Dhakal et al., 2013). UD flow is very low in the longitudinal direction and higher in the transverse direction. UD does suffer from resin bleed in the longitudinal direction.

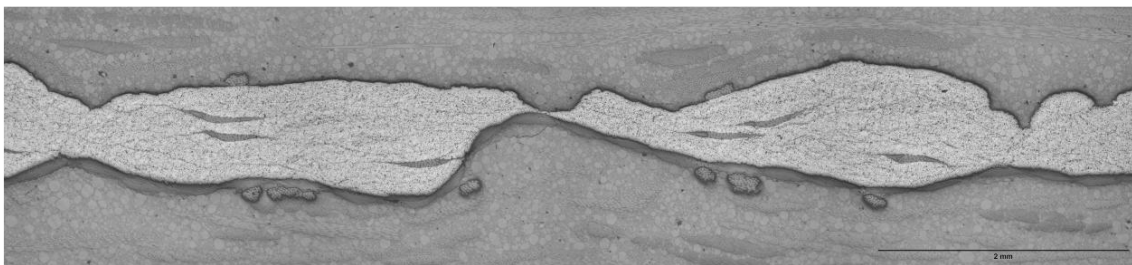


Figure 25: UD waviness inside hybrid

One way to alleviate UD flow is partial curing/staging of UD. It involves partially curing the UD before adding the SMC as shown in Figure 26.

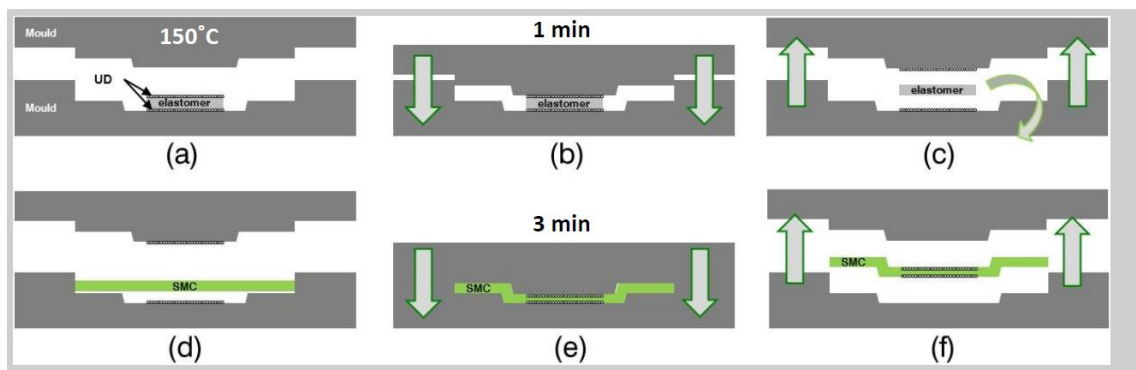


Figure 26: Two stage hybrid compression moulding

Due to fast curing times, partial curing needs to be precise. Low partial curing results in UD flow. High partial curing results in loss of tackiness and adhesion between SMC and UD. Potential downsides of partial curing are dry regions on SMC under the UD and SMC ripples near the UD-SMC interface. Corbridge

looked at different amounts of curing/staging from 25-75% and found 50% to be ideal.

Resin bleed at UD-SMC interface has been observed in hybrid composites. This leads to slight increase in the fibre volume fraction of the UD and may lead to dry spots. Additionally, as the resin bleed is not uniform, it may lead to variability in local modulus.

Debulking UD plies can improve adhesion of pre cured UD plies and SMC and leads to a lower void content. However, debulking is not practical for high volume manufacturing.

### **3.5.2 Adhesion of UD and SMC**

The adhesion at the interface of the UD and the SMC is a critical part of the composite. Same resin for the UD and SMC should be used when possible. It is critical for the resins to have similar curing times and temperatures.

However, a lot of SMCs in the market use Vinyl Ester and prepregs use epoxy. Co-curing of lightly cross-linked epoxy and vinyl ester results in good interfacial shear strength. Lightly cured epoxy has been used to improve adhesion of vinyl ester to carbon fibre (Xu and Drzal, 2001). Additionally, Polyester based gel coats have been known to adhere well to epoxy in the marine industry.

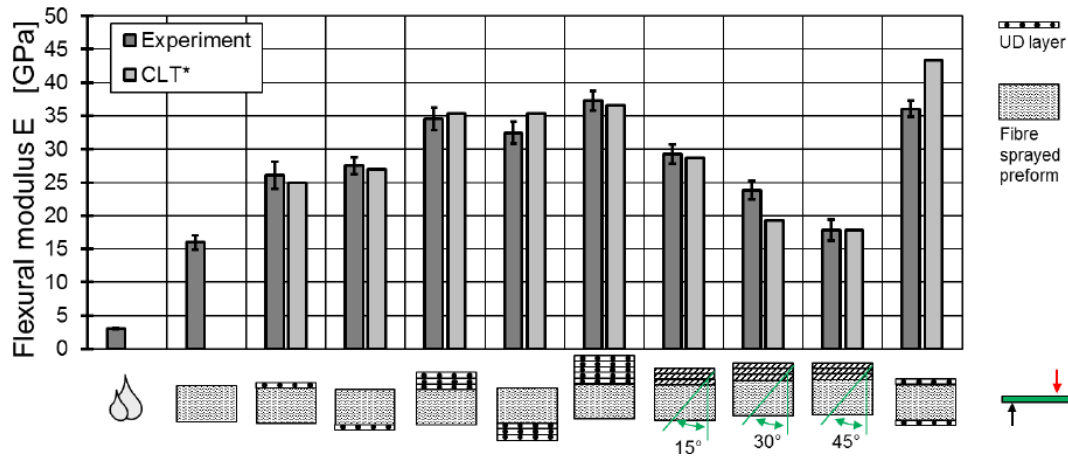
### **3.5.3 Difference in Compression Pressure**

Prepreg UD compression pressure is 5-35 bar whereas SMC compression pressure 80-120 bar. Higher pressure on prepreg can lead to resin bleed and fibre rich edges of UD. It may also cause fibre fracture and distortion. As higher pressure is necessary in SMC to reduce void content, hybrids are moulded at higher pressures.

### **3.5.4 Stacking of UD and SMC**

UDs and SMCs can be stacked in many ways. Figure 27 shows the different orientations that have been tested. UD-SMC-UD sandwich orientation has

resulted in good results in stiffness, strength, and flexural modulus. It is also easier to mould as the UDs can be placed on mould surfaces.

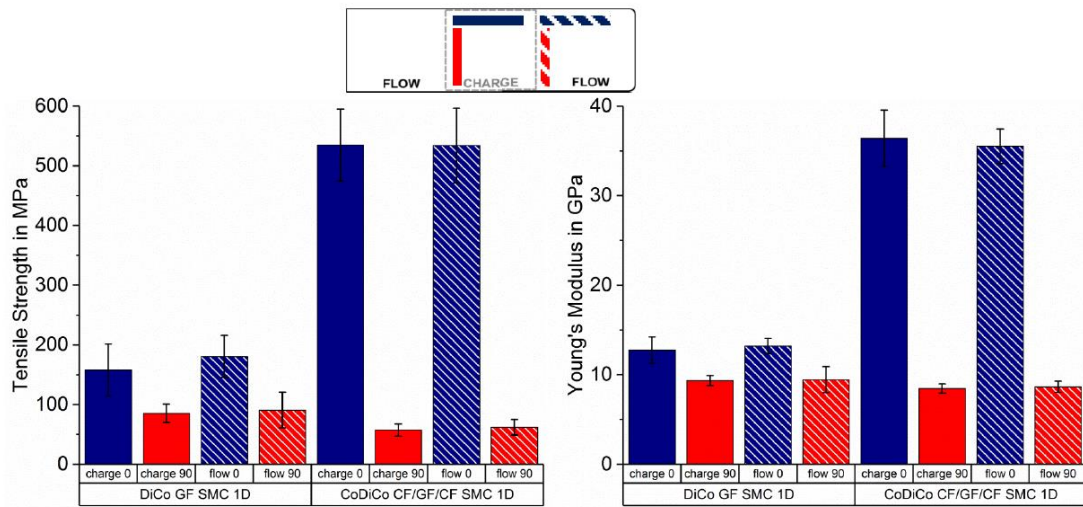


**Figure 27: Flexural modulus of different UD-SMC orientations** (Hopmann et al., 2017)

### 3.5.5 Charge Placement

If multiple layers of UD are used, they should be tapered to prevent stress concentrations. Interface angle should be less than 7 degrees to reduce the peel stress. (Evans et al., 2017)

A low flow moulding is preferred in hybrid composites as it reduces the risk of UD flow and increases part predictability. Figure 28 shows that there is a significant difference in the mechanical properties of SMC composites in the charge region and the flow region. However, in hybrid composites, the difference is negligible.



**Figure 28: Difference in mechanical properties of SMC and hybrid composite sections in charge region and flow region**

### 3.5.6 Predictability and Testing

Predictability of hybrid composites is higher than that of SMCs but lower than continuous fibre composites. Most hybrid strength prediction techniques are destructive and use a fibre angle-based approach. Vibration based models are being developed to predict fibre orientations but there has been no success in predicting failure location or load using them.

## 3.6 Mechanical Properties of Hybrid Composites

### 3.6.1 Modulus

The modulus of the hybrid composite can be predicted using Rule of Hybrid Mixtures (RoHM) as shown in Equation 3-1. It assumes that constant strain can be applied to both materials without any interaction.

#### Equation 3-1: Rule of Hybrid Mixtures

$$E = E_{UD}V_{UD} + E_{SMC}V_{SMC}$$

Where:

$E_{UD}$  is the modulus of the UD

$V_{UD}$  is the volumetric ratio of the UD in the hybrid composite

$E_{SMC}$  is the modulus of the SMC

$V_{SMC}$  is the volumetric ratio of the SMC in the hybrid composite

RoHM generally leads to slight overestimation of modulus (Venkateshwaran, Elayaperumal and Sathiya, 2012) (MIR et al., 2007). The potential reasons for variation in modulus are the orientation of fibres in UD and SMC. The impact of orientation of fibres in SMC is described in Equation 3-2.

#### Equation 3-2 Modulus of Random Fibre Composites

$$E_{SMC} = \eta_0 E_f V_f + E_m V_m$$

Where:

$\eta_0$  is the Krenchel efficiency factor

$E_f$ ,  $E_m$  are the modulus of the fibre and matrix respectively

$V_f$ ,  $V_m$  are the volume fraction of the fibre and matrix respectively

$\eta_0$  is assumed to be 0.375 when fibres are randomly oriented in a 2d plane. However, if the fibres flow in the z direction, the efficiency factor reduces.  $\eta_0$  is 0.2 for the randomly oriented fibres in a 3d plane (Matthews and Rawlings, 1999).

Misalignment of the UD due to placement or flow can cause significant reduction in stiffness and strength as well. The impact of the UD angle on UD strength can be predicted using the classical laminate model.

### 3.6.2 Strength

While RoHM works well for predicting the modulus, it isn't equally accurate at predicting the strength of hybrid composites. This is because specimen strength is highly dependent on the UD-SMC interaction and interface properties. Any region of imperfection or location of multiple fibre bundle edges can lead to stress build-up which cannot be predicted using the RoHM equation. However, it is the most accessible way to predict the strength and has been found to be accurate in cases such as Figure 29.

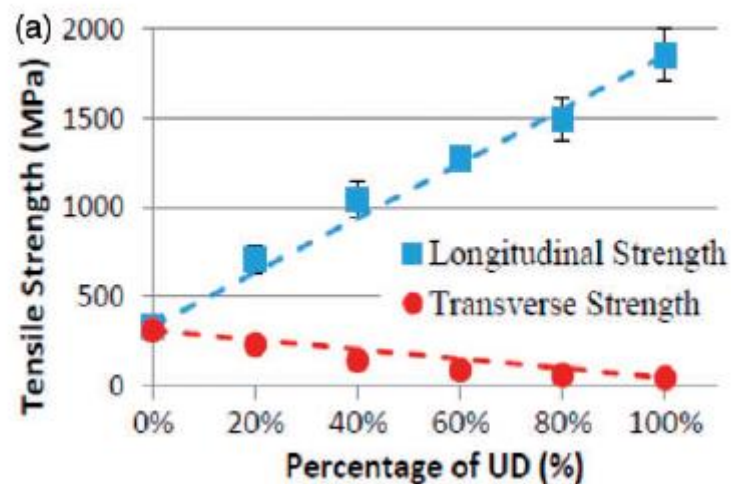


Figure 29: Difference in longitudinal and Transverse strength as a function of UD

(Evans et al., 2017)

## 3.7 Composite Joining Methods

Composites can be joined with metals in three key ways: (Jahn et al., 2016)

1. Adhesive Bonding
2. Mechanical Interlocking – using bolts, rivets or clinching
3. Adhesive bonding and Mechanical Interlocking

Table 8 summarises the advantages and disadvantages of the three methods. A combination of adhesive bonding and mechanical interlocking seems to be ideal for high loads.



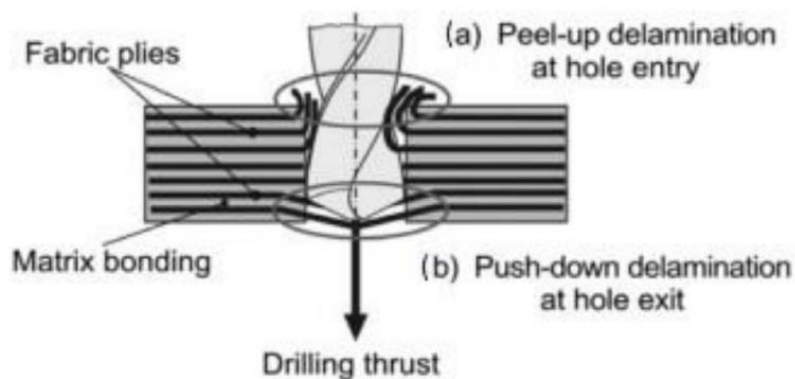
**Table 8: Advantages and Disadvantages of different composite joining methods**

<b>Joining Method</b>	<b>Advantages</b>	<b>Disadvantages</b>
<b>Adhesive bonding</b>	<ul style="list-style-type: none"> <li>• Uniform (fibre friendly) load introduction (Jahn et al., 2016)</li> <li>• No galvanic corrosion for dissimilar materials</li> <li>• Cost effective</li> <li>• Lightweight</li> </ul>	<ul style="list-style-type: none"> <li>• High material thickness can require high overlapping length</li> <li>• Durability and material degradation over time</li> <li>• Surface treatments</li> <li>• Long curing times</li> <li>• Humidity and Temperature constraints</li> <li>• Difficulty of Inspection</li> <li>• No Disassembly</li> </ul>
<b>Mechanical interlocking</b>	<ul style="list-style-type: none"> <li>• Higher load transfer(Jahn et al., 2016)</li> <li>• Reliable-measurable-high TRL</li> <li>• Easier maintenance/recycling</li> <li>• Easy Assembly</li> <li>• Relatively inexpensive</li> <li>• Easy Inspection</li> <li>• Ease of Regulatory Approval</li> </ul>	<ul style="list-style-type: none"> <li>• Weakness from Drilling – fibre damage, load transmission break,</li> <li>• Weakness from hole – load transmission break</li> <li>• Fibre Damage, yielding of matrix, loss of bolt clamp load impacts strength and fatigue (Caccese et al., 2009)</li> <li>• Relatively heavy</li> </ul>

		<ul style="list-style-type: none"> <li>• Risk of galvanic Corrosion</li> <li>• Stress Concentration at hole</li> <li>• Fibre Discontinuity</li> </ul>
<b>Adhesive bonding and Mechanical interlocking</b>	<ul style="list-style-type: none"> <li>• Better load distribution due to increased contact area (Kunc, Erdman and Klett, 2004)</li> <li>• Decreased stress concentration (Kunc, Erdman and Klett, 2004)</li> <li>• Higher joint rigidity (Kunc, Erdman and Klett, 2004)</li> <li>• Corrosion resistance</li> <li>• Water tightness</li> <li>• Easy Inspection</li> </ul>	<p>Expensive</p> <p>Time consuming</p> <p>Weakness from Hole</p> <p>Weakness from Drilling</p> <p>Limited Knowledge</p> <p>No disassembly</p>

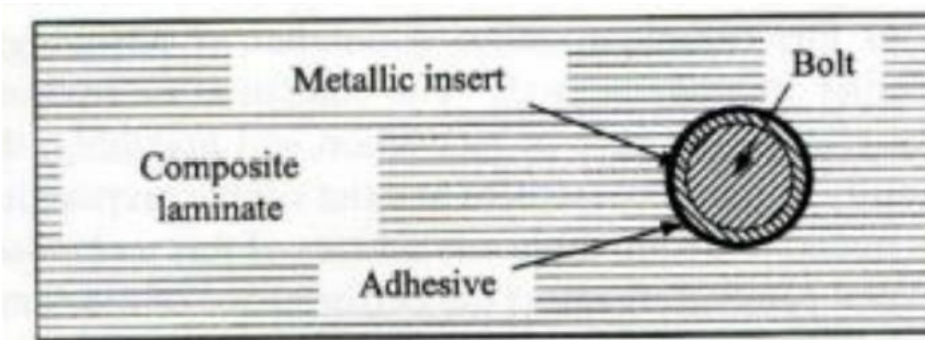
### 3.8 Inserts

As rivets and clinching have high potential for fibre damage and residual stresses, bolts are a better option. Bolts can be attached to composites using co-moulded inserts resulting in adhesive bonding and mechanical interlocking. The key benefit of a co-moulded insert is avoiding the drilling damage as shown in Figure 30.



**Figure 30 : Damage due to drilling** (Faraz, Biermann and Weinert, 2009)

Figure 31 shows co-moulded inserts that reduce stress concentrations and introduce relatively fibre friendly loads. They also shield the hole from repeated attachment of fasteners. A joint strength increase of up to 24% has been observed between samples with and without cylindrical inserts. (Camanho and Matthews, 2000)


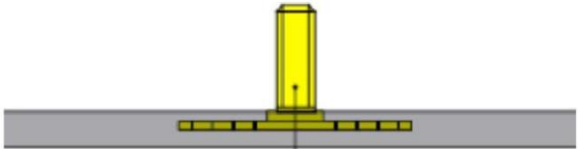


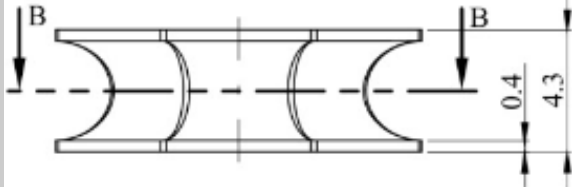
**Figure 31: Bonded insert for bolt in composite laminate** (Camanho and Matthews, 2000)

### 3.8.1 Location

Inserts can be located on the top, in the middle and through composites. Table 9 summarises the advantages and disadvantages of different insert locations. As the primary loading on the suspension arm is in-plane, through inserts are considered.

**Table 9: Locations of Inserts inside Composites**

Location	Advantages	Disadvantages	Application
 <p>Figure 32: Top Insert (BigHead, 2017)</p>	<ul style="list-style-type: none"> <li>• Can be added during or post moulding</li> <li>• No holes</li> <li>• Easy inspection</li> <li>• High bonding area</li> </ul>	<ul style="list-style-type: none"> <li>• Low Load transfer</li> <li>• Susceptible to peeling and over torquing</li> <li>• Poor pull out strength</li> </ul>	<ul style="list-style-type: none"> <li>• Joining of non-structural composite parts</li> </ul>
 <p>Figure 33: Middle/Embedded Insert</p>	<ul style="list-style-type: none"> <li>• Good pull out and bending strength</li> <li>• Good twisting strength</li> </ul>	<ul style="list-style-type: none"> <li>• Poor bearing strength.</li> <li>• Increased likelihood of delamination at</li> </ul>	<ul style="list-style-type: none"> <li>• Joining to structural and non-structural parts in medium load</li> </ul>

<p>(Gebhardt and Fleischer, 2014)</p>		<p>insert base</p> <ul style="list-style-type: none"> <li>• Hard to inspect</li> </ul>	<p>applications.</p> <ul style="list-style-type: none"> <li>• Parts where through access is not possible.</li> </ul>
 <p>Figure 34: Through Insert (Troschitz, Kupfer and Gude, 2019)</p>	<ul style="list-style-type: none"> <li>• Good in plane bearing strength</li> <li>• Good pull-out strength with the use of washers</li> <li>• High load transfer</li> </ul>	<ul style="list-style-type: none"> <li>• Component needs to have through access.</li> <li>• Relatively heavy</li> </ul>	<ul style="list-style-type: none"> <li>• High load transfer applications with in-plane loads.</li> </ul>

### 3.8.2 Modes of Failure

Composites with inserts can fail because of failure of the composite, failure of the insert or a combined failure of both. Figure 35 shows the critical macro failure modes due to in-plane loading. The subcritical micro damage modes in composites include matrix cracking, delamination, fibre/matrix shearing (Ataş and Soutis, 2013). While the failure modes of metals and composites are similar for in plane bearing load, metals tend to outperform composites because their ductility eases the stress concentrations (Duthinh and others, 2000).

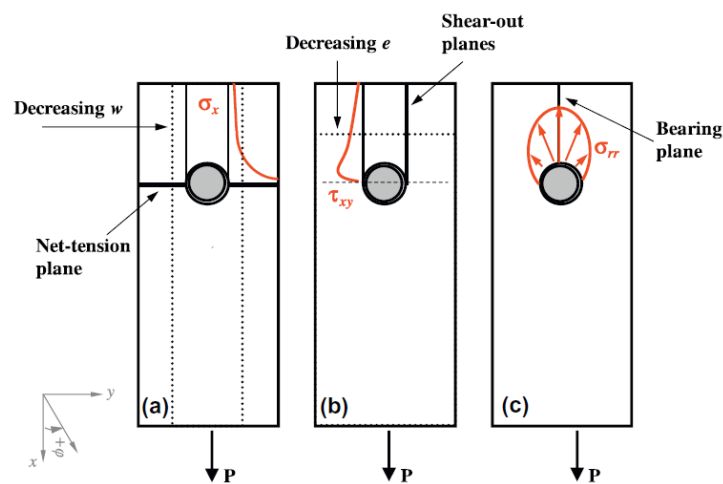


Figure 35: Modes of Failure in Composite plates (Ataş and Soutis, 2013)

#### 3.8.2.1 Net Tension Failure

Lower width increases the chances of a net tension failure as the area that can carry the load is significantly reduced by the hole. The net tension strength of a composite is expressed by Equation 3-3.

#### Equation 3-3: Net-Tensile Strength of a Specimen

$$\sigma_{net\ tension} = (W - D) * \sigma_{tensile}$$

Where:

W is the width of the specimen

D is the diameter of the hole

$\sigma_{tensile}$  is the tensile strength of the material

However, in the case of pin bearing, there is also shear stress on the material. For SMC composites, this shear stress further reduces the net tension load capacity by ~15%. (Caprino et al., 2002)

### 3.8.2.2 Shear Out Failure

Shear strength of the composite is dependent on the edge distance of the hole from the edge. The shear stress of a composite can be expressed by Equation 3-4. The specimen will fail in shear out failure when the shear stress exceeds the shear strength of the material.

#### Equation 3-4: Shear Stress on a Specimen

$$\sigma_{shear\ stress} = \frac{P}{2 * e * t}$$

Where:

P is the applied Load

e is the distance of the hole from the edge

t is the thickness of the material

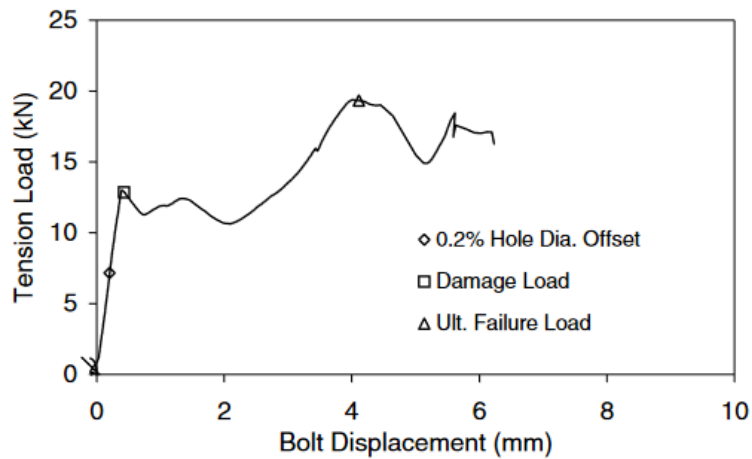
### 3.8.2.3 Bearing Failure

Bearing failure is caused by compressive stress on the material. Bearing stress is proportional to the projected area of the insert as shown in Equation 3-5.

#### Equation 3-5: Bearing Stress on a Material

$$\sigma_{bearing\ stress} = \frac{P}{A_{projected}}$$

Bearing failure is progressive in nature as shown in Figure 36. It results in matrix cracking, fibre buckling and delamination. It is gradual and observable and therefore the ideal failure mode. Bearing strength of materials is proportional to their compressive strength. Compressive strength of SMCs is hard to predict, however empirical data suggests that bearing strength can be up to 1.7 times the tensile strength.



**Figure 36: Typical Bearing failure load curve (Turvey and Wang, 2007)**

### 3.8.2.4 Geometric Design Parameters

To achieve bearing failure, there are different geometric design recommendations for continuous composites and SMCs to avoid net tension and shear out failure as shown in Table 10.

**Table 10: Recommended Part Width/Diameter and Edge Distance/Diameter Ratios for Bearing Failure in Single Pin Joints**

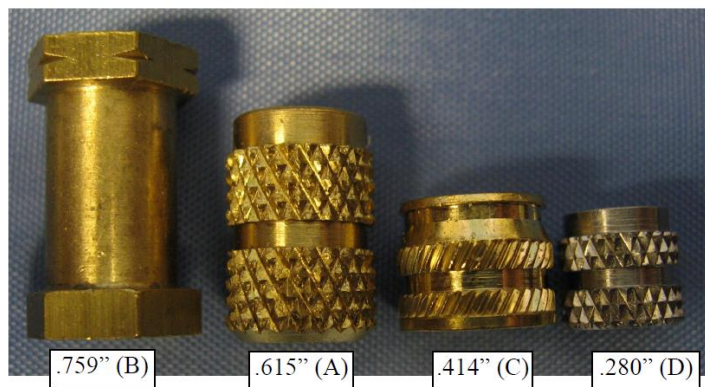
Material	Type	W/D Ratio	E/D Ratio
<b>Metals</b>	-	~2	~1
<b>SMC</b> (Caprino et al., 2002)	-	5	2
<b>UD</b> (ASTM International, 2021)	Quasi-Isotropic	6	3
<b>UD</b> (Collings, 1977)	[0°/90°]	>4	>5
<b>UD</b> (Collings, 1977)	[± 45°]	≥8	>4
<b>UD</b> (Collings, 1977)	[0°/± 45°]	≥4	≥4
<b>UD</b> (Collings, 1977)	[0°/60°]	≥4	≥4



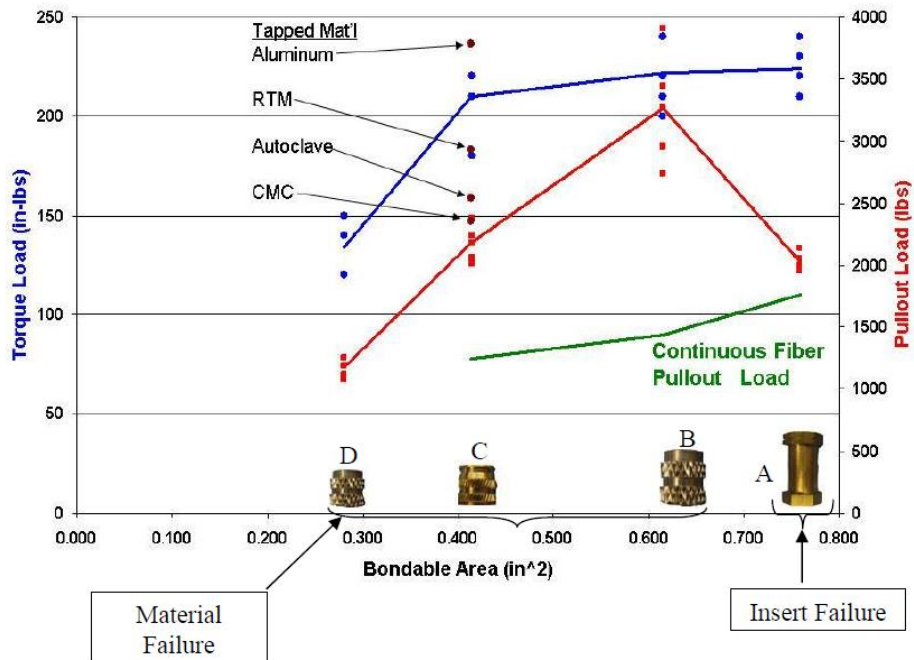
### 3.8.3 Shapes & Texture Inserts

Inserts can have different shapes and textures to improve their performance. While circular shape is the easiest to manufacture, a hexagonal shape can design to provide high torque resistance.

Different types of textures such as threads, knurls, screw arms, etc can be added to the insert surface to improve their adhesion and load transfer. Figure 37 shows a few commercially available texture options and Figure 38 displays their SMC panels and continuous fibre composites.



**Figure 37: Different insert options** (Reller, 2008)



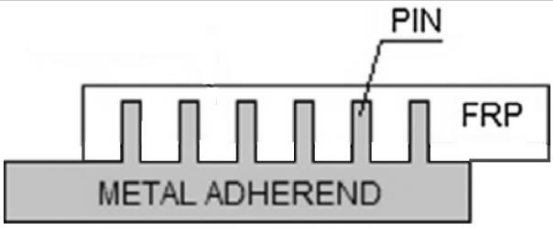
**Figure 38: Load capacity of inserts** (Reller, 2008)

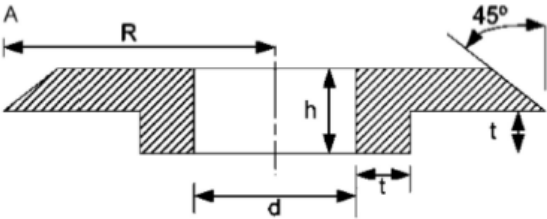
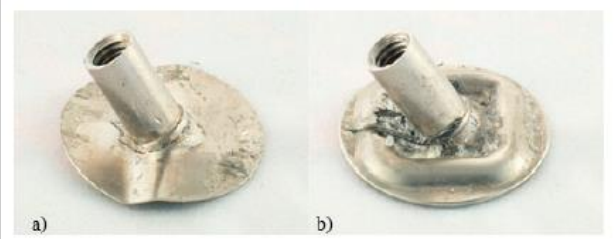
Figure 38 shows that high bondable area and diamond knurls lead to high pullout strength. They also show that textured inserts perform better in discontinuous fibre composites as opposed to continuous laminates.

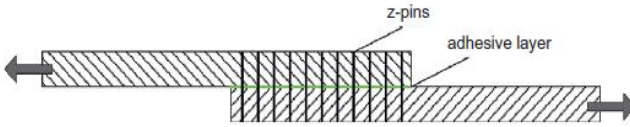
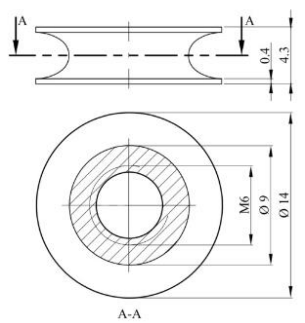
### 3.8.3.1 Additional Reinforcement options

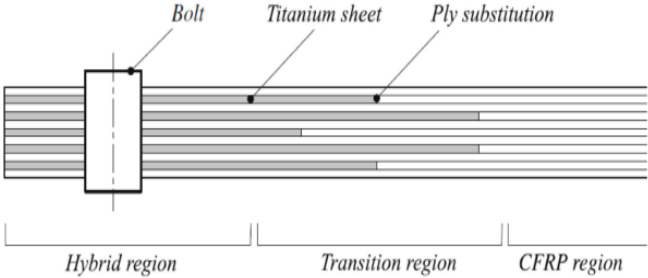
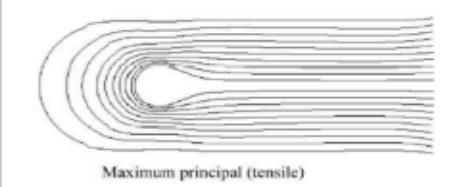
The principles, advantages and disadvantages of additional insert/joint reinforcement options is presented in Table 11.



**Table 11: Reinforcement Options for Composite Joining**

Name	Picture	Principle	Advantages	Disadvantages
<b>Pin Joining</b>	 <p><b>Figure 39 : Pin Joining of metal inserts in composites</b> (Graham et al., 2014)</p>	Can be manufactured using cold metal transfer or additive manufacturing	Increases joint mechanical strength. Leads to progressive failure	Expensive, time consuming

Name	Picture	Principle	Advantages	Disadvantages
<b>Tapered End</b>	 <p data-bbox="416 619 1050 703"><b>Figure 40: Optimised tapered ends for inserts</b> (Camanho et al., 2005)</p>	<p data-bbox="1084 336 1438 539">Provide additional load path and tapering prevents sharp changes in stress.</p>	<p data-bbox="1464 336 1794 539">Increases joint strength by 21%. (Mirabella and Galea, 1997)</p>	<p data-bbox="1821 336 2083 480">Added Mass. Needs to be co-moulded</p>
<b>Bead Pattern</b>	 <p data-bbox="409 1050 1059 1182"><b>Figure 41: Deformation of an insert with and without a bead pattern</b> (Gebhardt and Fleischer, 2014)</p>	<p data-bbox="1084 762 1438 1018">Higher moment of inertial leads to higher stiffness which in result leads to higher bending strength</p>	<p data-bbox="1464 762 1794 1129">It had no impact on tensile/pull out strength and led to a 38% increase in bending strength as opposed to a standard embedded insert</p>	<p data-bbox="1821 762 2083 970">Added mass. Adding manufacturing cost from welding.</p>

Name	Picture	Principle	Advantages	Disadvantages
<b>Z-pins/ Stitching</b>	 <p data-bbox="407 534 1057 619"><b>Figure 42: Z-pins reinforcement in bonded joints</b> (Löbel et al., 2013)</p>	<p data-bbox="1086 338 1435 592">Using rods made of titanium or composites to reinforce joints to increase toughness and ultimate strength.</p>	<p data-bbox="1464 338 1792 703">Act as crack arrestors. Change failure mode from delamination to fibre fracture. Increase strength and stiffness. Increase in bearing strength by 7.4-9.8%.</p>	<p data-bbox="1821 338 2083 756">Z-pins can cause local damage in laminates and lead to fibre rich regions. Complex manufacturing. Low Technology Readiness Level</p>
<b>Undercut</b>	 <p data-bbox="436 1235 1032 1319"><b>Figure 43: Through Insert design with an undercut</b> (Troschitz, Kupfer and Gude, 2019)</p>	<p data-bbox="1086 887 1435 1031">Material inside the undercut acts a barrier during pull-out test.</p>	<p data-bbox="1464 887 1792 1031">Increases the pull-out strength proportionally to the undercut volume.</p>	<p data-bbox="1821 887 2083 1198">Added mass. Non-uniform orientation of fibres can lead to variable pull in and push out strength.</p>

Name	Picture	Principle	Advantages	Disadvantages
<b>Titanium Foil</b>	 <p data-bbox="409 719 1055 804"><b>Figure 44: Hybrid Titanium sheet reinforcement</b> (Camanho et al., 2009)</p>	<p data-bbox="1086 336 1435 647">Hybrid composite utilising isotropic properties of titanium in thin sheets to reduce stress concentrations around the joint.</p>	<p data-bbox="1467 336 1794 488">Tensile Strength increase up 158%. (Camanho et al., 2009)</p>	<p data-bbox="1825 336 2085 536">Added mass. manufacturing complexity. High material cost</p>
<b>Fibre Steering</b>	 <p data-bbox="434 1094 1032 1174"><b>Figure 45: Fibre Steering around a hole</b> (Li, Kelly and Crosky, 2002)</p>	<p data-bbox="1086 863 1435 1062">Continuous fibres matching load direction around holes with no discontinuity</p>	<p data-bbox="1467 863 1794 1062">Bearing strength increase by up to 36%. (Li, Kelly and Crosky, 2002)</p>	<p data-bbox="1825 863 2085 1118">High Manufacturing Complexity. Added weight of roving bundles</p>

Name	Picture	Principle	Advantages	Disadvantages
<b>Holes</b>	 <p data-bbox="412 616 1055 699"><b>Figure 46: Bighead Insert with holes</b> (BigHead, 2017)</p>	<p data-bbox="1084 336 1438 483">Higher Interlocking with fibres and resin going through the holes.</p> <p data-bbox="1084 528 1438 611">Increased in-plane surface area of the insert</p>	<p data-bbox="1464 336 1796 534">Better load transfer. Lower Bearing stress due to high projected area</p>	<p data-bbox="1823 336 2083 483">Fibre bridging may prevent effective interlocking</p>
<b>Quasi Linear Inserts</b>	 <p data-bbox="412 986 1055 1021"><b>Figure 47: Quasi-Linear Insert</b> (Muth et al., 2018)</p>	<p data-bbox="1084 759 1438 906">Spread the load uniformly using three bolts instead of one.</p>	<p data-bbox="1464 759 1796 906">Fibre friendly load introduction and lower stress concentrations.</p>	<p data-bbox="1823 759 2083 957">Added mass, complexity, and manufacturing/assembly cost</p>

### **3.8.4 Adhesion**

One of the primary modes of failure observed in embedded inserts is the separation between the metal insert and the composite. Therefore, the strength of the final component can be increased by increasing the adhesion strength between the metal insert and the composite. The adhesive strength is a function of a variety of factors including the type of adhesive, surface area, surface energy of substrate and adhesive, etc.

#### **3.8.4.1 Adhesive**

The resin of the SMC also acts as the adhesive in hybrid systems. The goal of the adhesive is to not only provide strength but provide fibre friendly load transfer between the metal and fibres.

#### **3.8.4.2 Surface Treatment**

Surface energy of a metal substrate can be increased using surface treatments. Surface treatments also ensure reproducibility of the product and minimise the variability of the mechanical properties. A detailed overview of surface treatments for inserts and their impact is provided in Appendix C.

### **3.8.5 Material**

Material choice of the insert can have a significant impact on load transfer and failure mode. Numerical analysis has suggested that more compliant materials (Brass, Aluminium) and thinner inserts are ideal as stiff inserts may cause premature damage to composite (Camanho and Matthews, 2000). However, this analysis was based on embedded inserts.

Experimental data for through inserts showed marginal increase in joint strength from aluminium to steel insert (Nilsson, 1989). As composites have low thermal expansion, a metal with a low thermal expansion coefficient is desirable.

### **3.8.6 Corrosion**

There is a risk of galvanic corrosion when using carbon fibre and metals. Titanium and stainless steels have low galvanic potential and therefore low risk for galvanic



corrosion. There are multiple options for coatings on aluminium inserts to prevent corrosion, however they add a process and increase cost.

### **3.8.7 Pre-Load**

Pre-load is the initial compressive load applied on a joint. While bolt torque is measured when defining pre-load, the true variable at play is contact pressure. Higher torque and lower washer size increases contact pressure (Khashaba et al., 2006).

A lot of studies using all fibres and practically all matrices have shown benefits of preload. All observed increasing torque increasing bearing strength until a limit load and then the bearing strength plateaued. The increase has ranged anywhere from 14%-100% depending on material, geometry, stacking sequence, etc (Park, 2001)(Choi et al., 2018) (Galińska, 2020).

The bearing strength increases because of the friction between the laminate and the washer. Pre-load also causes a reduction in stress concentration around hole-edge (Choi et al., 2018). Lastly pre-load can also reduce impact of aging on degradation of mechanical properties.

On the other hand, a high pre-load can damage the composite in through thickness direction (Thoppul, Finegan and Gibson, 2009). Lastly, pre-load on composites reduces over time and this results in reduction of bearing strength. Therefore, to get reliable strengths, the creep profile of a material should be thoroughly investigated, or a minimum strength with no pre-load should be used.

### **3.8.8 Viscoelastic effects /Creep**

Polymers exhibit creep and relaxation over time under load. These effects are increased at higher temperatures and moisture (Thoppul, Finegan and Gibson, 2009). As preload increases mechanical properties, through thickness creep can reduce preload over time and reduce the benefits gained by pre-loading. The relaxation is dependent upon materials, fibre orientation, initial pre-load, time, temperature, humidity, etc.

Examples:

- 1.25-4.25% relaxation over 30 hours in CF-Epoxy laminates. Higher pre-load lead to lower relaxation (Thoppul, Gibson and Ibrahim, 2008)
- CF-SMC 50% loss of pre-load in first 100 hours and then gradient significantly reduced. (Finck et al., 2019)

### **3.8.9 Aging**

Aging is like creep; however, it can also occur when the part is not under load. It can be caused by moisture absorption, fibre degradation, matrix hydrolysis, etc (Galińska, 2020).

There are three key drivers of aging, i.e., temperature, humidity, and salt.

Example: In Glass fibre-polyester pultruded samples, single bolt joint strength was reduced by more than 50% when aged at 60 °C for 6.5 weeks and reduced by 60% when immersed in 60 °C water for 6.5 weeks. The effects of temperature were more significant than water. (Turvey and Wang, 2007).

Similar reduction has also been observed in Carbon Fibre/ Epoxy composites, so the effect is not limited to a particular resin or fibre.

Salt water exposure can result in reduction in joint strength up to 90% within 24 hours in GF/Epoxy composites. However, preloaded samples showed no reduction in strength (Ozen and Sayman, 2011).

## **3.9 Knowledge Gap**

SMC joints need to be wider than metal joints to avoid net-tension failure. While, SMC is poor in tensile loading, it is excellent in bearing. On the other hand, UD is poor in bearing and excellent in tension. Therefore, this unique combination allows the opportunity to strategically utilise their best properties in bolted connections and it hasn't been investigated yet. No one has attempted to change the failure mode of a SMC specimens using UD tapes.

Metal inserts allow for dispersion of stress concentration and easy attachment for bushes. Novel insert shape designs provide the opportunity to introduce stress in favorable conditions in hybrid composites.

### **3.10 Goals of a Hybrid Composite**

The goals of a hybrid composite are:

- UD fibres in the right location with right orientation and minimum waviness
- Low void content
- Good adhesion between UD and SMC
- Low residual stresses from shrinkage and thermal cycling
- Low and uniform shrinkage
- Predictable mechanical properties

### **3.11 Goals of an Insert**

An insert should be:

- Able to transfer loads from the bolt to the composite structure
- Lightweight
- Corrosion resistant
- Cost effective
- Able to reduce the stress concentration on the composite

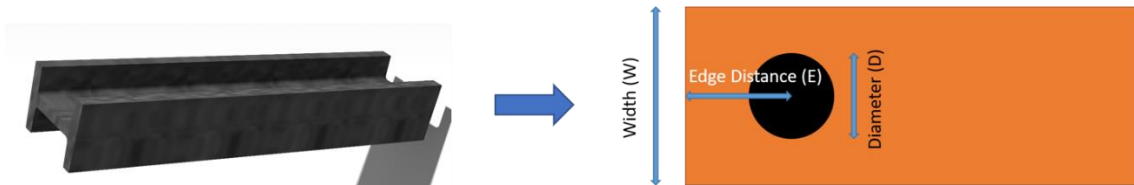


## 4 METHOD

The Method section is documented in the three stages of Design, Manufacturing and Testing.

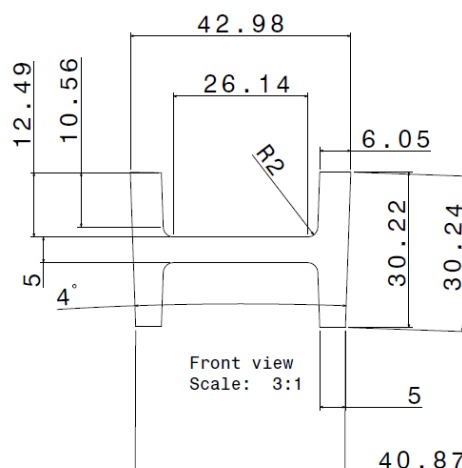
### 4.1 Design

The Design section outlines the steps that lead to the predicted mechanical properties of the specimens. While the I-beam was chosen to replicate the complex moulding of a suspension arm, the flanges were chopped off for mechanical testing as shown in Figure 48.



**Figure 48: I-Beam to Test Specimen**

Figure 49 shows the cross-section of the I-beam being moulded. After chopping off the flanges, the specimen length, width, and thickness were assumed to be 200 mm, 25 mm, and 5 mm respectively.



**Figure 49: Tapered I-Beam Cross-section Drawing**

#### 4.1.1 Material Properties

The material properties of the SMC and UD being moulded are shown in Table 12. The datasheets of both the materials can be found in Appendix B.

**Table 12: Material Properties of the Composites**

<b>Property</b>	<b>Carbon Fibre SMC</b>	<b>Carbon Fibre UD (Hexply M77)</b>
<b>Resin</b>	Vinyl Ester	Epoxy
<b>Tow</b>	12K	-
<b>Fibre Weight (%)</b>	50	62
<b>Fibre Volume (%)</b>	37	49.4
<b>Tensile Modulus (GPa)</b>	25.3	127
<b>Tensile Strength (MPa)</b>	108	1980
<b>Density (g/cm<sup>3</sup>)</b>	1.4	1.2
<b>Elongation (%)</b>	0.4	1.6
<b>Curing time at Temp (°C)</b>	35 s/mm at 135-145	7 min at 120 5 min at 130 3 min at 140
<b>Cost (£/kg)</b>	19	60

#### 4.1.2 Design Loads

As the volume and the placement of UD is a design variable, the maximum failure loads of a pure SMC specimen are initially considered. The failure loads in Table 13 are calculated using the equations in section 3.8.2.

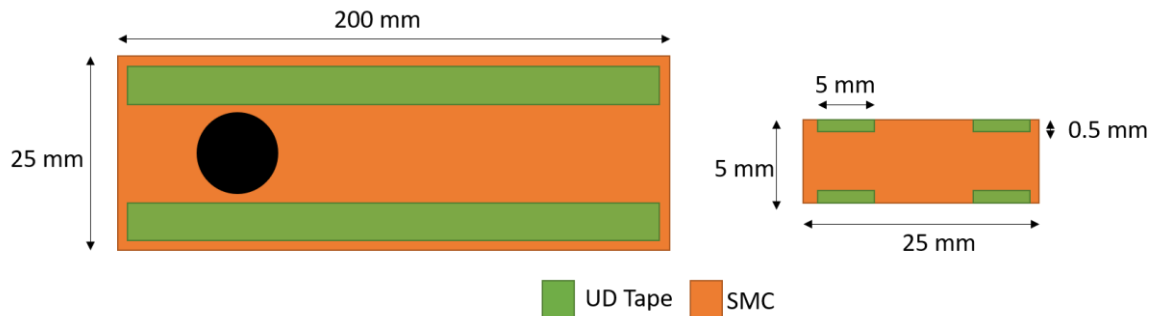
**Table 13: Predicted Pin-Bearing Failure Loads of SMC Specimen**

Net Tension Failure Load (N)	Bearing Failure Load (N)	Shear Out Failure Load (N)
6885	9180	29160

The specimen is predicted to fail in Net Tension, as it is the lowest failure mode. Therefore, the Net Tensile strength of the specimen is increased using hybridization and the bearing strength of the specimen is increased using inserts.

#### 4.1.3 Hybrid Structural Design

A UD-SMC-UD sandwich design was chosen based on literature as shown in section 3.5.2. Additionally, placing UD strips on top and bottom allows partial curing of the UD which prevents UD flow.<sup>5</sup> Lastly, UD on top and bottom would also increase the bending stiffness of the beam.



**Figure 50: Hybrid Specimen Layout**

The layout of the UD tapes and the SMC results in 8% volume of UD as displayed in Figure 50. UDs have a high tensile strength and stiffness, whereas SMC is notch insensitive and has a high bearing strength. Therefore, the SMC translates the bearing load from the pin to the UD using the adhesion. Table 14 outlines the failure loads of hybrid specimens.

<sup>5</sup> Cranfield holds a patent on partially curing UD in a hybrid composite structure.

**Table 14: Predicted Failure Pin-Bearing Failure Loads of UD-SMC Hybrid Specimens**

<b>RoHM Net-Tension Failure Load (N)</b>	<b>Bearing Failure Load (N)</b>	<b>Iso-strain Failure Load (N)</b>	<b>Shear Out Failure Load (N)</b>
22797	9180	10217	29160

The bearing failure loads and the shear out loads are the same as those stresses are still applied on the same cross-section of SMC. The RoHM Net-Tension assumes that SMC and UD will fail at the same time and adds the max load capacity of both the SMC and UD. The Iso-strain failure assumes equal strain in UD and SMC. As the elongation at failure of SMC is 0.4%, it is predicted that the SMC will fail before the UD which has an elongation to failure of 1.6% as shown in Figure 51.



**Figure 51: Net Tension Failure of Hybrid Specimen**



#### 4.1.4 Insert Design

The insert design is divided into insert material and insert shape.

##### 4.1.4.1 Insert Material

Table 15 displays the mechanical, thermal, electrochemical, and cost properties of different potential materials for the inserts.

**Table 15: Mechanical, thermal, electrochemical, and cost properties of material options** (Granta design, 2020)

<b>Material</b>	<b>Ultimate Tensile Strength (MPa)</b>	<b>Young's Modulus (GPa)</b>	<b>Density (kg/m<sup>3</sup>)</b>	<b>Thermal Expansion Coefficient (μ/ °C)</b>	<b>Galvanic Potential (V)</b>	<b>Cost (£/kg)</b>
<b>Aluminium 6082</b>	344	74	2700	23	-0.7	2
<b>Aluminium 7075</b>	580	76	2800	23.5	-0.7	4
<b>Stainless Steel 304</b>	500	205	8000	17	-0.1	2.5
<b>Stainless Steel 316</b>	600	205	8000	15	-0.14	3.2
<b>High Carbon Steel 1095</b>	720	215	7850	12.8	-0.47	0.67
<b>Titanium (Ti-6Al-4V)</b>	980	119	4430	8.9	-0.08	19.1
<b>Brass</b>	200	99	8400	18.5	-0.21	5.3

A simplified trade off table for material selection is showed in Table 16. As the primary composite material is Carbon Fibre SMC, it is critical that the insert shouldn't be prone to galvanic corrosion.<sup>6</sup> Secondly, cost is always a key factor for parts designed for mass-production. Lastly, the ultimate tensile strength of the material is important it determines the thickness of the insert.

**Table 16: Material Selection Trade-off Table**

Material	Galvanic	Cost	Ultimate Tensile
	Corrosion		Strength
Aluminium 6082	x	✓	✓
Aluminium 7075	x	✓	✓
Stainless Steel 304	✓	✓	✓
Stainless Steel 316	✓	✓	✓
High Carbon Steel 1095	x	✓	✓
Titanium (Ti-6Al-4V)	✓	x	✓
Brass	✓	✓	x

Therefore, the material chosen for the insert is SS316. Not only does it fulfil the selection criteria in Table 16, but it also has low thermal expansion, is easy to machine and has low lead times. SS316 was chosen over SS304 because of its superior mechanical properties and relatively minor cost difference.

#### 4.1.4.2 Insert Shape

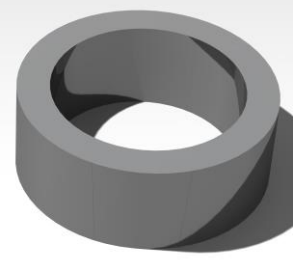

Inserts reduce stress concentrations and increase the projected area of load introduction and therefore reduce the bearing stress on the composite material. On the other hand, larger inserts decrease the W/D ratio of the specimen and in turn reduce the net tensile strength of the specimen as elaborated in section

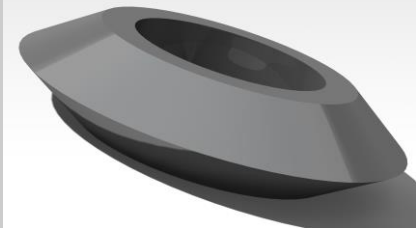
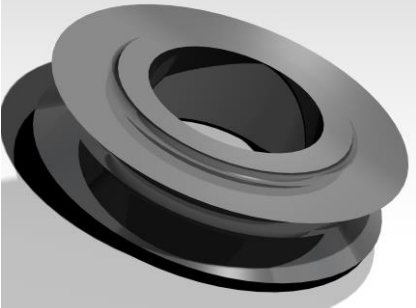
---



<sup>6</sup> While protective coatings can be applied to prevent it, their additional cost, processing, and complexity was not suitable for this project.

3.8.2.4. Therefore, depending on the composite material and expected failure mode, the thickness of the inserts can be varied. To ensure that the insert was not the weak point in the specimens, an insert thickness of 1.75 mm was chosen. This thickness ensured the insert was manufacturable, light, would not buckle during moulding and would still significantly ease the stress concentration. All variations of the insert have a base cylindrical thickness of 1.75 mm and are presented in Table 17. All inserts were sanded with a rough 80 grit sandpaper and cleaned with solvents before moulding.

Table 17: Insert Properties

Insert	Motivation	Projected Area (mm <sup>2</sup> )	Bearing stress at 10 kN load (MPa)	Mass (g)	Cost (£)
 <p data-bbox="344 791 600 823">Figure 52: Cylinder</p>	<p data-bbox="728 517 1238 823">A cylinder is the simplest insert shape in use. It increases the projected area and in turn decreases the bearing stress on the material. It is easy to manufacture and can be cut from a tube.</p>	67.5	148	2.42	2.68
 <p data-bbox="293 1198 649 1230">Figure 53: Knurled Cylinder</p>	<p data-bbox="728 884 1238 1302">Knurling is a popular gripping technique used in the plastics industry. A diamond knurl with a pitch of 1.6 mm is chose because it is the deepest standard sized knurl on the market. The diamond grooves allow fibre-interlocking and efficient load transfer</p>	67.5	148	2.01	7.93




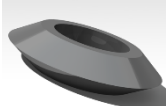
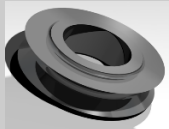
Insert	Motivation	Projected Area (mm <sup>2</sup> )	Bearing stress at 10 kN load (MPa)	Mass (g)	Cost (£)
 <p data-bbox="309 699 633 730">Figure 54: Flying Saucer</p>	<p data-bbox="728 427 1238 627">The Flying Saucer increases the bearing strength of the specimen by increasing the projected area in the middle of the specimen.</p>	84	119	5.94	3.4
 <p data-bbox="365 1121 577 1153">Figure 55: Yoyo</p>	<p data-bbox="728 794 1238 1042">The Yoyo increases the bearing strength of the specimen by increasing the projected area near the location of the UDs at the top and bottom of the specimen.</p>	84	119	5.57	5.33



Insert	Motivation	Projected Area (mm <sup>2</sup> )	Bearing stress at 10 kN load (MPa)	Mass (g)	Cost (£)
 <p data-bbox="344 715 598 751">Figure 56: 2d Yoyo</p>	<p data-bbox="728 424 1236 624">As bearing stress is dependent on the projected area, a 2d Yoyo is 2d projection of Yoyo insert with lower weight.</p>	84	119	2.8	20.85
 <p data-bbox="344 1217 598 1254">Figure 57: Butterfly</p>	<p data-bbox="728 812 1236 1066">The butterfly insert increases the projected area of the insert in line with the cylinder. It does not further reduce the W/D ratio of the specimen.</p>	91.5	109	3.2	21.82

### 4.1.5 Design of Experiments

Table 18 outlines the nine experiments that are conducted with their specific composite material and insert. Three repetitions of each specimen were moulded totalling 27 test specimens.

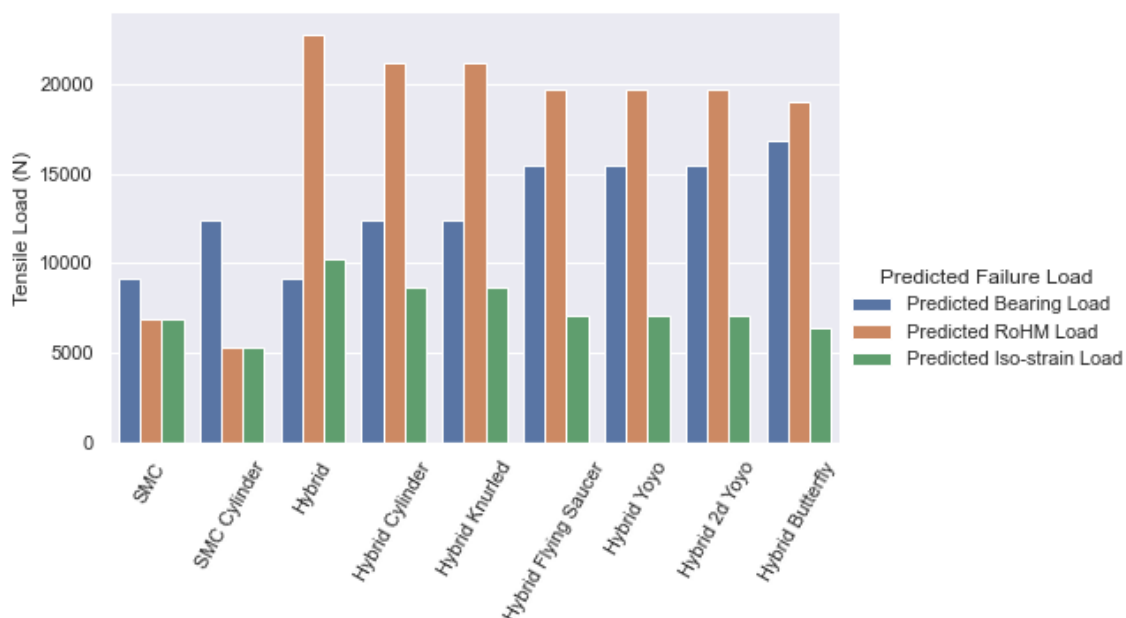
**Table 18: Design of Experiments**

Specimen Type	Composite	Insert
1	SMC	None
2	SMC	 Cylinder
3	SMC-UD Hybrid	None
4	SMC-UD Hybrid	 Cylinder
5	SMC-UD Hybrid	 Knurled Cylinder
6	SMC-UD Hybrid	 Flying Saucer
7	SMC-UD Hybrid	 Yoyo

<b>8</b>	SMC-UD Hybrid	 2d Yoyo
<b>9</b>	SMC-UD Hybrid	 Butterfly

#### 4.1.6 Predicted Strength and Modulus

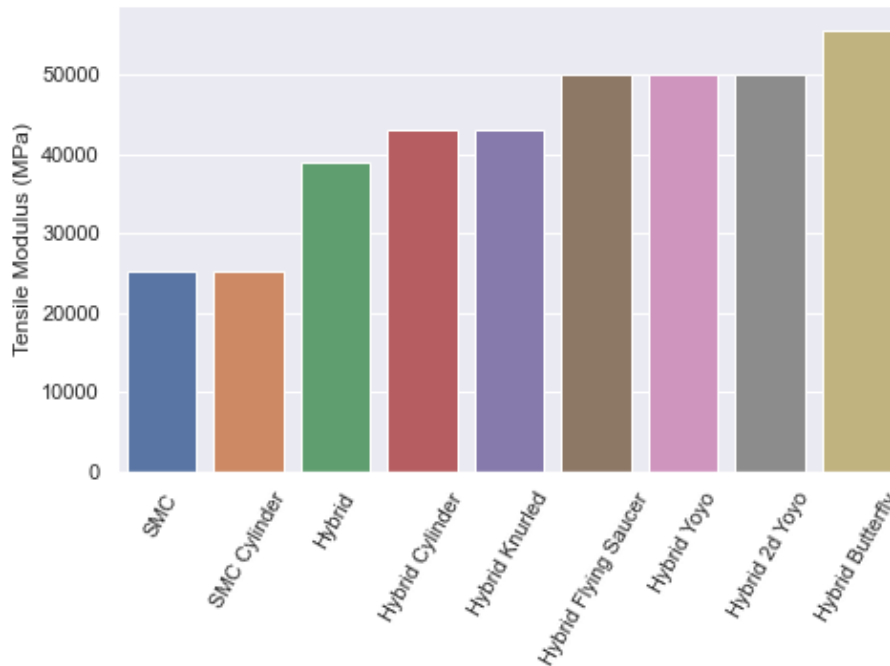
Figure 58 displays the predicted strength of the composite structure using different methods. The bearing load prediction is derived from an empirical ratio of bearing strength to tensile strength of 1.7. The RoHM load assumes that all UD and SMC will fail at the same point. The Iso-strain load assumes that the specimen is under equal strain throughout its cross-section and will fail when the strain reaches 0.4% (max elongation of SMC).



**Figure 58: Predicted Failure Loads of all Configurations**



Figure 59 displays the predicted modulus of all experiments calculated using RoHM as described in section 3.6.1.



**Figure 59: Predicted Modulus based on Rule of Hybrid Mixtures**

#### 4.1.7 Summary of Hypothesis's being tested

- Adding UD tapes around the hole increase the failure strength of a SMC composite.
- Adding UD tapes to a pin loaded SMC specimen changes its failure mode.
- A cylindrical insert increases the strength of a hybrid specimen.
- Increasing the projected area of an insert increase the failure strength of a hybrid specimen.
- Location of load introduction has an impact on failure load of hybrid composite specimen.
- A 2d insert with the same projected shape and area as a 3d symmetric insert have same performance in hybrid composites.
- Increasing the projected area in plane with the cylinder increase the bearing strength of the composite.

## 4.2 Manufacturing

The manufacturing of the specimens was done using a compression moulding machine that can both heat up the mould and apply high pressure as shown in Figure 60.



**Figure 60: Compression Moulding Press**

The male and female moulding tools used to make the I-Beams are shown in Figure 61.



**Figure 61: Male and Female Moulding Tool**

#### **4.2.1 Charge Design**

The charge design was based on few rules adopted from industrial best practices:

- Charge weight is final weight +5%
- Pyramid stacking sequence
- No complex charge shapes
- No small cuts of SMC

There is a variation in the SMC density, which meant that the charge weights varied by a small amount in different mouldings. Due to the high volume of the flanges compared to the web-section in the I-beam, only low flow charge design was manufacturable.

#### 4.2.1.1 Low Flow Charge Design

A hole was punched in the SMC charge and placed in the mould as shown in Figure 62. Using a punched hole avoided the formation of any knit lines or weld lines.

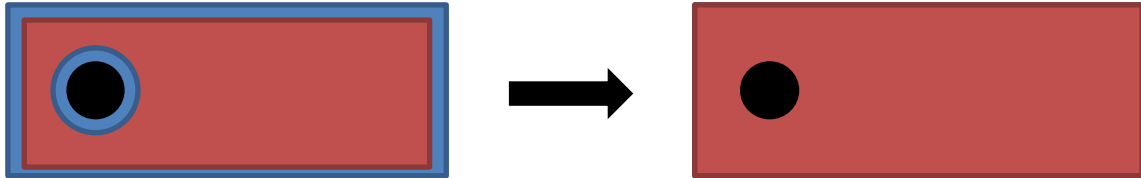


Figure 62: Charge Design with a Punched Hole

#### 4.2.2 SMC Moulding

Figure 63 shows an illustration of the SMC moulding process. The charge was loaded into the mould at 80°C, compressed at 100 bars and then heated all the way to 140. It was held at 140 for 5 mins before cooling down. This cycle ensured complete curing of the SMC.

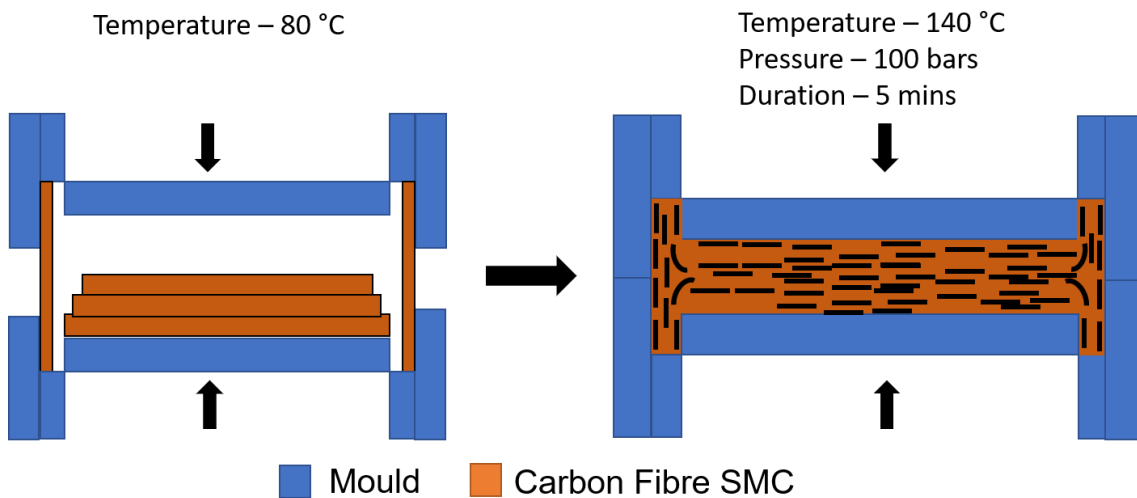


Figure 63: SMC I-Beam Moulding Process

Figure 64 shows one of the moulded SMC specimens. Some cosmetic marks from the moulding process are visible on the specimen.

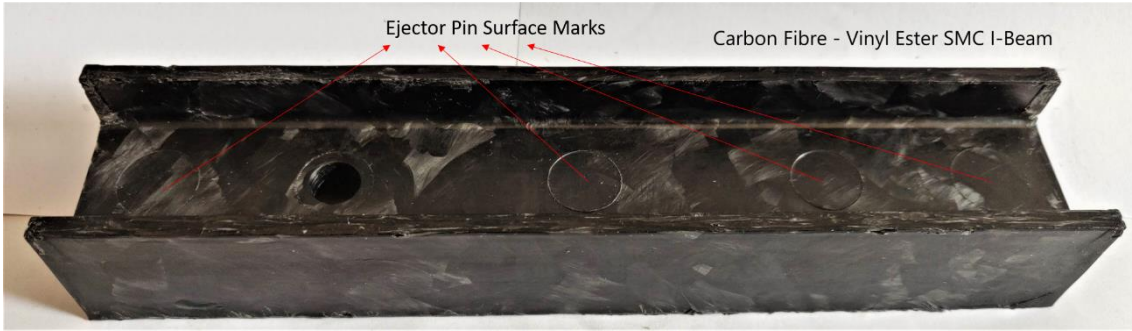


Figure 64: SMC Moulded Specimen

### 4.2.3 Hybrid I – Beam Moulding

The moulding process of the hybrid I-beam is illustrated in Figure 65. A silicon elastomeric tool was used for partial curing of the UD to prevent UD flow. It was observed that wiping the tool with a solvent prior to moulding increased the surface energy of the tool and ensured UD adhesion to the tool.

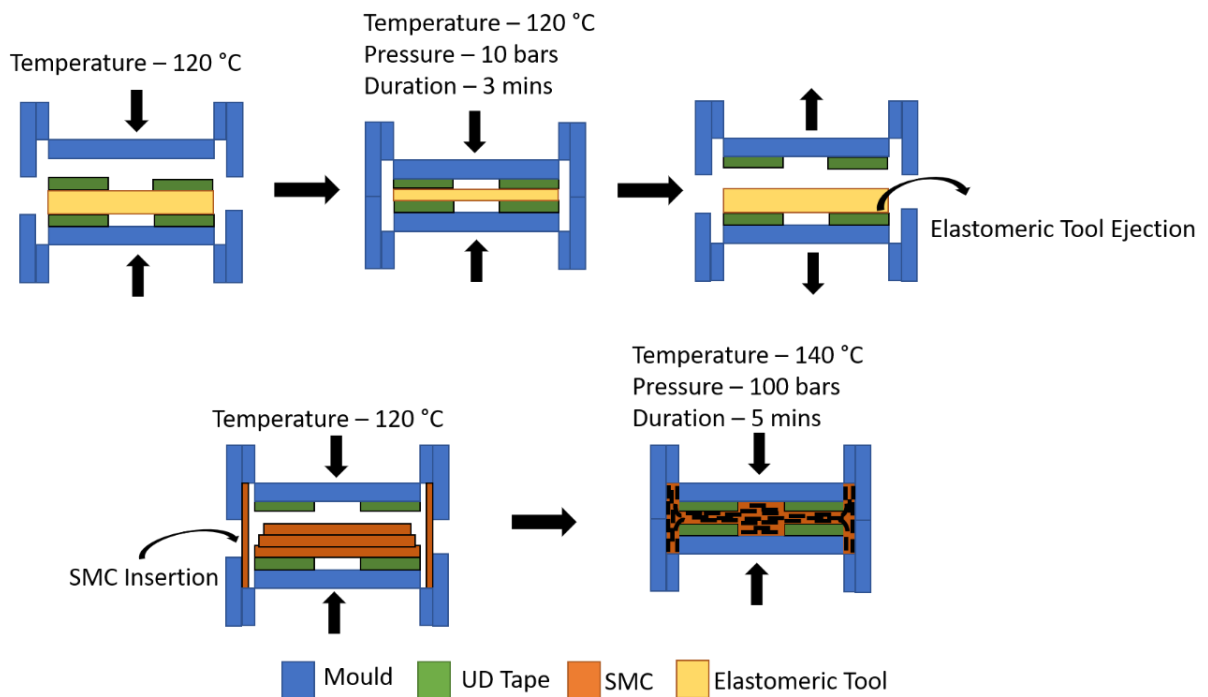


Figure 65: Hybrid I-Beam Moulding Process

#### 4.2.3.1 Elastomer Designs

The Elastomeric tool went through a couple of iterations as shown in Figure 66. These advancements ensured higher confinement of the UD during partial curing and led to more consistent mouldings.

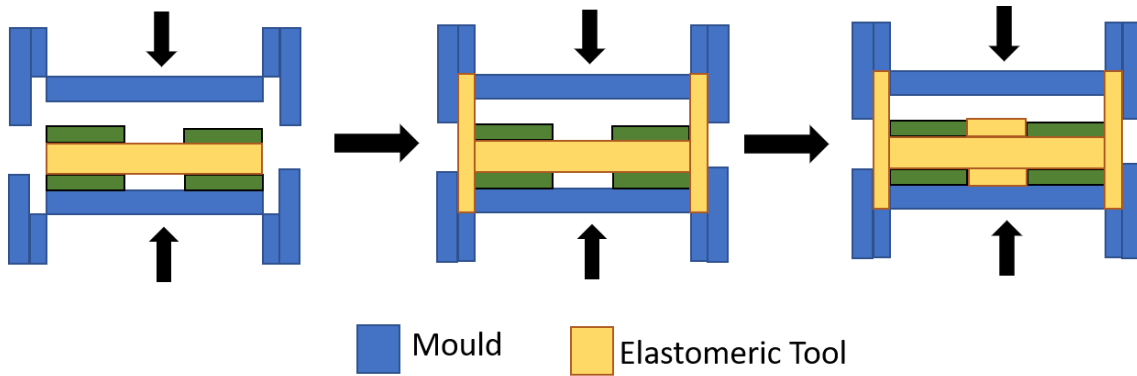


Figure 66: Elastomeric Tool Iterations

An example of the resultant hybrid moulding is presented in Figure 67.

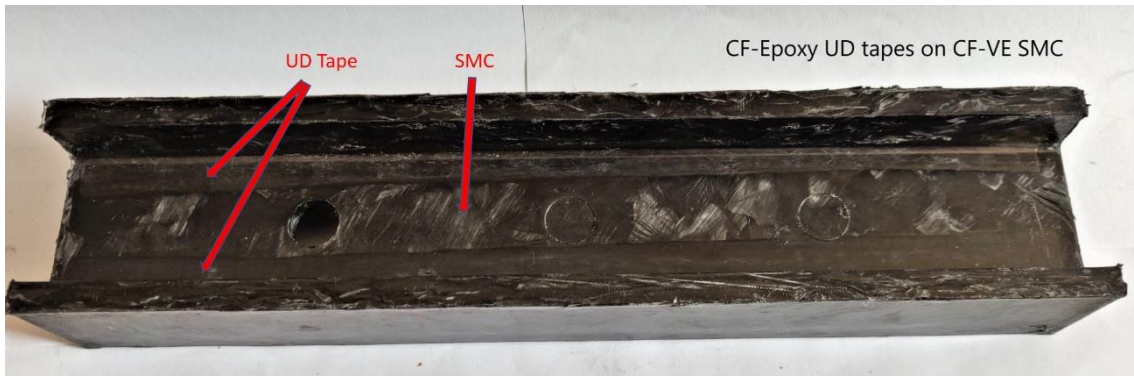


Figure 67: Hybrid I-Beam Moulding

## 4.3 Testing

### 4.3.1 Sample Preparation

To perform pin-bearing test based on the ASTM 5961 standard, the flanges of the I-beam were chopped off leading to a flat specimen. The bottom quarter of the specimen was sanded, and steel tabs were bonded using epoxy. The resulting test specimens along with their respective inserts are displayed in Figure 68

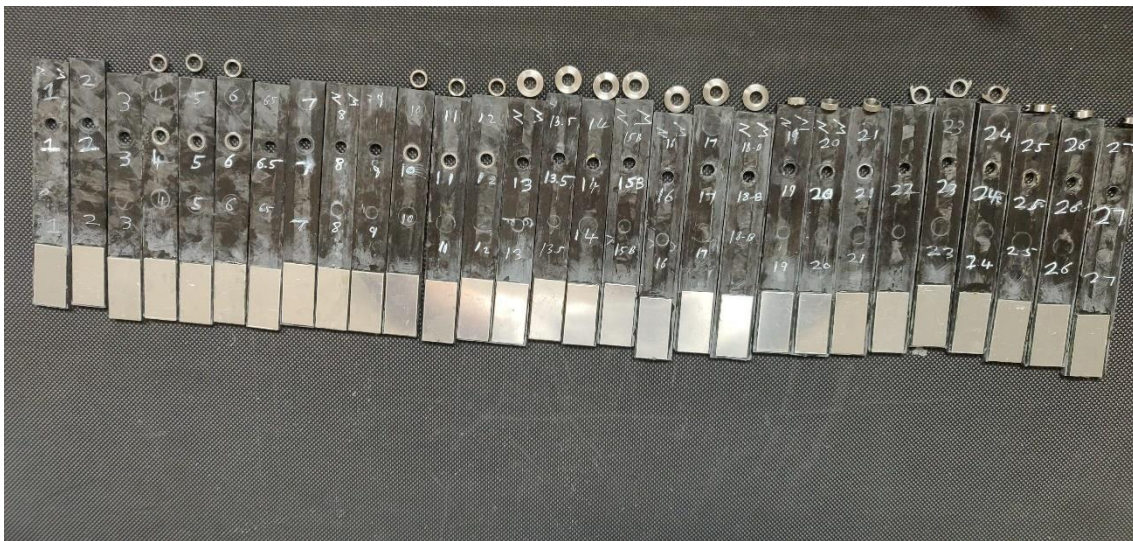


Figure 68: Specimens with their respective inserts

### 4.3.2 Machine Set up

The pin-bearing test set up of the machine is displayed in Figure 69. A laser extensometer was used to measure the displacement of the specimen under load. As per the ASTM 5961 standard, the specimen was torqued up to 5 Nm. A higher bearing strength and stiffness is expected with higher torques, but higher torques add an unpredictable variable.



**Figure 69: Pin-Bearing Test Set Up**



## 5 RESULTS

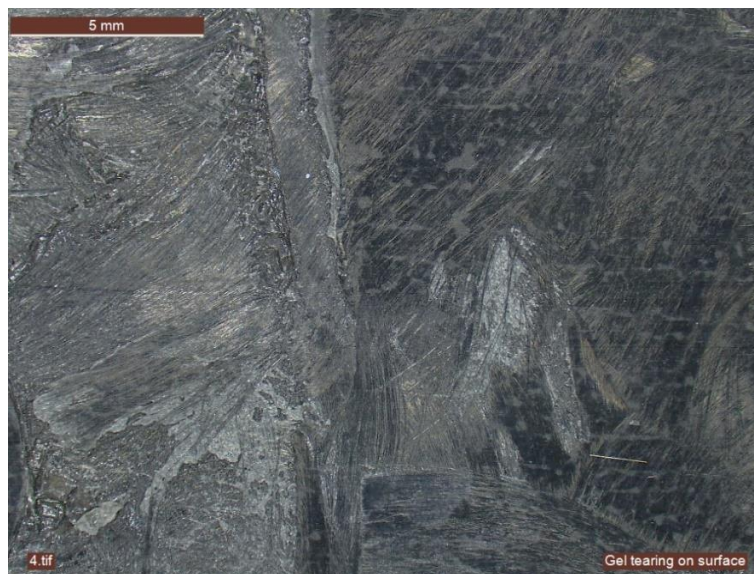
This section describes the results of the moulding and the testing of the specimens. The chapter is divided in qualitative and quantitative results.

### 5.1 Qualitative Results

#### 5.1.1 Moulding Results

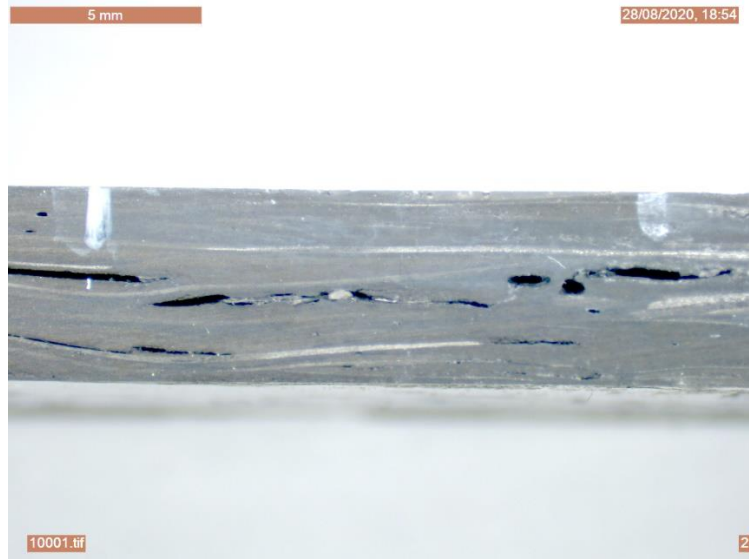
The moulding process was iterative, and the results generally got better with experience. Due to the mould release agent in the SMC, the cylindrical inserts did not stick inside the specimen and were held in place with friction. All the other inserts were mechanically locked in the material.

Figure 70 shows an example of gel tearing on the surface of SMC Specimens. This phenomenon occurred when the SMC could dwell in mould before compression moulding. Even at temperatures as low as 70°C, the outer layers of the SMC started gelling. This was mitigated by eliminating dwell time.



**Figure 70: Gel Tearing on Surface**

After chopping off the flanges, voids were observed in early specimens as shown in Figure 71. The number of visible voids decreased with higher charge mass and higher pressure.



**Figure 71: Voids in Specimens**

In some specimens, UD-SMC delamination was observed as shown in Figure 72. These were a couple of mm long and may have occurred due to the use of silicon elastomeric tool.



**Figure 72: UD-SMC Delamination**

The minimum force that can be applied consistently by the press is 10kN. This led to a pressure of 50 bars on the UD during the partial curing cycle and in turn led to resin bleed from the UD. This resin bleed caused dry spots on the surface of the UD as shown in Figure 73.



**Figure 73: Dry Region from Resin Squeeze Out**

A resin-rich region was observed at the interface of UD and SMC in a few specimens as shown in Figure 74. This occurred because the UD tape formed a step over the SMC.



**Figure 74: Resin-rich Region at the UD-SMC Interface**

High fibre waviness was observed at the cross-section near the insert in few specimens as shown in Figure 75. This was likely due to the high flow of SMC in the region. Waviness of fibres is detrimental to joint strength, as curved fibres cannot translate tensile loads efficiently.



**Figure 75: Fibre Waviness near Insert**

Figure 76 and Figure 77 show the successful flow of fibres into the Flying Saucer and Yoyo inserts validating the charge pattern.



**Figure 76: Fibre Flow around Flying Saucer Insert**



**Figure 77: Fibre Flow around Yoyo Insert**

### 5.1.2 Test Results

Almost all specimens displayed some degree of asymmetric failure on one side as shown in Figure 78. This was likely due to the local variability of modulus in SMC.



Figure 78: Asymmetric Failure of Specimens

## 5.2 Quantitative Results

### 5.2.1 Geometric Properties

The geometric properties of the specimens are detailed in Table 19. The mould closed with a gap of 5 mm, however the SMC sprung to higher thickness after moulding. This spring back was proportional to the amount of the charge placed in the mould.

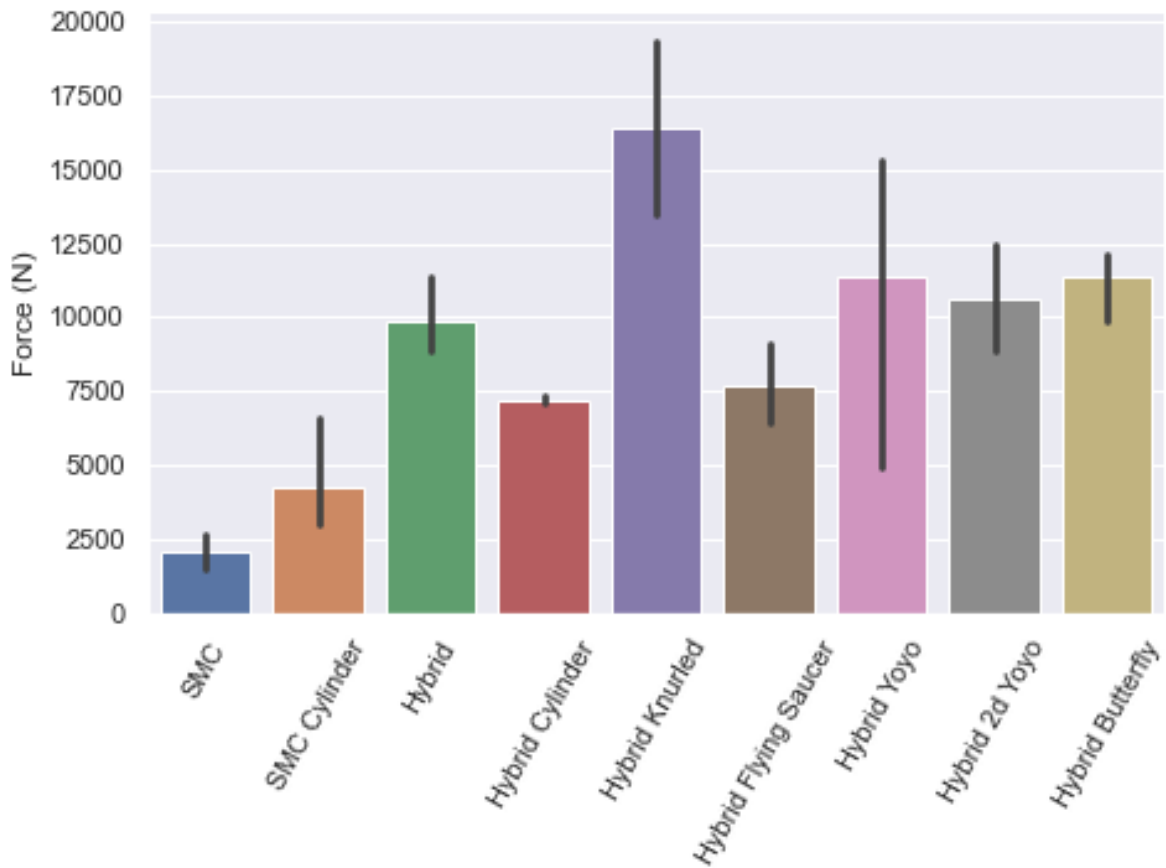
The flat specimens were made by chopping off the flanges. This involved sawing the flanges and filing the edges which introduced a variation in the specimen width.

**Table 19: Specimen Geometric Properties**

	<b>Thickness (mm)</b>	<b>Width (mm)</b>
<b>Mean</b>	5.45	29.43
<b>Standard Deviation</b>	0.37	1.56
<b>Min</b>	4.88	26.32
<b>Max</b>	6.01	32

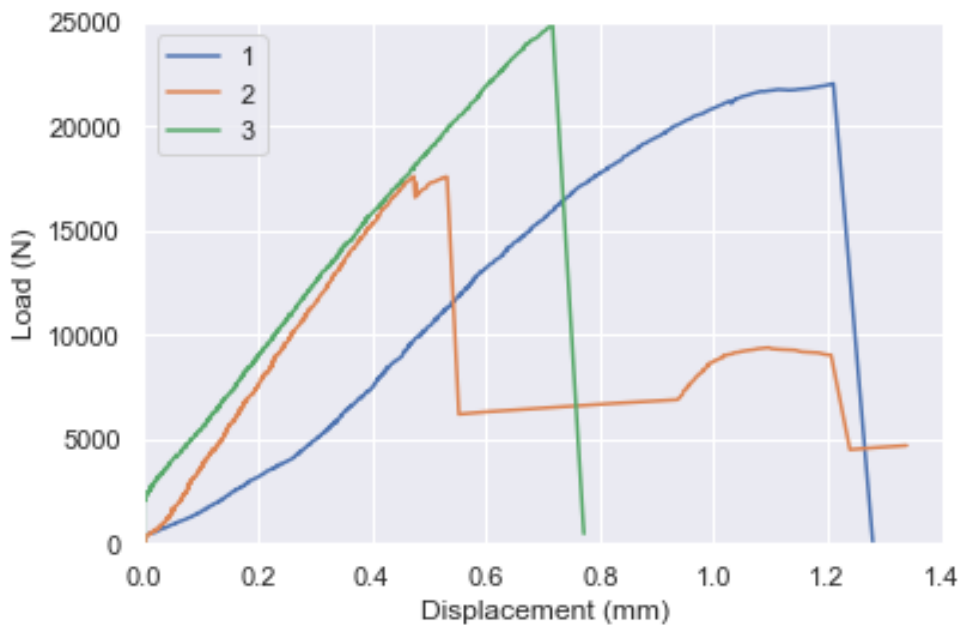
### 5.2.2 Mechanical Properties

The failure mode of all specimens was either net-tension failure or combination of bearing and net-tension failure. The failure load of all specimens was multiplied by a scaling factor to account for the differences in the cross-section area. Figure 79 displays the resultant bar graph. The hybrid specimen with the knurled insert performed the best followed by the Yoyo, 2d Yoyo and the Butterfly Inserts.



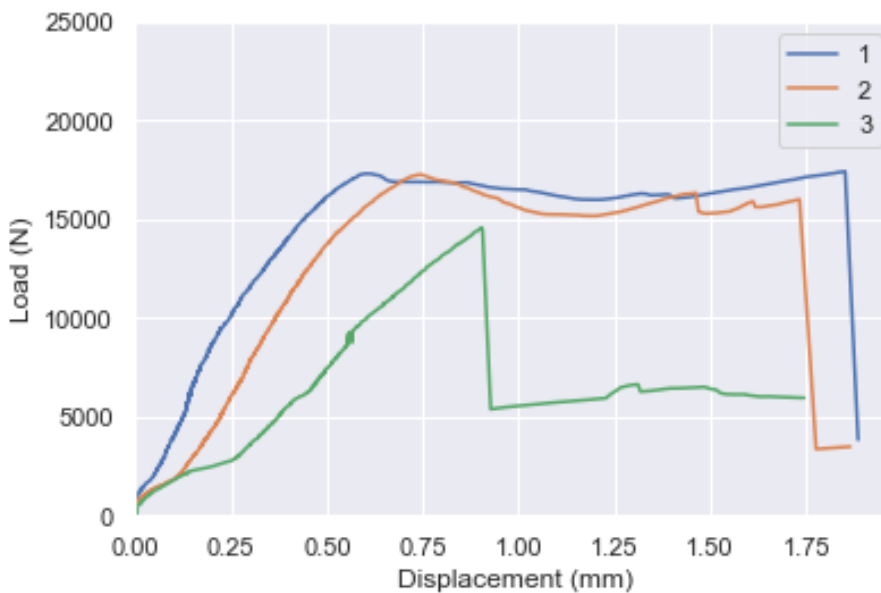
**Figure 79: Failure Loads Proportional to the Cross-Section Area of the Specimens**

Figure 80 shows the Load-Displacement graph of the hybrid specimens with knurled inserts. The second specimen had two partial failures instead of a single complete failure. This was observed in a lot of specimens and is attributed to modulus variability of the SMC leading to higher local loadings on the UD tapes on one side.



**Figure 80: Hybrid Specimen with Knurled Insert**

The butterfly inserts displayed a unique progressive bearing failure where the joint retained significant load capacity after max load as shown in Figure 81.



**Figure 81: Hybrid Specimen with Butterfly Insert**

The Load-Displacement graphs of all the other inserts can be found in Appendix A.

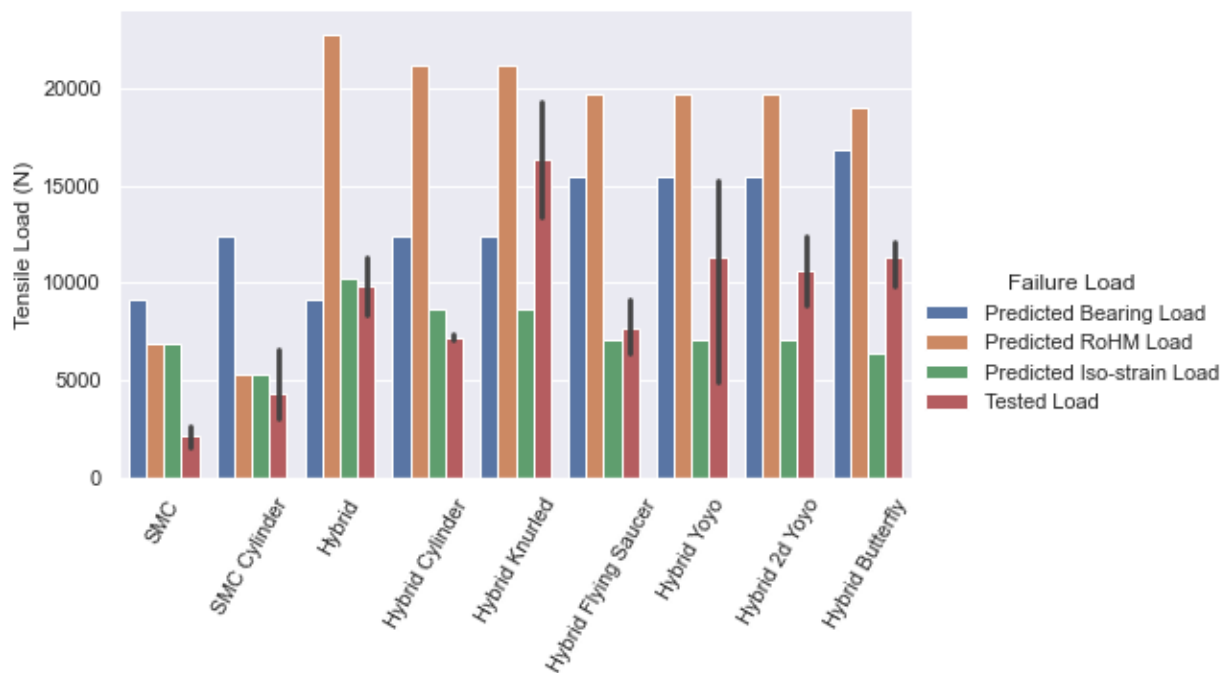


## 6 Discussion

### 6.1 Mechanical Performance

#### 6.1.1 Strength

A comparison of the predicted and tested loads of the experiments is presented in Figure 82. The primary failure mode of all specimens was either net-tension or bearing followed by net-tension. The Knurled, Flying Saucer and Butterfly displayed explicit bearing failures in tested specimens.



**Figure 82: Comparison of Predicted and Tested Failure Loads**

It can be observed that the SMC specimens didn't perform as predicted. The two likely reasons are the inherent variability of SMC moulding and the fact that these were the first few mouldings and the processing parameters got better with more mouldings.

The hybrid specimen increased the strength of SMC by about 200 % with < 7% UD placement in critical region. The tested strength of hybrid specimen was similar to the predicted bearing strength and iso-strain strength. This predictability is one of the key benefits of hybrid composites.

The cylindrical inserts in both the SMC and the Hybrid were held in the specimen with friction and therefore had no adhesion and poor mechanical interlocking. This led to the specimens behaving strangely as the inserts settled in during testing.

Knurled inserts had the best performance and further increased the strength of the hybrid specimens by 60%. There are two key reasons for the high performance:

- It gripped the SMC on front and the sides, significantly improving the stress distribution in the specimen as displayed in Figure 83.
- It occupied the lowest amount of critical space around the hole, which increased the composite material in the region increasing its net tensile strength.



**Figure 83: Gripping Effect of the Knurled Insert**

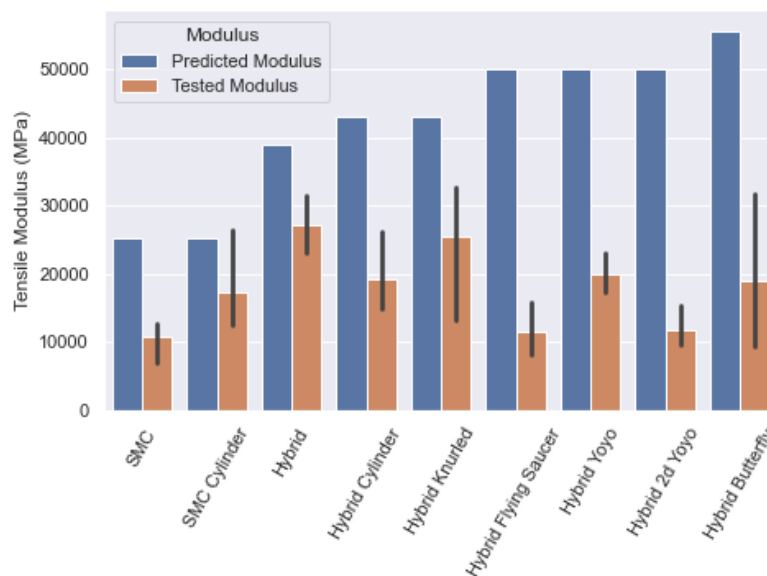
The specimens with the Yoyo insert had a significantly higher strength than the ones with the Flying Saucer insert. This showed that the load introduction close to UD is better than load introduction in the middle. This also proves the assumption of iso-strain is not true in hybrid composites. An iso-strain material would be immune to changes in the location of load introduction.

The Yoyo insert performed marginally better than the 2d Yoyo with the same projected area. This aligns well with the theory that projected area is a good variable to predict bearing stress<sup>7</sup>. The 2d Yoyo is half the weight of the Yoyo insert and is four times the cost. Mass production of inserts using casting will bring down the cost, but the additional complexity may not be worth the weight savings.

The Butterfly inserts had a very progressive failure dominated by bearing. This was likely due to its high projected area and because it did not occupy the critical area around the insert. The progressive failure mode is valuable as it allows for detection and repair without catastrophic disassembly. Overall, the strength of all specimens was significantly dominated by the Width/Diameter ratio.

### 6.1.2 Stiffness

A comparison graph of the predicted tensile modulus and tested tensile modulus is displayed in Figure 84. A high degree of variability is observed in the tested modulus. The standard hybrid specimens and the hybrid specimens with the Knurled inserts had the best performance.



**Figure 84: Comparison of Predicted and Tested Modulus**

<sup>7</sup> The literature states that it's an approximation and works within 5% of actual bearing strength.

The hybrid specimens with the best tested performance had a modulus like the predicted modulus of the SMC. In hindsight, this is because the bearing load is directly applied only to the SMC in the current hybrid configurations.

The predicted modulus was calculated using the RoHM, which would have been valid in calculating the bending stiffness. However, as the loading was primarily applied via the SMC, the predicted modulus was wrong.

## **6.2 Manufacturing Process**

During compression moulding, the mould always closed with a gap of 5 mm, however the resulting specimen's thicknesses ranged from 4.88 to 6.01 mm. The final thickness of the specimen was proportional to the amount of charge placed in the mould. There are two key phenomenon taking place here:

- The SMC shrinks as it cures. The SMC has additives that reduce the overall shrinkage, but local shrinkage is still observed.
- When more charge than the mould capacity is added, some of the resin will squeeze out as flash, however, the rest will be compressed and will spring back after the load is released.

High charge and high-pressure lead to lower void contents. However, they also make it difficult to obtain net-shape parts. Therefore, a spring back allowance must be designed in moulds to achieve consistent net shape parts with low voids.

Fibre Waviness was observed in the critical region near the insert due to high flow. The punched holes should be as small as possible to minimize flow in the region.

It was observed that wiping or spraying the mould with a solvent before partial curing of UD increased its surface energy and improved the adhesion of the UD to the mould.

The minimum force of the press (10 kN) was too high for the UD and led to resin bleed. The impact of this resin bleed is not conclusive. A thinner elastomeric tool can be used to ensure that the mould closes before significant force is applied to the UD.

Resin-rich regions were observed at the UD-SMC interface. UD tapering should be applied in both dimensions to avoid resin rich regions at the interface.

### 6.3 Comparison with aluminium

Table 20 shows the comparative performance of the hybrid composite with different Aluminium alloys under similar pin loading conditions.

**Table 20: Comparison of Hybrid Composite and Aluminium under Pin Loading**

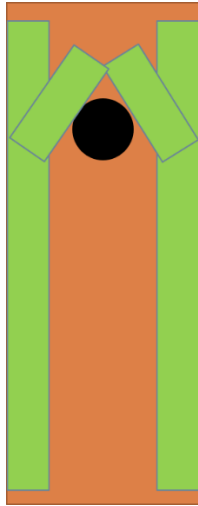
<b>Property</b>	<b>Hybrid Composite with Knurled Insert</b>	<b>Al 6060</b>	<b>Al 6082 T6</b>
<b>Tensile Load (N)</b>	16000	5400	11250
<b>Tensile Modulus (GPa)</b>	26	69.5	69.5
<b>Density (kg/m<sup>3</sup>)</b>	1522	2700	2700

The tensile strength of the hybrid composites is significantly higher than those of the Aluminium alloys even with a significantly lower density. However, in its current configuration, the stiffness of the hybrid composite is limited by the stiffness of the SMC

### 6.4 Proposed Design

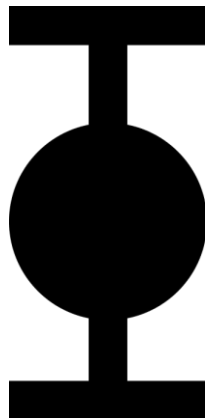
To improve the consistency of hybrid specimens, the asymmetric failure needs to be addressed. The primary cause of asymmetric failure is variable modulus and low elongation at failure of the current SMC. Replacing the current Vinyl Ester based SMC with a higher elongation epoxy SMC should significantly improve reliability. Additionally, SMC with thinner tows should further reduce variability as they would have smaller stress concentrations at bundle ends.

To increase the stiffness of the hybrid specimen, additional UD tapes at angle of 45 ° near the loading point are proposed as shown in Figure 85.



**Figure 85: Angled UD Strips to Increase Stiffness**

Given the progressive failure of the Butterfly Insert, an optimised insert with a similar design philosophy is proposed in Figure 86.



**Figure 86: Tie Fighter Insert Design**

## 7 Conclusion

This report investigates the variables affecting bearing load introduction in hybrid composites. The two key variables in this design were the UD placement and the insert design. Complex I-sections were compression moulded using SMC and UD-SMC hybrid composites with novel inserts. These specimens were then tested in a pin-bearing condition.

The conclusions of the moulding process are:

- SMC springs back after compression moulding and should be accounted for in mould design.
- Wiping the mould with solvents before partial curing allows the UD to stick to the mould.
- UD tapering should be used in all directions when possible.

The conclusions of the design process are:

- Placing the UD strips around the hole in hybrid composites synergistically utilises the high tensile strength of UDs and the high bearing strength of SMCs.
- Hybrid composites increased the tensile strength of the specimen by over 200% by using < 7% UD.
- Knurled inserts further increased the performance of hybrid composites by 60% because of their ability to grip the SMC.
- Location of load introduction via an insert is more important than the projected area of the insert.
- Increasing the projected area of the insert in-line with the loading direction leads to progressive failure.
- Width/Diameter ratio is one of the most critical factors in insert performance.
- Hybrid composites have a significantly higher strength when compared to Aluminium alloys, but smart solutions are needed to achieve high stiffness.

## 8 Recommendations and Future Work

The projected showed very promising results. It demonstrated that in narrow beams, knurled insert is the ideal choice because of it's low form factor and gripping capacity. Further work can be conducted to increase the strength, stiffnes, attractiveness and reliability of the hybrid composites.

- Hybrid design with 45° UD tapes should be investigated as a means to increase joint stiffness.
- Torque relaxation over time in hybrid composites should be studied.
- Process Cost Comparison between compression moulding and aluminum forging should be conducted.
- Alternate elastometric tool material should be investigated because of manufacturing concerns with silicon.
- The high aspect ratio SMCs made by Mitsubishi should be considered for higher predictability.
- Hybrid specimens should be manufactured using CF UD and Epoxy based SMC because of their higher elongation and stiffness.
- Hybrid Specimens with CF UD and Glass Fibre Epoxy should be investigated as a low cost alternative.



## REFERENCES

Akiyama, K. (2011) *Development of PCM technology*.

ASTM International (2021) *D7248/D7248M-21 Standard Test Method for High Bearing - Low Bypass Interaction Response of Polymer Matrix Composite Laminates Using 2-Fastener Specimens* ASTM International, West Conshohocken, PA

Ataş, A. and Soutis, C. (2013) 'Subcritical damage mechanisms of bolted joints in CFRP composite laminates', *Composites Part B: Engineering*, 54, pp. 20–27.

Bale, J.S. and others (2015) 'The discontinuous carbon fiber composite: a review of the damage characteristics', *LONTAR Jurnal Teknik Mesin Undana (LJTMU)*, 2(1), pp. 9–14.

BigHead (2017) *Composite panel production for automotive applications: bigHead® Bonding Fasteners help provide fast, secure and precise results*. Available at: <https://www.bighead.co.uk/fr/discover-bighead/news/2017/12/composite-panel-production-automotive-applications-bighead-bonding-fasteners-help-provide-fast-secure-precise-results/> (Accessed: 12 July 2021).

Bond, M.D., Harper, L.T., Turner, T.A. and Warrior, N.A. (2019) 'Full-field strain measurement of notched discontinuous carbon fiber composites', *Polymer Composites Group, Division of Materials, Mechanics and Structures, The University of Nottingham*

Bücheler, D., Griesbaum, P. and Henning, F. (2018) 'New Developments in Compounding of CF SMC', *4 th International Composite Congress*. Stuttgart: Fraunhofer ICT.

Caccese, V., Berube, K.A., Fernandez, M., Melo, J.D. and Kabche, J.P. (2009) 'Influence of stress relaxation on clamp-up force in hybrid composite-to-metal bolted joints', *Composite Structures*, 89(2) Elsevier, pp. 285–293.

Camanho, P.P., Fink, A., Obst, A. and Pimenta, S. (2009) 'Hybrid titanium--CFRP laminates for high-performance bolted joints', *Composites Part A: Applied*

*Science and Manufacturing*, 40(12) Elsevier, pp. 1826–1837.

Camanho, P.P. and Matthews, F.L. (2000) 'Bonded metallic inserts for bolted joints in composite laminates', *Proceedings of the Institution of Mechanical Engineers, Part L: Journal of Materials: Design and Applications*, 214(1) SAGE Publications Sage UK: London, England, pp. 33–40.

Camanho, P.P., Tavares, C.M.L., De Oliveira, R., Marques, A.T. and Ferreira, A.J.M. (2005) 'Increasing the efficiency of composite single-shear lap joints using bonded inserts', *Composites Part B: Engineering*, 36(5) Elsevier, pp. 372–383.

Candotape (2016) *What is Surface Energy, and Why is it Important in Bonding?*. Available at: <https://www.can-dotape.com/blog/what-is-surface-energy-and-why-is-it-important-in-bonding/> (Accessed: 31 May 2021).

Caprino, G., Giorleo, G., Nele, L. and Squillace, A. (2002) 'Pin-bearing strength of glass mat reinforced plastics', *Composites Part A: Applied Science and Manufacturing*, 33, pp. 779–785.

Choi, J.-I., Hasheminia, S.M., Chun, H.-J., Park, J.-C. and Chang, H.S. (2018) 'Failure load prediction of composite bolted joint with clamping force', *Composite Structures*, 189, pp. 247–255.

Collings, T.A. (1977) 'The strength of bolted joints in multi-directional cfrp laminates', *Composites*, 8(1), pp. 43–55.

Corbridge, D.M. (2018) *Compression moulding of hybrid carbon fibre composites for structural applications*. University of Nottingham.

Dhakal, H.N., Zhang, Z.Y., Guthrie, R., MacMullen, J. and Bennett, N. (2013) 'Development of flax/carbon fibre hybrid composites for enhanced properties', *Carbohydrate Polymers*, 96(1), pp. 1–8.

Duthinh, D. and others (2000) '*Connections of fiber-reinforced polymer (FRP) structural members: a review of the state of the art*'

Evans, A.D., Harper, L.T., Turner, T.A. and Warrior, N.A. (2017) 'Joint design of continuous/discontinuous hybrid carbon fibre composites', *21st International conference on composite materials*.

Fan, J.-D., Lee, L.J., Kim, J. and Im, Y.-T. (1989) 'Cure analysis of sheet molding compound in molds with substructures', *Polymer Engineering & Science*, 29(11), pp. 740–748.

Faraz, A., Biermann, D. and Weinert, K. (2009) 'Cutting edge rounding: An innovative tool wear criterion in drilling CFRP composite laminates', *International Journal of Machine Tools and Manufacture*, 49(15) Elsevier, pp. 1185–1196.

Feraboli, P., Peitso, E., Deleo, F., Cleveland, T. and Stickler, P.B. (2009) 'Characterization of Prepreg-Based Discontinuous Carbon Fiber/Epoxy Systems', *Journal of Reinforced Plastics and Composites*, 28(10), pp. 1191–1214.

Finck, D., Seidel, C., Hausmann, J. and Rief, T. (2019) 'Creep-induced screw preload loss of carbon-fiber sheet molding compound at elevated temperature', *Materials*, 12(21) Multidisciplinary Digital Publishing Institute, p. 3598.

Galińska, A. (2020) 'Mechanical Joining of Fibre Reinforced Polymer Composites to Metals—A Review. Part I: Bolted Joining', *Polymers*, 12(10) Multidisciplinary Digital Publishing Institute, p. 2252.

Gebhardt, J. and Fleischer, J. (2014) 'Experimental investigation and performance enhancement of inserts in composite parts', *Procedia CIRP*, 23 Elsevier, pp. 7–12.

Graham, D.P., Rezai, A., Baker, D., Smith, P.A. and Watts, J.F. (2014) 'The development and scalability of a high strength, damage tolerant, hybrid joining scheme for composite–metal structures', *Composites Part A: Applied Science and Manufacturing*, 64, pp. 11–24.

Granta design (2020) *CES Edupack ANSYS*,

Hitchen, S.A. and Kemp, R.M.J. (1996) 'Development of novel cost effective hybrid ply carbon-fibre composites', *Composites Science and Technology*, 56(9), pp. 1047–1054.

Hopmann, C., Magura, N., Stender, S., Böttcher, A. and Fischer, K. (2017) 'Cost-Efficient Manufacturing of Quality Assured Hybrid CFRP/GFRP-Parts', *SAMPE Europe Conference*. Stuttgart: SAMPE.

Jahn, J., Weeber, M., Boehner, J. and Steinhilper, R. (2016) 'Assessment strategies for composite-metal joining technologies--a review', *Procedia Cirp*, 50 Elsevier, pp. 689–694.

Jeong, J.-H., Kim, K.-T. and Im, Y.-T. (1996) 'Plane-strain compression molding analysis of sheet molding compounds in flat and cross-sectional T-shape molds', *Journal of Materials Processing Technology*, 57(3), pp. 320–331.

Khashaba, U.A., Sallam, H.E.M., Al-Shorbagy, A.E. and Seif, M.A. (2006) 'Effect of washer size and tightening torque on the performance of bolted joints in composite structures', *Composite Structures*, 73(3), pp. 310–317.

Kia, H.G. (1993) *Sheet molding compounds: science and technology*. Hanser Verlag.

Kunc, V., Erdman, D. and Klett, L. (2004) 'Hybrid joining in automotive applications', *Proceedings of the International SAMPE Technical Conference*, pp. 3943–3956.

Lee, C.-C. and Tucker, C.L. (1987) 'Flow and heat transfer in compression mold filling', *Journal of Non-Newtonian Fluid Mechanics*, 24(3), pp. 245–264.

Li, R., Kelly, D. and Crosky, A. (2002) 'Strength improvement by fibre steering around a pin loaded hole', *Composite Structures*, 57(1–4) Elsevier, pp. 377–383.

Löbel, T., Kolesnikov, B., Scheffler, S., Stahl, A. and Hühne, C. (2013) 'Enhanced tensile strength of composite joints by using staple-like pins: Working principles and experimental validation', *Composite Structures*, 106, pp. 453–460.

Matthews, F.L. and Rawlings, R.D. (1999) '10 - Short fibre composites', in *Composite Materials*. Woodhead Publishing Series in Composites Science and Engineering. Woodhead Publishing, pp. 287–325.

Mazumdar, S. (2001) *Composites manufacturing: materials, product, and process engineering*. CrC press.

MIR, B.J., TAJVIDI, M., GHASEMI, E. and Hermanson, J.C. (2007) 'Prediction of the elastic modulus of wood flour/kenaf fibre/polypropylene hybrid composites', *IRANIAN POLYMER JOURNAL (ENGLISH)*

- Mirabella, L. and Galea, S.C. (1997) 'An experimental investigation into the use of inserts to enhance the static performance of thin composite bolted lap joints', *Proc. 11th Int. Conf. on Composite Materials.*, Vol.6, pp. 148–157.
- Muth, M., Schwennen, J., Bernath, A., Seuffert, J., Weidenmann, K.A., Fleischer, J. and Henning, F. (2018) 'Numerical and experimental investigation of manufacturing and performance of metal inserts embedded in CFRP', *Production Engineering*, 12(2) Springer, pp. 141–152.
- Nilsson, S. (1989) 'Increasing Strength of Graphite/Epoxy Bolted Joints by Introducing an Adhesively Bonded Metallic Insert', *Journal of Composite Materials*, 23(7), pp. 642–650.
- Olsson, J., Lundström, S. and Olofsson, K. (2009) 'Compression moulding of SMC: coupling between the flow and the local void contents', *International Conference on Composite Materials: 27/07/2009-31/07/2009*.
- Orgéas, L. and Dumont, P.J.J. (2011) 'Sheet molding compounds', *Wiley encyclopedia of composites*, Wiley Online Library, pp. 1–36.
- Ozen, M. and Sayman, O. (2011) 'Failure loads of mechanical fastened pinned and bolted composite joints with two serial holes', *Composites Part B: Engineering*, 42(2), pp. 264–274.
- Papathanasiou, T.D. and Guell, D.C. (1997) *Flow-induced alignment in composite materials*. Woodhead publishing.
- Park, H.-J. (2001) 'Effects of stacking sequence and clamping force on the bearing strengths of mechanically fastened joints in composite laminates', *Composite Structures*, 53(2), pp. 213–221.
- Reller, D.L. (2008) *Effect of pullout and torsional strength of composites with co-molded thread inserts*. The University of Texas at Arlington.
- REVELLINO, M., SAGGESE, L. and GAIERO, E. (2000) '2.22 - Compression Molding of SMCs', in Kelly, A. and Zweben, C. (eds.) *Comprehensive Composite Materials*. Oxford: Pergamon, pp. 763–805.
- Sasdelli, M., Karbhari, V.M. and Gillespie, J.W. (1993) 'On the use of metal

inserts for attachment of composite components to structural assemblies-a review', *International Journal of Vehicle Design*, 14(4) Inderscience Publishers, pp. 353–369.

Selezneva, M. and Lessard, L. (2016) 'Characterization of mechanical properties of randomly oriented strand thermoplastic composites', *Journal of composite materials*, 50(20) SAGE Publications Sage UK: London, England, pp. 2833–2851.

Sentis, D.F., Cochereau, T., Orgéas, L., Dumont, P.J.J., Du Roscoat, S.R., Laurencin, T., Terrien, M. and Sager, M. (2017) 'Tensile behaviour of uncured sheet moulding compounds: Rheology and flow-induced microstructures', *Composites Part A: Applied Science and Manufacturing*, 101 Elsevier, pp. 459–470.

Thoppul, S.D., Finegan, J. and Gibson, R.F. (2009) 'Mechanics of mechanically fastened joints in polymer–matrix composite structures – A review', *Composites Science and Technology*, 69(3), pp. 301–329.

Thoppul, S.D., Gibson, R.F. and Ibrahim, R.A. (2008) 'Phenomenological Modeling and Numerical Simulation of Relaxation in Bolted Composite Joints', *Journal of Composite Materials*, 42(17), pp. 1709–1729.

Troschitz, J., Kupfer, R. and Gude, M. (2019) 'Process-integrated embedding of metal inserts in continuous fibre reinforced thermoplastics', *Procedia CIRP*, 85 Elsevier, pp. 84–89.

Turvey, G.J. and Wang, P. (2007) 'Failure of pultruded GRP single-bolt tension joints under hot–wet conditions', *Composite Structures*, 77(4), pp. 514–520.

Venkateshwaran, N., Elayaperumal, A. and Sathiya, G.K. (2012) 'Prediction of tensile properties of hybrid-natural fiber composites', *Composites Part B: Engineering*, 43(2), pp. 793–796.

Visweswaraiah, S. and others (2017) 'Conditions for notch sensitivity in hybrid fibre architectures of randomly oriented strands combined with laminate groups', *COMPTEST 2017*, , pp. 20–25.

Visweswaraiah, S.B., Selezneva, M., Lessard, L. and Hubert, P. (2018)

'Mechanical characterisation and modelling of randomly oriented strand architecture and their hybrids--a general review', *Journal of Reinforced Plastics and Composites*, 37(8) SAGE Publications Sage UK: London, England, pp. 548–580.

Vander Voort, G.F., Lampman, S.R., Sanders, B.R., Anton, G.J., Polakowski, C., Kinson, J., Muldoon, K., Henry, S.D. and Scott Jr, W.W. (2004) 'ASM handbook', *Metallography and microstructures*, 9 ASM International Materials Park, OH, pp. 40002–44073.

Woodhead Publishing (2012) '18 - Fracture processes of aerospace materials', in Mouritz, A. P. (ed.) *Introduction to Aerospace Materials*. , pp. 428–453.

Wulfsberg, J., Herrmann, A., Ziegmann, G., Lonsdorfer, G., Stöß, N. and Fette, M. (2014) 'Combination of carbon fibre sheet moulding compound and prepreg compression moulding in aerospace industry', *Procedia Engineering*, 81 Elsevier, pp. 1601–1607.

Xu, L. and Drzal, L.T. (2001) 'Improvement of adhesion between vinyl ester resin and carbon fibers', *Proceedings of the 13th International Conference on Composite Materials (ICCM'01)*., pp. 1–10.





# APPENDICES

## Appendix A Force Displacement Graphs

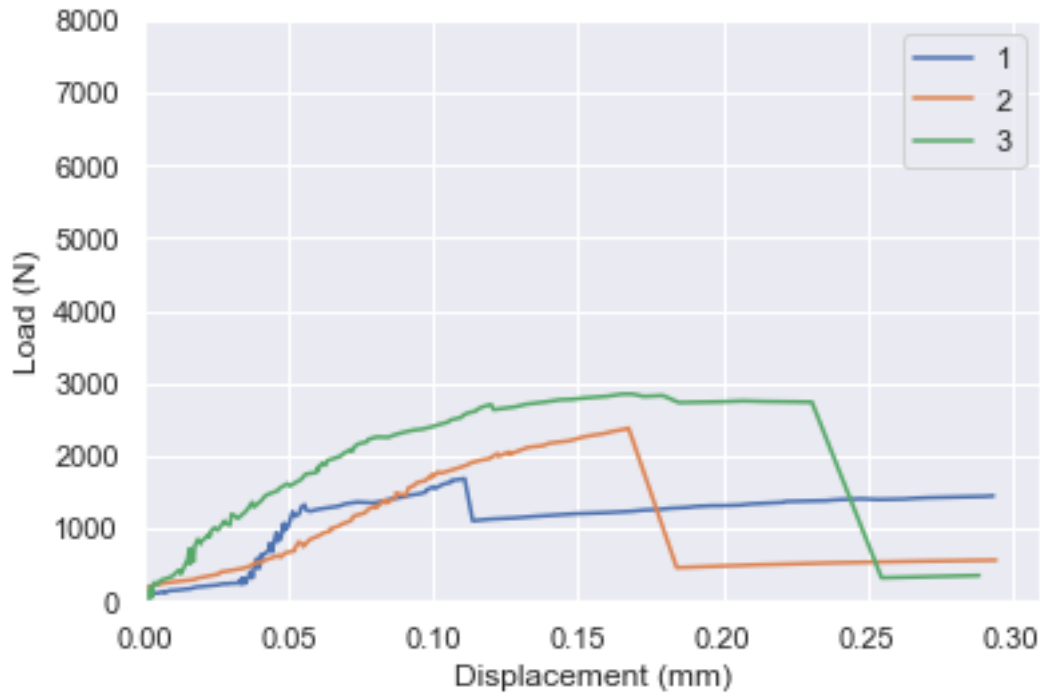
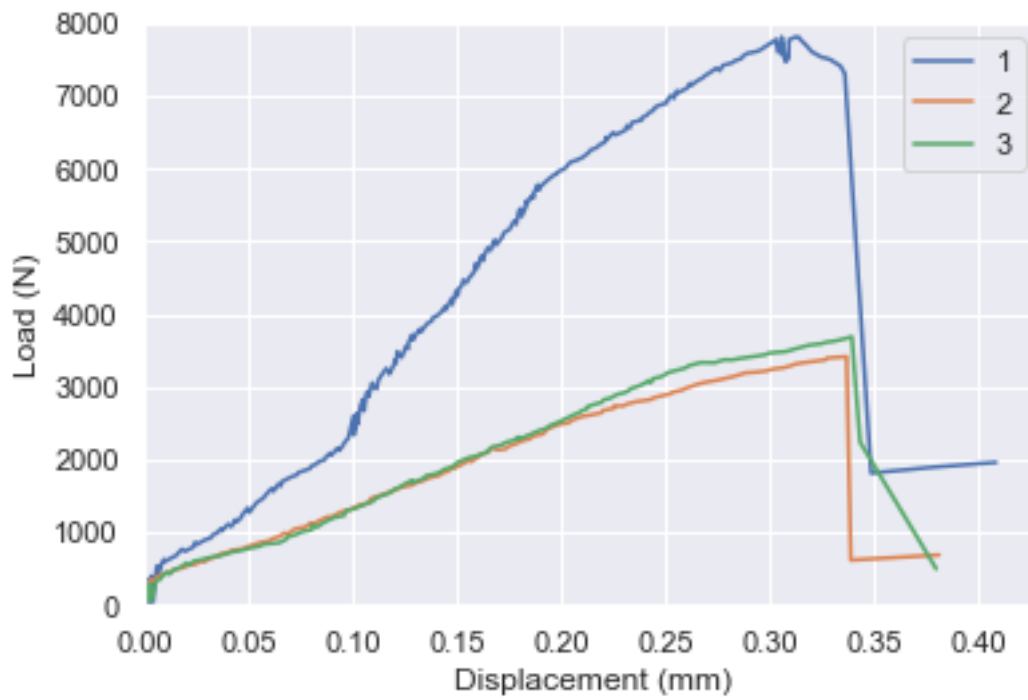
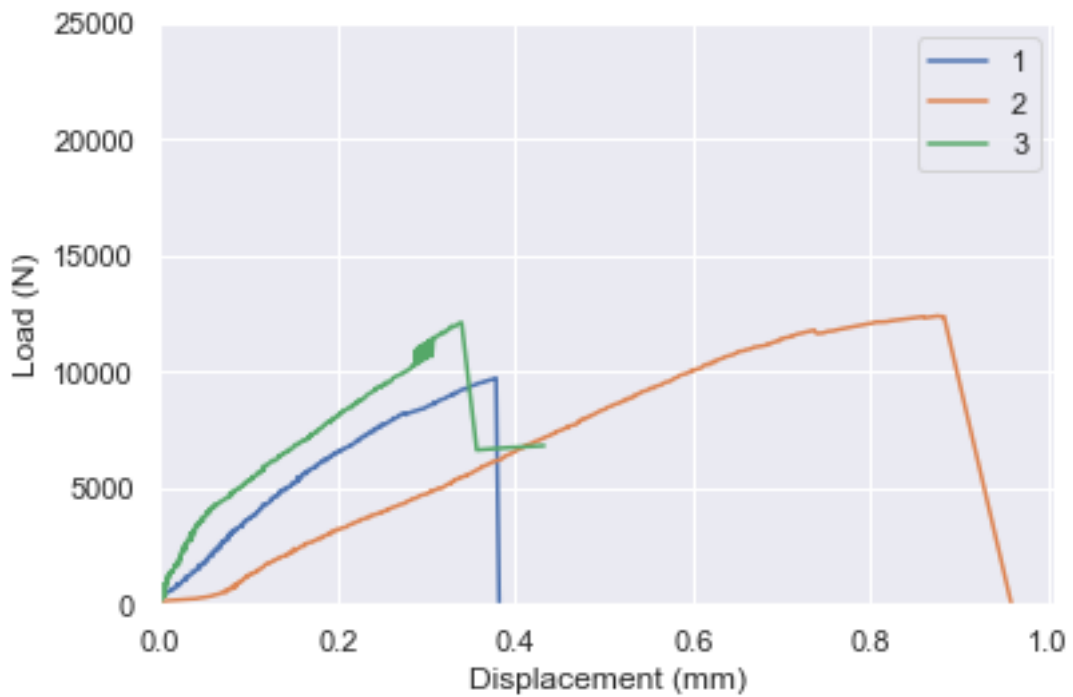


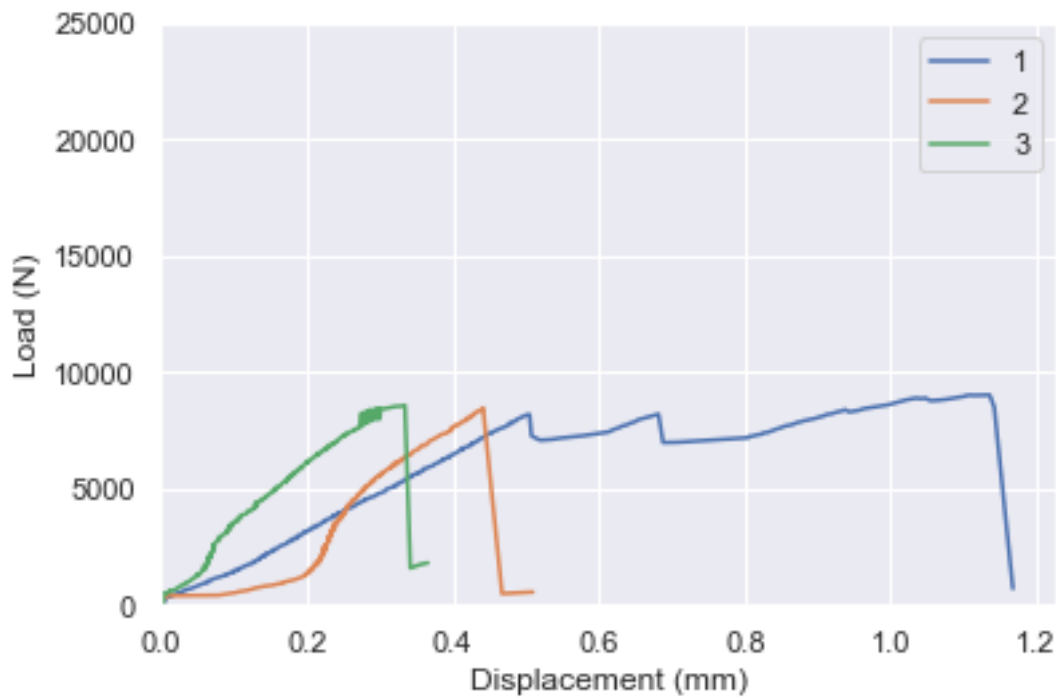
Figure 87: SMC Specimen



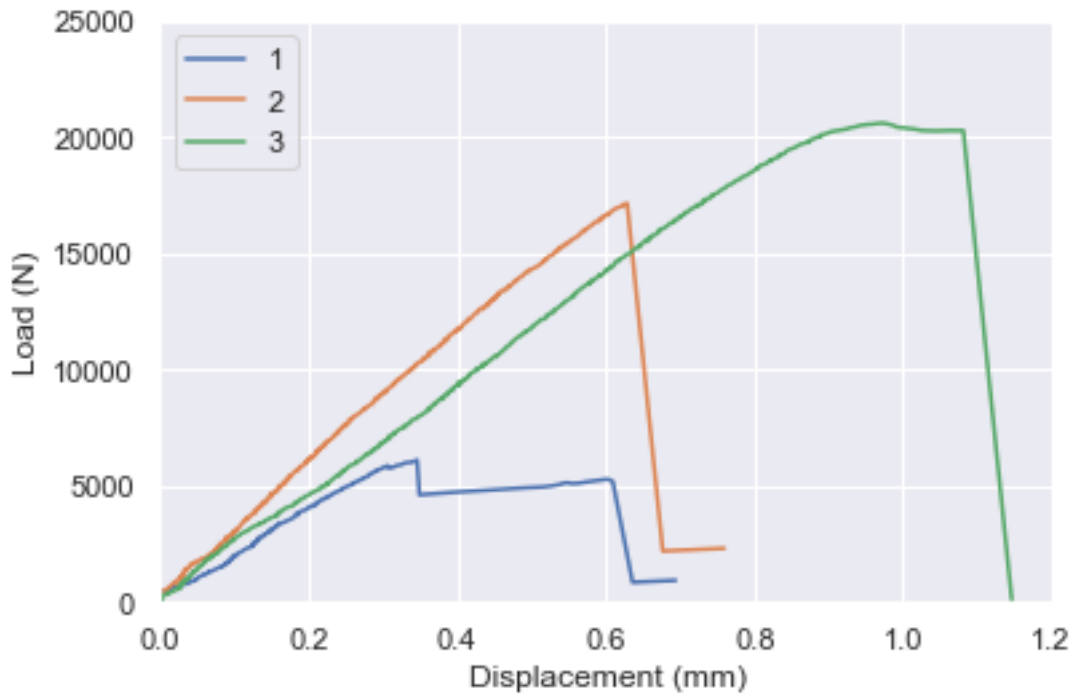
**Figure 88: SMC Specimen with Cylindrical Insert**



**Figure 89: Hybrid Specimen**



**Figure 90: Hybrid Specimen with Cylindrical insert**



**Figure 91: Hybrid Specimen with Yoyo Insert**

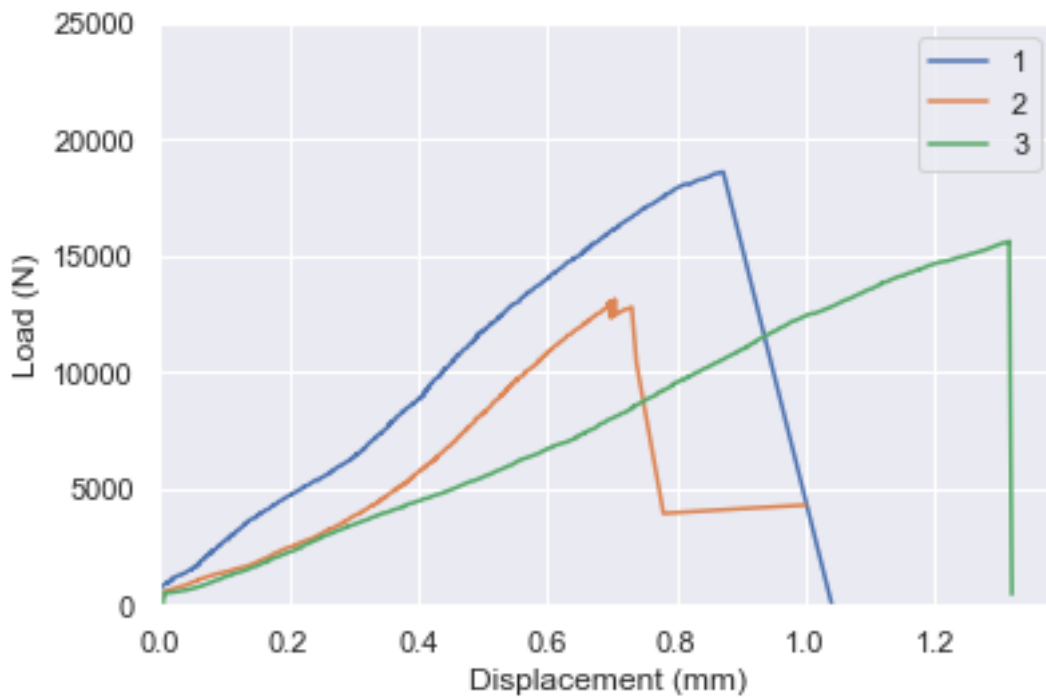


Figure 92: Hybrid Specimen with 2d Yoyo Insert

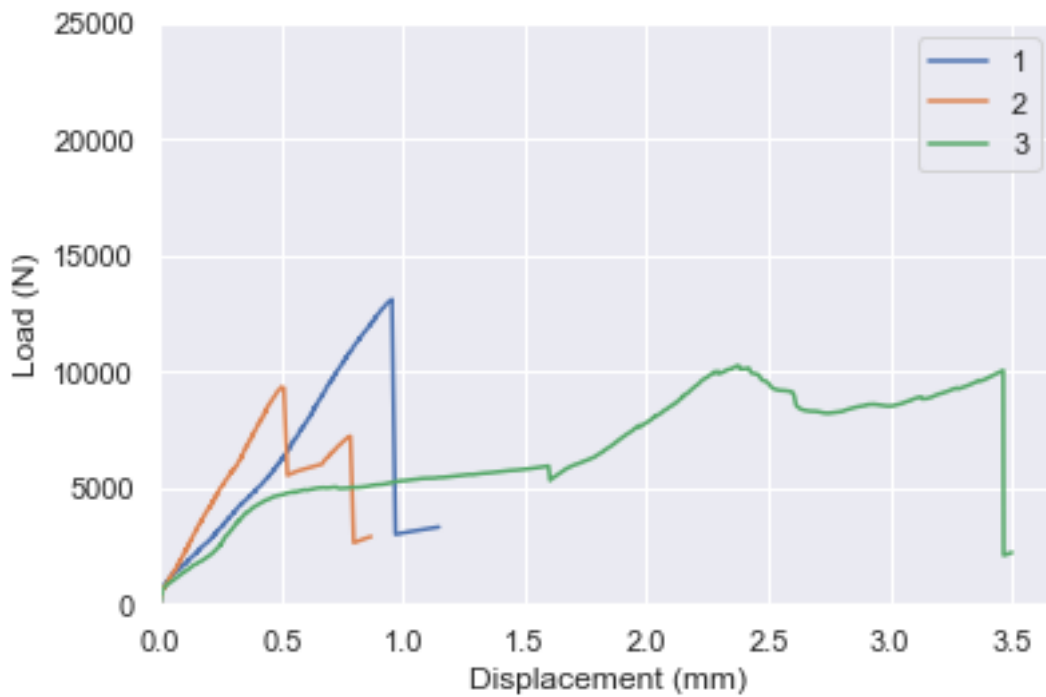


Figure 93: Hybrid Specimen with Flying Saucer

# Appendix B Datasheets

## B.1 Carbon Fibre UD



**HexPly® M77**  
fast curing epoxy resin matrix for prepregs



Product Data Sheet

### Description

HexPly® M77 is a fast curing hotmelt, thermosetting epoxy resin matrix, specifically designed for prepreg applications at which short cure cycles are required. M77 is recommended for curing at 120 – 150°C and is suitable for a range of pressures (5 – 35bar). M77 can be used for manufacture of large industrial components, suitable for cure of thin and thick sections.

### Resin Matrix Properties

#### Dynamic Thermal Properties by DSC (ISO 11357-5)

(cure -40 to 270°C @10°C/min) <sup>(1)</sup>

Uncured T<sub>g</sub>: 5 – 15°C

T<sub>Onset</sub>: 118 – 132°C

T<sub>Peak</sub>: 132 – 142°C

Enthalpy: 340J/g +/-20%

*(1) Data obtained from neat resin upon delivery*

#### Isothermal Cure Properties by DSC

Temperature	Cure Time (95%) <sup>(2)</sup>
120°C	≤9min
130°C	≤6min
140°C	≤3min
150°C	≤1.5min

*(2) time to 95% conversion (ISO 11357-5), total scan time 15min @120 – 140°C, 2min @150°C*

- Optimum cured T<sub>g</sub>: 130°C +/-5°C (following a 15min cure @130°C) <sup>(3)</sup>
- Typical cured T<sub>g</sub>: 130°C +/-5°C (following a 2min cure @150°C) <sup>(3)</sup>  
*(3) according to ISO 11357-2 using a 10°C/min ramp rate, -40 to 270°C; based on 95% conversion*
- Density (ISO 1183-1): 1.15 – 1.25g/cm<sup>3</sup>
- Color: Off white - Yellowish
- Tack: Moderate

## B.2 Carbon Fibre SMC

---

# Polynt-SMCarbon® 24 CF50-12K

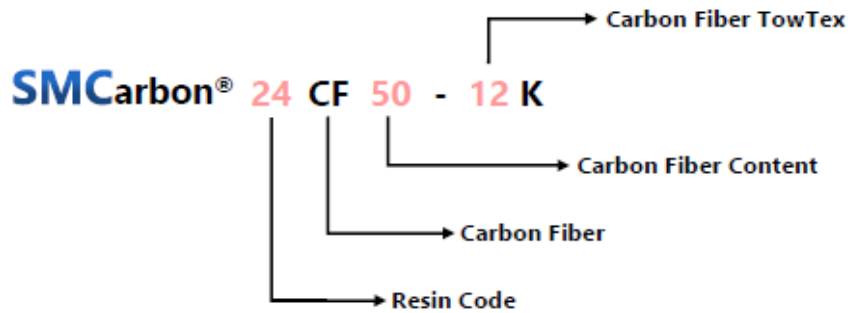
### Generic Information

---

Sheet moulding compound based on vinyl ester resin and reinforced with carbon fibres for compression moulding. This material has great potential for weight reduction and allows a high degree of design freedom. The SMCarbon-Series is particularly suitable for structural applications where high mechanical properties are required.

### Code Description

---



### Material Description

---

Packaging:	roll	Fiber length:	25 mm
Material width:	500 mm – 1200 mm	Fiber tow tex :	12 K
Shelf life at -18°C:	6 months	Nominal fiber content $w/w$ :	50 %
Shelf life at RT 23°C:	8 weeks	Areal weight:	1.200 g/m <sup>2</sup> – 1.800 g/m <sup>2</sup>
		Typical cure temperature:	135 – 145 °C
		Typical moulding pressure:	80 – 120 bar
		Typical cure time:	35 s/mm

### Storage and Handling

---

Store the product in its original sealed packaging at 23°C. Leave product to reach room temperature before unrolling, to prevent condensation. The usual precautions when handling uncured synthetic resins and fine fibrous materials should be observed, and a Safety Data Sheet is available for this product. The use of clean disposable inert gloves provides protection for the operator and avoids contamination of material and components.

---

## Mechanical Properties on cured material

---

Properties were determined on compression-moulded specimens according DIN EN 14598.

Properties	Method	Unit	Value
Density	ISO 1183 A	g/cm <sup>3</sup>	1,40
Shrinkage	ISO 2577	%	-0,09
Tensile Modulus	ISO 527-4	N/mm <sup>2</sup>	25.300
Tensile Strength	ISO 527-4	N/mm <sup>2</sup>	108
Flexural Modulus	ISO 14125	N/mm <sup>2</sup>	22.600
Flexural Strength	ISO 14125	N/mm <sup>2</sup>	285
Impact Strength	ISO 179	KJ/m <sup>2</sup>	45
Glass Transition Temperature	ISO 11357-2	°C	150
Heat distortion temperature	ISO 75-2	°C	> 200

# Epovia<sup>®</sup> Optimum RF 5000

## Resin Epoxy Vinylester Urethane

Version : October 2015

### Appearance

Clear Ambercoloured liquid resin

### Main resin characteristics

Epoxy Vinylester Urethane Resin  
Thickening with magnesium oxide

### Moulding information

SMC / BMC

### Other possible process

Pultrusion

### Main applications

Industrial parts

### Other possible applications

### Shelf life and storage

- Store in the shade out of direct sunlight below 30°C in sealed containers
- The shelf-life will be reduced if the resin is exposed to higher temperatures
- Use within shelf life specified on the container.

### Precautions for handling

Please find the current SDS on internet [www.cpccomposites.com](http://www.cpccomposites.com)

Characteristics, Methods and Conditions	Values (Average values)
<b>Liquid properties</b>	
-Specific gravity at 23 °C :	1.05 – 1.10 g/cm <sup>3</sup>
-Viscosity (dPa.s) : V23	Brookfield at 23°C
Spindle 2 Speed 50 rpm :	22
-Solid content (%) : PC53	60
-Reactivity :	
	Méthod : R 03 (100g)
	Test temperature : 130 °C
	Catalyst system : 1 % TBPB
	Tube Ø 18 ht 75 mm
	Gel time : 180 s
	Peak time : 230 s
	Peak temperature : 260 °C
<b>Mechanical properties (cured resin non reinforced)</b>	
Post cure (4 hrs at 80°C) and (2 hrs at 120°C)	
<b>-Tensile ISO 527 (1999)</b>	
-Tensile strength (MPa) :	35
-Tensile modulus (MPa) :	3500
-Elongation at break (%) :	1.25
<b>-Flexural ISO 178 (2003)</b>	
-Flexural strength (MPa) :	80
-Flexural modulus (MPa) :	3000
<b>Thermomechanical properties (cured resin non reinforced)</b>	
-HDT ISO 75-2 A (1999) (°C):	130



## B.3 Glass Fibre SMC

### *Technical data sheet*

## SMC 24/50 RN-1090

### material properties

characteristics	method	unit	value
surface weight	ISO 10352	g/m <sup>2</sup>	1800
fibre content	ISO 1172	%	50
fibre length	PA 3.01	mm	25
curing time @ 145°C	ISO 12114/2	s/mm	14
specific density	ISO 1183 A	g/cm <sup>3</sup>	1,63
shrinkage	ISO 2577	%	0,08
flexural modulus	ISO 14125	N/mm <sup>2</sup>	13.200
flexural strength	ISO 14125	N/mm <sup>2</sup>	320
tensile strength	ISO 527-4	N/mm <sup>2</sup>	170
tensile modulus	ISO 527-4	N/mm <sup>2</sup>	12.000
impact strength	ISO 179	KJ/m <sup>2</sup>	130
heat distortion temperature	ISO 75-2 A	°C	>200

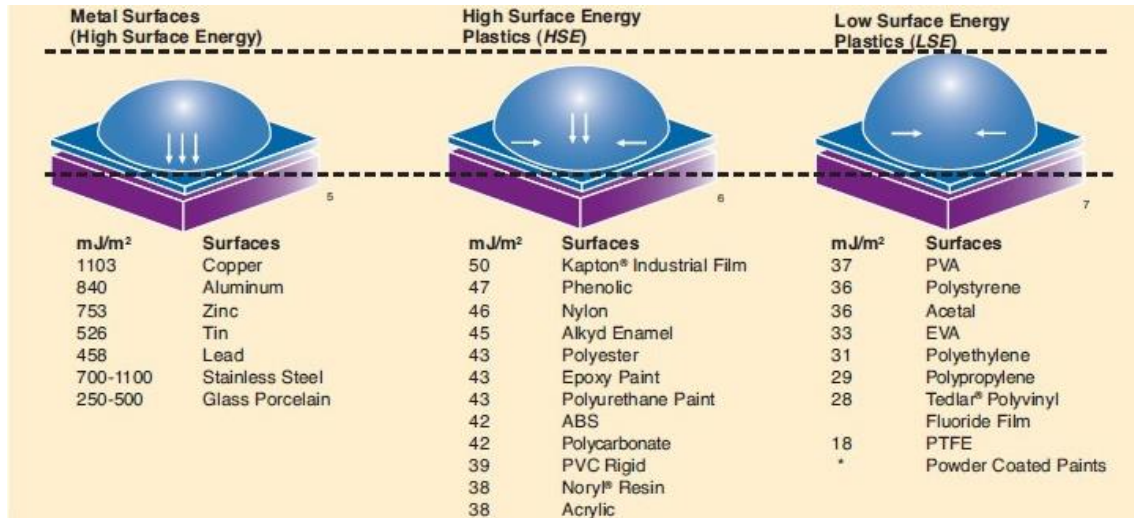
Properties were determined on compression-moulded specimens according DIN EN 14598

### storage and processing recommendation

storage condition	store dry at max. 25 °C and out of direct sun light
moulding time	30 s/mm
moulding pressure	80-120 bar
moulding temperature	145 °C

This technical leaflet issued in the month of May 2021 replaces any other version printed before.

## Appendix C Adhesion of Metals and Composites

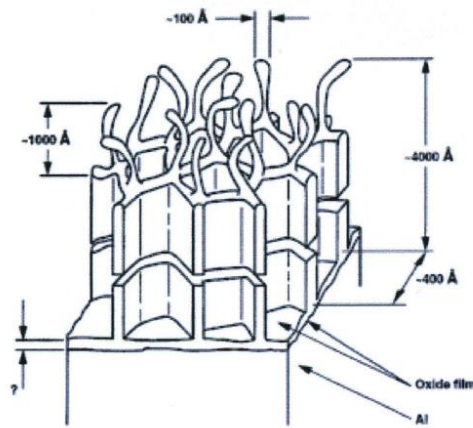


**Figure 94: Surface Energy of different materials** (Candotape, 2016)

The surface energy of a lot of materials is displayed in Figure 94. This surface energy can be increased with surface treatments.

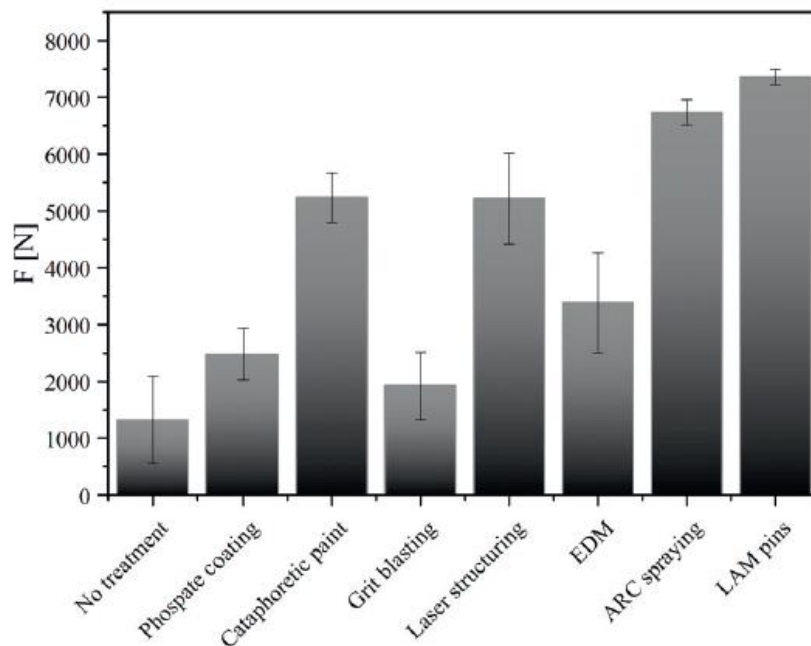
The surface treatments can be broadly divided into coatings and mechanical treatments and their effectiveness can vary metal to metal.

The recommended surface treatment for aluminium inserts is Phosphoric acid Anodising. Figure 95 shows the surface structure of Aluminium after Phosphoric Acid Anodization which increases its surface energy and therefore enhances the adhesion between the metal and the substrate.



**Figure 95: Aluminium surface microstructure after Phosphoric Acid Anodization** (Vander Voort et al., 2004)

Figure 96 displays the strength of the lap joints of stainless-steel samples with carbon fibre coupons using different surface treatments. It can be observed that the surface treatments only increase the tensile strength of the joint, but also reduce the variability of the joint.



**Figure 96: Tensile strength of stainless-steel carbon fibre lap joints with different surface treatments on metal** (Gebhardt and Fleischer, 2014)

Figure 97 displays the impact of the surface treatments on the strength of the standard insert. It can be observed that impact of the surface treatments isn't

nearly pronounced in inserts as opposed to lap joint tests. This is primarily because substrate adhesive failure is one of the failure modes of the insert. The added adhesive strength does not necessarily influence the delamination and insert deformation. Therefore, even though the impact of surface treatments on final strength is moderate, their impact on reduction of variability is valuable.

	<b>Tensile tests</b>	<b>Bending tests</b>
<b>Untreated inserts</b>	100%	100%
<b>Cataphoretic painting</b>	110%	131%
<b>Laser structuring</b>	119%	112%
<b>Arc spraying</b>	128%	141%
<b>Laser additive manufacturing pins</b>	142%	127%

**Figure 97: Tensile and Bending strengths of embedded inserts with different surface treatments** (Gebhardt and Fleischer, 2014)

## Appendix D Risk Assessment & Mitigation Plan

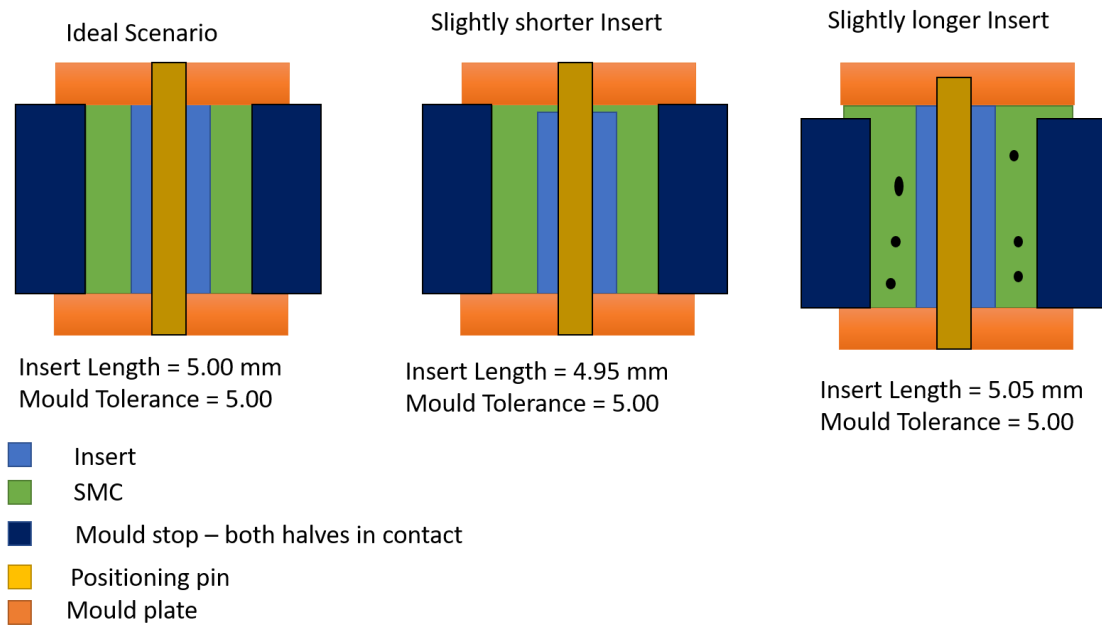
Table 21: Risk Assessment and Mitigation Plan

Risk	Mitigation Plan
Risk of irritants in SMC resin	Wear gloves, lab coat
Itching/Irritation from Fibres	Always wear gloves when handling uncured fibres
Styrene from vinyl ester	Cross flow ventilation
Heavy Steel Moulds	Wearing gloves and always moving moulds in the presence of someone in the lab
Hot Moulds	Wait till mould have cooled before unloading them from the machine
High Compression Load	Closing the press door before applying load
Tensile Loading test	Using an acrylic shield and/or safe distance between specimen and humans
Plague	Had 2 shots, had the plague, wear mask indoors and social distancing (when possible)

## Appendix E

### E.1 Insert Tolerance and Manufacturing Load

During Manufacturing, the inserts will be under compression loads from the mould. The insert shouldn't yield or buckle under these loads. The compression pressure on the complete cross-section during moulding is 100 bars. Therefore, the compression load on the insert is proportional to the cross-sectional surface area of the insert.



**Figure 98: Impact of Insert Tolerance on Loading**

Figure 98 shows the importance of the tolerance of the inserts. Therefore, to ensure mould closure and predictable compression loading on the insert, the length of the insert should be 5mm or less.

## E.2 Medium Flow Trapezoidal

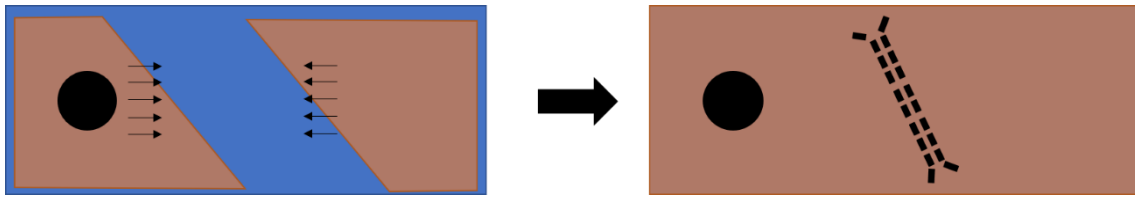


Figure 99: Medium Flow Trapezoidal Charge Design

## E.3 Hybrid Flat Sample Moulding

About halfway through the project, it was realised that there was a shortage of SMC material and new material wouldn't arrive in time. Therefore, last few samples were moulded as flat samples as shown in Figure 100. This ensured that all the mouldings could be done with the existing material.

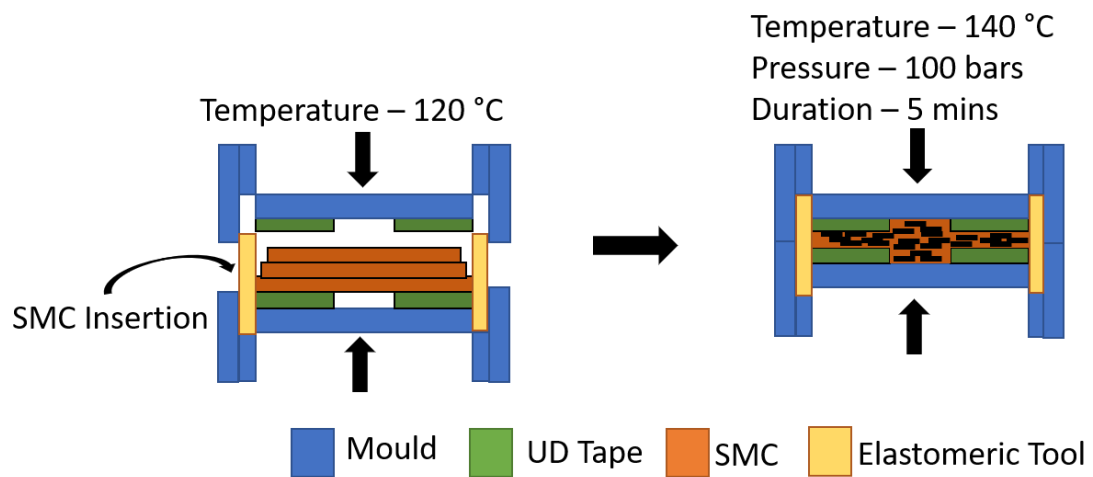


Figure 100: Hybrid Flat Sample Moulding